2013-05-30

L1-Optimal Control of Variable-Speed Variable-Pitch Wind Turbines

Jafarnejadsani, Hamidreza

UNIVERSITY OF CALGARY

ℓ_1-Optimal Control of Variable-Speed Variable-Pitch Wind Turbines

by

Hamidreza Jafarnejadsani

A THESIS

SUBMITTED TO THE FACULTY OF GRADUATE STUDIES

IN PARTIAL FULFILMENT OF THE REQUIREMENTS FOR THE

DEGREE OF MASTER OF SCIENCE

DEPARTMENT OF MECHANICAL AND MANUFACTURING ENGINEERING

CALGARY, ALBERTA

MAY, 2013

Abstract

The fast-growing technology of large scale wind turbines demands control systems capable of enhancing both the efficiency of capturing wind power, and the useful life of the turbines. Control based on ℓ_1 performance is an approach to deal with persistent exogenous disturbances which have bounded magnitude (ℓ_1-norm) such as realistic wind disturbances and turbulence profiles.

In this study, we use a linear matrix inequality (LMI) approach for solution of the ℓ_1-optimal control problem. We develop an LPV model of a variable-speed variable-pitch (VS-VP) wind turbine in the transition region (between power point tracking and power regulation regimes). Then, we derive an LPV ℓ_1-optimal controller using LMI methods.

We also develop an efficient method for computing the ℓ_1-norm of a closed-loop system. As the control synthesis problem is non-convex, we use the proposed method to design optimal output feedback controllers for a linear model of a wind turbine at different operating points using genetic algorithm (GA) optimization. The locally optimized controllers were interpolated using a gain-scheduled technique with guaranteed stability. The controller is tested with comprehensive simulation studies on a 5 MW wind turbine using FAST software. The proposed controller was compared with a well-tuned PI controller. The results show improved power quality, and decrease in the fluctuations of generator torque and rotor speed.

Acknowledgements

I would like to thank Dr. Jeff Pieper for his academic and financial support and guidance throughout the M.Sc degree. I would also like to thank Julian Ehlers, a fellow Ph.D student, for his help with the FAST simulation software. I thank my parents for their support and encouragement and also all that have helped make this work possible.

This thesis is dedicated to my parents for their love & support.

Table of Contents

List of Tables

List of Figures

List of Symbols

$\mathbb{R}$	The real numbers
$\mathbb{R}^n$	n –space, all n-tuples of real numbers
$X^{n\times m}$	Space of $n \times m$ with entries in X
$\det(A)$	Determinant of matrix A
A^{-1}	Inverse of matrix A
A^T	Transpose of matrix A
$A\|_{n\times m}$	$n \times m$ matrix A
$[s_{ij}]_{n\times m}$	$n \times m$ matrix s with entries s_{ij}
$\dim(A)$	Dimensions of matrix A
$diag(A, B, \dots)$	Diagonal matrix with diagonal entries $A, B, \dots$
$\mathcal{F}_\ell(A, B)$	Lower linear fractional transformation
$G_1 * G_2$	Linear fractional transformation interconnection of systems G_1 and G_2
$T: x \to y$	Map T from x to y
$A(z), B(z), \dots$	Discrete-time transfer function
$\neq$	Negated equality
$\approx$	Similar
$\equiv$	Equality by identity
$:=$	Equality by definition
$\|x\|$	Absolut value of x
$\bar{x}$	Average of variable x
$\dot{x}$	Time derivative of variable x
sup	Suprimum
min	Minimum
max	Maximum
inf	Infimum
$\|x\|_p$	p norm of x
$\|R\|_*$	Star norm of operator R
ℓ_p	Space of real sequences supported by nonnegative integers such that if $x \in \ell_p$ then $\|x\|_p = \sum_{k=0}^{\infty} \|x(t)\|^p < \infty$
ℓ_∞	Space of all bounded sequences of real numbers supported by nonnegative integers such that if $x \in \ell_\infty$ then $\|x\|_\infty = \sup_k \max_i \|x_i(t)\| < \infty$
$\|R\|_{\infty-ind}$	Induced norm of operator R on input/output signal in ℓ_∞ space
$\mathcal{H}_2$	Space of linear time-invariant operator with bounded energy contained (RMS value) in the impulse response
$\mathcal{H}_\infty$	The space of linear-time-invariant ℓ_2-stable operators
$\mathcal{RH}_\infty$	Space of systems that have finite-dimensional realization and are stable
$co\{a, b, \dots\}$	Convex hull of a set
$\subset$	Subset/Subspace
$\in$	Element of

$\notin$	Not an element of
$\forall$	For any/all
$\subseteq$	Subset
$\delta(t)$	Dirac delta function
$s.t.$	Subject to

List of Acronyms

CPU	Central Processing Unit
DOF	Degree of Freedom
GA	Genetic Algorithm
LFT	Linear Fractional Transformation
LMI	Linear Matrix Inequality
LP	Linear Programming
LPV	Linear Parameter-Varying
LQR	Linear Quadratic Regulator
LTI	Linear Time-Invariant
LTV	Linear Time Variant
MIMO	Multi-Input Multi-Output
NN	Neural Network
OP	Operating Point
PI	Proportional-Integral
PID	Proportional-Integral-Derivative
PLMI	Parameterized Linear Matrix Inequality
RBF	Radial Basis Function
RMS	Root Mean Square
SISO	Single-Input Single-Output
VSVP	Variable-Speed Variable-Pitch

Chapter 1: Introduction

1.1 Wind Turbine Systems

Today, wind turbine systems are one of the fastest growing technologies. In order to be competitive, optimizing control systems are used in large-scale wind turbines. These systems enable the wind turbine to work efficiently and produce the maximum power output in varying wind conditions while keeping torque variations low so as to avoid fatiguing structural components. In addition, because wind turbines are usually installed in remote areas such as offshore installation, these control systems can be used in condition monitoring for the purpose of maintenance. A thorough review of the advances in wind turbine control systems is performed in Bianchi *et al.* (2007).

Wind turbines are facing turbulent winds with varying speed. In high wind speeds, in order to prevent conditions such as overrunning, a control mechanism should limit the speed of rotation of the blades. In large wind turbines, blades with variable pitch angle are used. Active control of blade pitch angle can limit the rotor speed by changing the angle of attack in the blades to reduce aerodynamic lift and also, in limiting cases, to cause stall effects. In addition, pitch control can enable the system to track the optimal tip-speed-ratio to have the maximum power output in different wind conditions. In smaller wind turbines, passive control of the rotor speed is used to limit the speed of wind turbine using stall effect in a certain wind speeds. The disadvantage of passive stall control of wind turbine is that it causes more stress in blades and reduces their lifespan. In addition, it wastes the useful wind power because of the drop in aerodynamic torque caused by the stall effect in the blades (Bianchi *et al.* 2007).

In recent decades, fixed speed generators were common in wind turbines because of low cost and capability of direct connection to the grid with specific frequency. As a consequence of using fixed speed generators, wind turbines had to work at a certain speed. Therefore, they could not adapt to variable wind speeds to track optimal rotor speed or the so-called optimal tip-speed-ratio. To be more adaptable to variable wind speeds and to be more efficient, variable speed wind turbines with variable speed generators, which can be connected to the grid via electronic convertors, are the modern choice of alternative technologies. These convertors enable the generator to work in variable speed with a frequency which is isolated from the grid frequency. Therefore, control on the turbine speed for tracking the optimal rotor speed becomes possible (Achermann, 2005). Although, fixed speed wind turbines with stall controlled blades prevailed in large wind turbines for many years, recently, with a fast growth in the wind turbine industry, variable speed wind turbines with variable pitch blades are successful options because of their efficiency to capture more wind power and capability to achieve higher power qualities. Moreover, as the size of wind turbines increases, concerns about mechanical stresses in the blades and the structure and also failure of wind turbine components like the drive-train increases. Therefore, variable speed wind turbines with an active control of the rotor speed and blade pitch angle can alleviate the loads and stresses on the different parts of the wind turbines. As a result, higher power efficiency, longer lifespans, and improved power quality makes these wind turbines competitive economically, despite their higher initial costs (Burton *et al.* 2001, Hansen *et al*. 2005).

As shown in Fig. 1.2, the wind turbine control system consists of several subsystems. The aerodynamic block shows the conversion of wind force to mechanical torque in blades. The mechanical subsystem consists of two blocks. Drive-train block describes the conversion of the

mechanical torque in the rotor to the rotational speed in the generator. The structure block describes the movement of tower, basement and mechanical parts in the nacelle because of thrust force of wind. The electrical subsystem shows the conversion of mechanical power of rotating shaft to electricity in the generator and connection to the grid. Actuator subsystem describes the dynamics of servomotors used for pitch control and the dynamics in yawing.

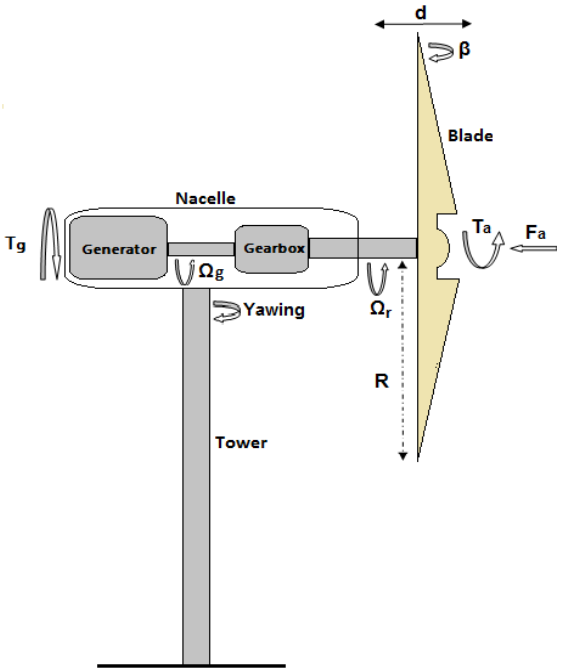

Figure 1.1 Wind turbine with horizontal axis.

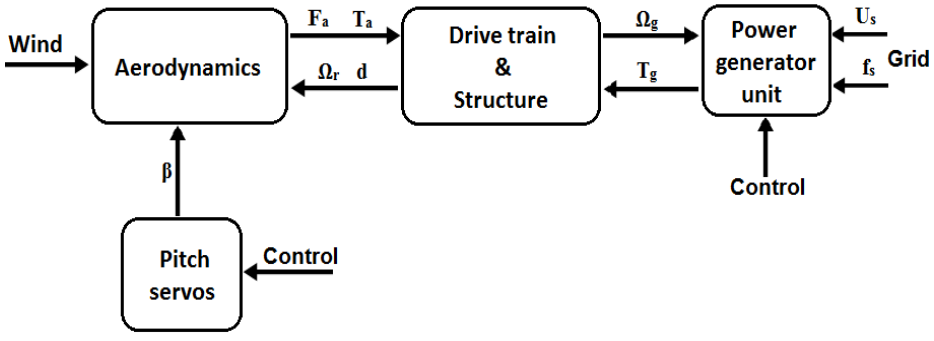

Figure 1.2 Subsystem-level block diagram of a variable-speed, variable-pitch (VS-VP) wind turbine.

Energy capture, power quality, and mechanical loads are the three main control objectives in wind turbine. These control objectives are briefly discussed in the following paragraphs:

1.1.1 Energy Capture

The generation capacity of a wind turbine, which determines the amount of wind energy capture, is restricted to the physical and economic constraints. The ideal power curve for a typical wind turbine at different wind speeds is shown in the Fig. 1.3. It is observed that the range of operation of wind turbine is limited to minimum wind speed, V_{min}, and maximum wind speed, V_{max}. At wind speeds below V_{min} and above V_{max}, the turbine is kept at rest. Although, wind energy can be captured at these speeds, considering the mechanical loads and power quality and cost of maintenance, it is more economical in the long term to keep the wind turbine at rest in these conditions. In addition, most of the energy is captured at nominal wind speeds and very low and very high wind speed conditions are rare (Bianchi *et al.* 2007).

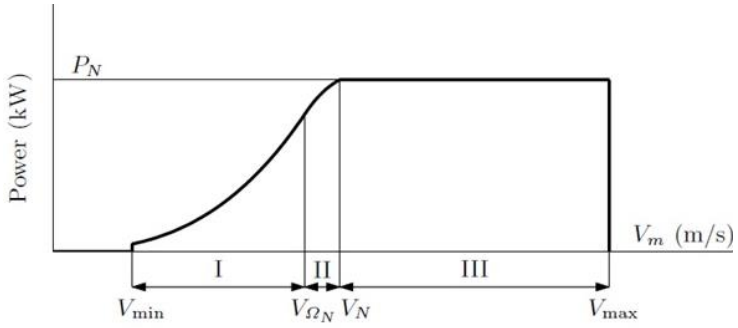

Figure 1.3 Ideal power curve.

Above the rated wind speed V_N , the captured power in the ideal power curve remains constant. The maximum power capture at V_N and higher wind speeds is limited to the size of wind turbine and its generation capacity. However, using larger turbines increases cost per kW. As is shown in Fig.1.3, three regions can be identified in the range of operation of wind turbine. For the wind speeds below the rated wind speed, wind turbine captures the maximum available

power of the wind flow. As shown in equation below, it is a cubic relation relative to the wind speed, theoretically. This region is specified as Region I.

$$P = C_{P_{max}} F_a V = \left(\frac{1}{2}\right) \rho \pi R^2 C_{P_{max}} V^3 \tag{1.1}$$

In Region III, which is called the rated power area, the power is kept constant. In this region, there is more wind power available than the captured power. Therefore, turbine works at lower efficiency with power coefficient less than $C_{P_{max}}$. Region II is a transient region between Regions I and III. A control strategy for Region II that alleviates the transient loads while ensuring reasonable power efficiency is important so that we will discuss it extensively in Ch. 3 of this thesis. In some designs, this region is ignored by connecting the maximum power region to the constant power region (Bianchi *et al.* 2007).

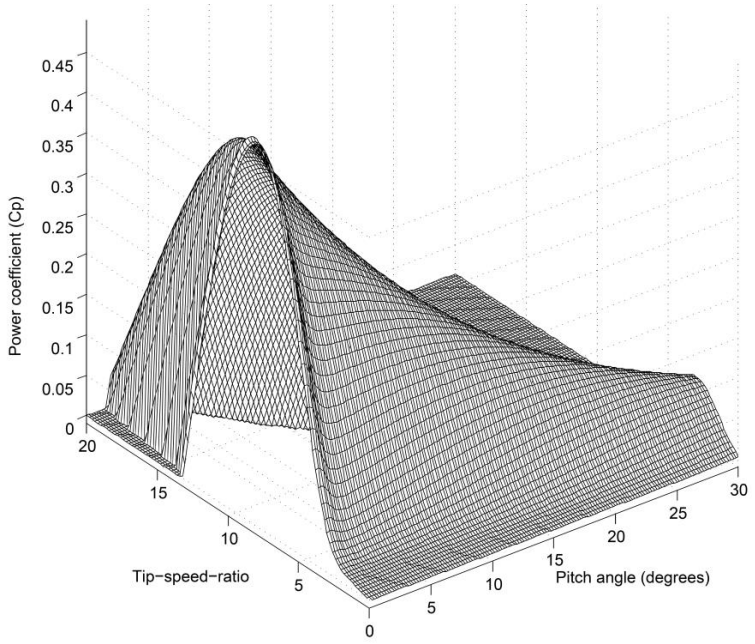

Figure 1.4 The power coefficient surface as a function of tip-speed-ratio and pitch angle.

1.1.2 Mechanical Loads

As the wind turbine works at its maximum capacity, more mechanical loads are induced in different parts that decrease the useful life of the turbine and cause fatigue in the components. Consequently, the long term cost of power generated increases. Therefore, alleviation of mechanical loads should be considered along with the other control objectives.

Static and dynamic loads are two type of mechanical loads induced in wind turbine. Static load is the result of aerodynamic forces induced by mean wind speed. In wind turbine design, dynamic loads are more important. The temporal distribution of wind speed field over the area swept by the blades induces dynamic loads in different parts. As a consequence, variation in the aerodynamic torque and also variation in the loads on the turbine structure and drive-train happens. As an alternative classification, dynamic loads can be divided to low frequency and high frequency loads. Transient loads which are induced by turbulence and gusts are low frequency loads. These loads are very important especially in the higher wind speeds and should be considered in the control strategy for determining the components rating. If a tight control strategy is designed in order to just follow the steady-state control curve, it induces a significant amount of extra loadings. High frequency loads are caused by cyclic loads around the peaks at multiples of rotor speed and propagate through the drive-train. They can excite vibration modes of some parts of the turbine. As the size of turbine increases, there are more moving bodies that may be affected by high frequency vibration. Control strategy has a critical effect on damping these harmful vibrations. For example, pitch control may excite some resonance modes in the turbine structure that should be monitored and considered in the control system design (Battista *et al.* 2000, Leithead and Connor 2000, Sørensen *et al.* 2005).

1.1.3 Power Quality

Important factors for power quality are stability of voltage and frequency at the point of connection to the grid and by emission of flicker. Low power quality can cause additional costs of investment in power lines. Frequency variations are result of power balance. If the load on the generator is more than the power supplied to it, the generator will decelerate and the frequency reduces. The inverse happens if the power demand be less than power supplied to the generator. Then the rotor accelerates and the frequency goes up. However, for the case of small-scale wind farms that connect to the network this problem does not occur. For large scale wind farms and also isolated farms, power balance can cause frequency variances that should be regulated. Therefore, monitoring and conditioning of power quality should be considered in the control systems design (Lalor *et al.* 2005, Larsson 2000, Muljadi and Butterfield 2001).

1.2 Control Design for Wind Turbines

In 1970s and 1980s, several large wind turbines were designed using fixed speed synchronous generators. These wind turbines had stiff drive train and large rotor with high inertia. The classical control design in this era for wind turbine was based on Proportional-Integral-Derivative (PID) approach. It was found that the turbulent wind flow easily excites the first torsion mode of large drive-trains. Several control designs were proposed to regulate the power output and also add damping to the closed loop system using pitch control (Kos 1978, Rothman 1978, Svensson and Ulen 1982, Hinrichsen and Nolan 1984, and Wasynczuk *et al.* 1981).

In the later wind turbine control designs, Linear Quadratic Regulator (LQR) approach was used to alleviate the load on mechanical components like drive-train, tower, and blades in addition to regulating the power. Liebst (1985) designed a LQR control for KAMeWa wind turbine with blade flap, lag, and pitch; drive-train torsion; generator torsion; and tower bending were the wind turbine DOF modeled in the study. Mattson (1984) used a state estimator in combination with LQR to overcome the limit in measurement of the states needed in the controller. He designed the controller based on the linear model containing drive-train torsion and tower fore-aft bending DOF.

The flexible structure of wind turbine and the aerodynamic forces which act on the wind turbine are highly nonlinear. In pitch control, the input gain that is the partial derivative of aerodynamic torque, vary at different operating points with wind speed, rotor speed, and pitch angle. Therefore, one controller which is designed based on the linear model at one operating point may result in poor performance at other operating points or even an unstable closed-loop system (Wright, 2004). To address this problem several scheduling or switching techniques have been suggested to design multiple controllers at different turbine operation points. Some work has been performed to design gain-scheduled and switching controllers by Kraan (1992) and Bianchi *et al.* (2007). However, switching between controllers may raise some problems regarding the stability and performance at switching points. However, there are some gain-scheduling and linear parameter varying methods, which guarantee the stability in switching between local controllers like the study by Bianchi and Pena (2011), Xie and Eisaka (2004), and Apkarian *et al.* (1995). Wind speed can be used as scheduling parameter in wind turbine controllers. The anemometers which are installed on the nacelle, can measure the wind speed. However, anemometers measure the wind speed at one point and the downstream wind flow

behind the blades is affected by the turbine structure itself. Therefore, wind speed measurement is not accurate and is not well-correlated to the wind speed that is experienced by wind turbine blades. This makes the practical implementation of controller scheduling difficult. Ehlers *et al.* (2007) and Østergaard *et al.* (2007) have addressed this problem by introducing indirect estimation of effective wind speed.

1.2.1 Gain-Scheduling Techniques

Wind turbines are nonlinear systems. Gain scheduled controllers are one of the well-known tools that make it possible to use linear control theory for these nonlinear systems. Gain scheduling strategies are widely used in practice (Rugh and Shamma, 2000). The design of gain scheduled controller is in three steps:

1. For a collection of operating points, the LTI models of nonlinear plant are derived and parameterized by scheduling parameters. These variables may be functions of operating points.
2. The LTI controller is designed for each LTI model. Any appropriate linear control method that stabilizes the plant can be used in this step. Design objectives can be stated in terms of bounds on the induced norms of certain input-output operators such as design of LTI controller using H_∞-control or ℓ_1-optimal control synthesis that will be presented in the following chapters.
3. Finally, the gain scheduling strategy is planned. One simple method is switching or interpolating between the LTI controllers according to the scheduling parameters. But, these methods cannot guarantee the stability and performance of the real nonlinear system. However, in several studies, gain scheduling methods with guaranteed stability have been developed. Designing the controllers in the framework of linear parameter

varying (LPV) systems, is one of the well-established gain-scheduling techniques with guaranteed stability and performance.

1.2.2 Adaptive Control

Adaptive control is another modern approach that is used in nonlinear systems like wind turbines. Adaptive control allows the controller gains adapt to changing conditions. Some work was performed by Bossanyi (1987), Freeman and Balas (1999) for adaptive control of wind turbines. Also, in studies by Mayosky and Cancelo (1999), Boukhezzar and Siguerdidjane (2009), and Jafarnejadsani and Pieper (2013), neural networks are used for adaptive control of large-scale wind turbines. Jafarnejadsani et al (2013) proposed an adaptive control based on Radial-Basis-Function (RBF) neural network (NN) which is for different operation modes of variable-speed variable-pitch (VS-VP) wind turbines including torque control at speeds lower than rated wind speeds, pitch control at higher wind speeds, and smooth transition between these two modes. The adaptive neural network control approximates the non-linear dynamics of the wind turbine based on input/output measurements and ensures smooth tracking of optimal tip-speed-ratio at different wind speeds. The robust NN weight updating rules were obtained using Lyapunov stability analysis. The validity of results was verified by simulation studies on a 5 MW wind turbine simulator (Jafarnejadsani *et al.* 2013).

1.2.3 Modeling and Simulation

To develop and validate analytical codes for wind turbine loads and response predictions, several studies has been performed and a thorough review of wind turbine design codes can be found in Molennar (2003). FAST (Fatigue, Aerodynamics, Structures and Turbulence) is one of aero-elastic wind turbine simulators. In our study, the proposed control method was validated using the FAST software. FAST code was first developed at Oregon State University (Wilson *et*

al. 1999) and validated and refined by National Renewable Energy Laboratory (NREL). For simulation, we used the parameters of the NREL-Offshore-Baseline-5MW wind turbine which was developed by Jonkman *et al.* (2009) at NREL. In addition, an aerodynamic subroutine package named AeroDyn (Laino and Hansen 2003) that was developed at University of Utah is used in FAST. The AeroDyn subroutine calculates the aerodynamic forces on a wind turbine blade that is the core element in wind turbine simulation code.

In this study, FAST was used for both extraction of the linear model for control design and for closed –loop simulation. We extracted linear model of wind turbine in a few operating conditions based on just a subset of the total modeling DOF contained in FAST including flexible drive-train, generator torsion, and aerodynamic forces. However, additional DOF can be switched on in the FAST. The effect of unmodeled modes and controller design based on addition of DOF in steps was studied by Wright (2004) in detail. Wright applied modern state-space control design methods to a two-bladed teetering hub upwind machine at the National Wind Technology Center (NWTC). The design objective was to regulate turbine speed and enhance damping in several low-damped flexible modes of the turbine. Starting with simple control algorithms based on linear models, complexity was added incrementally until the desired performance was firmly established.

1.3 ℓ_1-Optimal Control Synthesis

The majority of the results in robust control considers quadratic-type performance and stability criteria and also ℓ_2 signal norms, $\mathcal{H}_2$ and $\mathcal{H}_\infty$ system norms, and also integral quadratic constraints. Overviews on robust control are given in Skogestad and Postlethwaite (2005) and in

Sanchez-Pena and Sznair (1998). The quadratic criterion has been successfully applied to many real-world problems and it can address the system behaviour in terms of energy, dissipativity, or frequency- domain properties. However, some other time-domain properties such as control error, the response overshoot, and the maximum values of control inputs can only be addressed indirectly by quadratic criteria and with numerous design iterations. The mentioned time-domain properties can be addressed directly using ℓ_∞ signal norm

$$\|v\|_\infty \coloneqq \sup_t \max_i |v_i(t)| \tag{1.2}$$

ℓ_∞-norm measures the maximum amplitude of the components v_i of a signal vector v over time. To obtain a corresponding measure for a stable system G, often the so-called ℓ_∞-gain

$$\|G\|_{\infty-ind} \coloneqq \sup_{0<\|w\|_\infty<\infty} \frac{\|Gw\|_\infty}{\|w\|_\infty} \tag{1.3}$$

is used. The gain characterizes the worst- case amplitude of the system output $z = Gw$ normalized by the maximum amplitude of the input w under the assumption of zero initial conditions. In other words, the ℓ_∞-gain describes how well a system attenuates persistent disturbances and stabilizing controller can be designed based on the minimization of the ℓ_∞-gain. As a common situation, it is desired to keep z small if z is the control error. It can be shown that, for LTI systems, the ℓ_∞-gain is equal to the ℓ_1-norm of the system's impulse response. Therefore, the name ℓ_1-optimal control is used for the field of ℓ_∞-gain disturbance attenuation. In addition, many other control objectives such as set-point control, following the reference commands, minimization of resource consumption, or filtering problems can be addressed in ℓ_∞-gain framework. In this work we use discrete-time design approach to propose an efficient computation method for ℓ_∞-gain of the closed-loop system and we develop the procedure for optimization of the controller based on search-based optimization methods such as genetic

algorithms. In addition, we used linear matrix inequality (LMI) approach to find an upper bound on the ℓ_∞-gain and designing the ℓ_1-optimal controller for continuous-time systems.

While there are a vast amount of contributions in the field of robust linear control concerned with $\mathcal{H}_2$ and $\mathcal{H}_\infty$ control, the ℓ_1-optimal control has also seen a number of basic and promising results. The synthesis methods proposed so far in the control literature treat nominal control design in terms of linear programs (LPs) and also norm computations. In summary, although there have been a number of basic results, the literature has paid less attention to ℓ_1 control than to quadratic-type performance frameworks.

Although, some promising works have been performed for designing the output feedback control in ℓ_1-norm framework using linear programing, these approaches requires too much computational effort to calculate the ℓ_1-norm and also the theory to come up with convex optimization problem is very difficult and in some type of problems impossible. In addition, the proposed output feedback controllers in ℓ_1 control literature usually results in high order output feedback controllers. In this study, we propose a method for approximation of ℓ_1-norm that results in a new norm calculation which, as shown in this study, represents desirable characteristics of the ℓ_1-norm. This new norm can be computed efficiently, so it is possible to use search-based optimizations such as genetic algorithms, because the computational cost of ℓ_1-norm calculation of output feedback-controlled closed loop system is low. Therefore, the controller parameters can be optimized using search-based methods without concerning about convexity of the problem or any conservatism that are usually imposed for simplification of the non-convex problems to the convex optimization problems, which can be solved using approaches such as LMIs or LPs.

The main concern in the robust control is to certify the stability of an uncertain system and to quantify its performance. The uncertainty may be real parametric, LTI, linear time varying (LTV), or nonlinear. During the last three decades, numerous methods have been developed for analysis of linear systems subject to different classes of uncertainties or perturbations. There are two main approaches to robust control problems. First, there is the small gain approach, where stability and performance are investigated using scaled system norms and uncertainties with bounded ℓ_2- or ℓ_2-gain or bounded ℓ_∞- or ℓ_∞-gain are particularly well-studied. Some important contributions can be found in Doyle and stein (1981), Packard and Doyle (1993), Shamma (1994), Khammash and Pearson (1991), Dahleh and Kammash (1993), and Dahleh and Diaz-Bobillo (1995). The second main approach to robust analysis relies on Lyapunov stability and performance characterizations via dissipation inequalities, Riccati equations, and LMIs. Some contribution in state-space realization of different type of uncertainties using the mentioned approach can be found in Helmersson (1995), Gahinet (1996), Apkarian and Tuan (2000), Scherer (2000b).

Although, there have been a number of results on uncertain systems in ℓ_1-control literature, there are still many open questions. In our study, the goal is to design a ℓ_1-optimal control for the nonlinear system of wind turbine that is modeled as a linear parameter varying (LPV) system. Some contributions in investigation on conditions to compute the ℓ_∞-gain of systems with parametric uncertainties or the upper bound can be found in the work of Rieber *et al.* (2006b) and Rieber *et al.* (2008). We briefly review on the nominal ℓ_1 performance analysis, to set the computational approaches into prospective. Also, conservative upper bound on ℓ_∞-gain is presented using LMI method. As part of our contribution in this study, we came up with new upper bound in the problem of computing ℓ_∞-gain. Although, the proposed upper bound may not

be less conservative compared to the so-called star norm or the one suggested in the work of Rieber (2007), the computation of our proposed upper bound is very efficient, so that it is suitable in some search-based optimizations of the controller based on ℓ_1 performance. In addition to computational efficiency, the new upper bound conveys the desired characteristics of the ℓ_∞-gain. In an example, we have studied our new method for computation of ℓ_∞-gain using a discrete-time state-space model of an aircraft system.

1.3.1 ℓ_1-Optimal Controller Synthesis

ℓ_1 control problem was formulated in Barabanov and Granichin (1984) and Vidyasagar (1986). The standard ℓ_1 control problem formulation treats finite-dimensional discrete-time LTI plant G as described in the following development. Consider the state-space realization

$$\begin{bmatrix} x(k+1) \\ z(k) \\ y(k) \end{bmatrix} = \begin{bmatrix} A & B_1 & B_2 \\ C_1 & D_{11} & D_{12} \\ C_2 & D_{21} & D_{22} \end{bmatrix} \begin{bmatrix} x(k) \\ w(k) \\ u(k) \end{bmatrix} \tag{1.4}$$

where $x(k) \in \mathbb{R}^n$ is the states vector, $y(k) \in \mathbb{R}^{n_y}$ is the measurement input, and $w(k) \in \mathbb{R}^{n_w}$is the disturbance input. Also, it is assumed that (A, B_2) is stabilizable and (A, C_2) is detectable that is necessary and sufficient for the existence of a stabilizing LTI output-feedback controller K with realization

$$\begin{bmatrix} x_K(k+1) \\ u(k) \end{bmatrix} = \begin{bmatrix} A_K & B_K \\ C_K & D_k \end{bmatrix} \begin{bmatrix} x_K(k) \\ y(k) \end{bmatrix} \tag{1.5}$$

Note that G is the closed-loop map from w to z. The control design goal is to find the internally stabilizing controller such that the closed-loop ℓ_1 performance $\|G\|_1$ is minimized. The well-known Youla Parameterisation (Youla *et al.* 1976) of all stabilising controllers can be used to convert the problem into a more tractable form. In Appendix A ,the Youla

Parameterisation is described in more detail. All asymptotically stable closed-loop transfer matrices are written as

$$\hat{G}(z) = \hat{H}(z) - \hat{U}(z)\hat{Q}(z)\hat{V}(z) \tag{1.6}$$

where $\hat{Q}$ is a free stable parameter, and $\hat{H}$, $\hat{U}$, and $\hat{V}$ are the fixed stable transfer matrices. Finally the standard ℓ_1 control problem can be formulated as a minimization problem

$$\gamma \coloneqq \inf_{Q \in \ell_1^{n_y \times n_u}} \|H - U * Q * V\|_1 \tag{1.7}$$

This optimization problem is an infinite-dimensional with infinitely many constraints. Some solutions to this problem can be found in Dahleh and Pearson (1987b), Diaz-bobillo and Dahleh (1993), Dorea and Hennet (1997), and Khammash (2000). We briefly discuss the Khammash Q -scaled method. All stable Q parameters can be parameterizad by infinite sequence $Q = \{Q(0), Q(1), Q(2), \dots\}$ corresponding to $\hat{Q} = Q(0) + Q(1)z^{-1} + Q(2)z^{-2} + \cdots$
A restriction on Q can be imposed to make the problem finite-dimensional. It can be assumed that $Q(k) = 0$ for $k > N$ and $\|Q\|_1 \leq \gamma_Q$ for some given N and γ_Q so that it leads to the suboptimal problem

$$\bar{\gamma}_N \coloneqq \inf_{Q \in \ell_1^{n_y \times n_u}} \|H - U * Q * V\|_1$$

$$s.t.\ Q(k) = 0 \text{ for } k > N \text{ and } \|Q\|_1 \leq \gamma_Q \tag{1.8}$$

In this solution of this suboptimal problem, $\bar{\gamma}_N$ is an upper bound on the ℓ_1-gain (Khammash, 2000).This problem can be transformed into a finite-dimensional LPs that allow computationally efficient controller synthesis. The main drawback of the approaches based on linear programing is that they result in high order controllers especially in larger-sized problems. Some practical application of ℓ_1 control can be found in Spillman and Ridgely (1997), Malaterro

and Khammash (2000), Rieber *et al.* (2005b). To the knowledge of the author, application of ℓ_1 framework in wind turbine control system is only investigated extensively in our report.

1.4 ℓ_1-Optimal Control of a LPV model of VS-VP Wind Turbine in the Transition Region

In control of the wind turbines, wind acting on the blades is an exogenous disturbance. Although, this disturbance is persistent and has infinite energy, it has bounded magnitude (Dahleh and Diaz-Bobillo 1995). In ℓ_1-optimal control, the ℓ_∞-norm is the criterion used to measure the input disturbances and output signals. Therefore, time-domain performance specifications like overshoot, bounded magnitude, bounded slope, and actuator saturation can be directly addressed (Schuler *et al.* 2010).

The fast-growing technology of large scale wind turbines demands control systems capable of enhancing both the efficiency of capturing wind power, and the useful life of wind turbines. There exists a transition region between the torque control strategy at low wind speed, and the pitch control strategy used at high wind speed. This study treats the problems of ensuring smooth transition between these strategies, and capturing maximum power around the nominal operating point in transition region. Control based on $\boldsymbol{\ell_1}$-norm performance is an approach to deal with persistent exogenous disturbances like infinite energy ($\boldsymbol{\ell_2}$-norm) and bounded magnitudes ($\boldsymbol{\ell_1}$-norm) wind disturbances facing wind turbines. In addition, time-domain performance measures such as overshoot and actuator saturation can be directly addressed by $\boldsymbol{\ell_1}$-optimal control. In this work, a state-feedback controller is derived by means of a linear matrix inequality (LMI) solution of an upper bound on the $\boldsymbol{\ell_1}$-norm of the closed loop system. We developed a LPV model of variable-speed variable-pitch (VS-VP) wind turbine in the transition

region. This LPV model provides a suitable framework for a LMI approach. The LPV model results in a set of parameterized LMIs (PLMIs) with quadratic parameter dependence which are transformed into LMIs using a relaxation technique. Then, we tested the proposed parameter-dependent feedback controller with simulation of a simplified model of a 5MW wind turbine.

Over the operation range of wind turbines at different wind speeds, three regions can be identified. At low wind speeds (Region I), the wind turbine captures maximum power using torque control to track the optimum rotor speed. At high wind speeds (Region III), the wind turbine works at constant rotor speed and the power generation is kept constant at rated power by means of active pitch control. A transition region (Region II) exists near the rated wind speed where the controller switches between the maximum-power and rated-power regions. The transition region includes the nominal best operating point of the wind turbine realizing maximum extraction at the rated value of power. Therefore, in addition to smooth transition between Regions I and III, the power generation efficiency is an important control objective in the Region II. The wind turbine dynamics exhibit poor controllability around the nominal operating point, because of switching between the two different control systems at low and high wind speed regions (Bianchi *et al.* 2007). There are strategies that propose controllers for the entire range of operation. However, these strategies are potentially conservative. Here, we design a controller for transition region which satisfies the control objectives, *i.e.* maximum energy capture while rotor speed and generator torque do not exceed their rated values in the presence of wind gusts as external disturbances. This control allows a smooth transition between two separate controllers that are being designed for low and high wind speed regions.

In this work we drive a linear parameter varying (LPV) model of the nonlinear dynamics of a wind turbine in the transition region. This LPV model provides a second order

approximation of the derive-train dynamics, which is more accurate than a linear model because it is able to capture the extremum point that exists in the turbine's torque characteristics in the transition region. This eliminates the problem of poor controllability in the transition region. LPV wind turbine model was presented in Bianchi *et al.* (2007). In Rieber *et al.* (2005) and Rieber and Allgower (2003), the ℓ_1-optimal control designed in the framework of LPV systems.

Linear matrix inequalities (LMIs) are a well-established method in control to solve problems, which involve matrix variables. LMIs allow the efficient consideration of optimization criteria such as ℓ_1 and H_∞-constraints for performance and robustness in the design of controllers (Schuler and Weiland, 2004). In this study, we take the LMI approach to ℓ_1-optimal control problem to find an upper bound on ℓ_1-norm. In a few papers such as Abedor *et al.* (1996) and Khosravi and Jalali (2008), the LMI constraints on ℓ_1-norm are presented and the controllers are derived. ℓ_1-optimal control is first treated in the work of Dahleh and Diaz-Bobillo (1995) and Dahleh and Pearson (1987). A novel synthesis method was developed by Khammash (2000). To derive the feedback controller for a closed loop system with ℓ_1-optimal matrix inequalities, we used techniques and tools described in Turner *et al.* (2007) for transforming the matrix inequality problem into suitable LMI-format for solution.

1.5 Gain-Scheduled ℓ_1-Optimal Control of a VS-VP Wind Turbine at High Wind Speeds Using Genetic Algorithms

In order to alleviate mechanical load and improving the power quality, recent large-scale wind turbines operate with active pitch control combined with variable speed generator (Ackermann and Soder, 2002 and Gardner *et al.* 2003). In more simple control of variable-speed

variable-pitch (VS-VP) wind turbines, the generator torque and pitch angle are controlled separately. In low wind speed, the pitch angle is fixed while the torque control makes it possible for wind turbine to operate at variable speed to capture the maximum wind power. At high wind speeds, the pitch control limits the captured wind power and the rotor speed while the generator torque is unchanged (Constant torque strategy in Region III) (Bossanyi 2000). The constant torque in high wind speeds results in higher pitch activities for regulation of the generated power, so that it induces extra load in the components. Therefore, constant torque at high speeds does not fully exploit the capabilities of VSVP wind turbines.

In some works such as Leithead and Connor (2000), two independent feedback loops are designed to track the speed reference and the torque reference for the cases that both pitch control and generator torque are active simultaneously. However, this decentralized approach does not get optimal results. A multivariable or centralized approach in which the pitch angle and generator torque are involved simultaneously for an optimal control design, can perform better. In this report, we use the multivariable approach to design the pitch and torque controls in a ℓ_1 performance framework and using the gain-scheduling techniques for the LPV model of the wind turbine at high wind speeds (Region III).

1.5.1 Gain-Scheduling with Guaranteed Stability

In numerous applications in nonlinear systems, gain-scheduling has successfully been used. In this method, the linear model of nonlinear system is obtained at different operating points and linear controller is designed for each region of operation. Based on the value of scheduling parameters, the controllers are changed. However, there is a concern in stability and performance of system in switching between controllers. Some works have been performed to improve the stability and performance such as imposing certain dwell time (Hespanha and Morse

1999). The well-established linear parameter varying (LPV) systems theory can guarantee the stability and performance in the whole range of operation. The problem of this method is the computational effort needed to obtain the LPV controller that limits application of LPV to lower order systems. Also, all the controllers are designed simultaneously, so that the performance at design points may be degraded. In some applications, it is desired to design the optimal controller at each operating point independently (Bianchi and Pena 2011). Some work on the controllers designed independently can be found in Chang and Ramussen (2008), Stilwell and Rugh (2000), Blanchini *et al.* (2009), Hespanha and Morse (2002). Bianchi and Pena (2011) presented a methodology which considers the interpolation of LTI controllers designed for different operating points in order to produce a gain-scheduled controller. They formulated a stability-preserving interpolation scheme with a performance level guarantee in the state-space framework. In this study, we used the gain-scheduling technique proposed by Bianchi and Pena (2011) for interpolation of ℓ_1-optimal controllers designed for each wind turbine operating point at different wind speeds in Region III. We also established the measure of performance level in the interpolating points to the ℓ_1 performance case using LMIs as $\mathcal{H}_\infty$ performance case was the only one discussed in Bianchi and Pena (2011). In addition, we derived the equivalent stability criteria in terms of LMIs for discrete-time systems as in Bianchi and Pena (2011), the stability criteria was presented only for continues-time systems.

1.5.2 Control Optimization Using Genetic Algorithms

The optimal control problems of the type described above are generally solved numerically. The earlier numerical methods were based on finding a solution of the two-point boundary value problem given by the Euler-Lagrange equation which is necessary condition for optimality, or satisfies Hamilton-Jacobi-Bellman equation, which is sufficient condition of

optimality. These methods are called indirect methods. Some of the main drawbacks of indirect methods are given in Fabin (1996) and Fabin (1998). Most of recent works on optimal control problem, use direct methods, in which, the optimal solution is obtained by direct minimization of the performance index subject to constraints. The direct methods can be applied by using discretization technique or parameterization technique. However, the direct methods are less accurate than indirect method and sometimes have several minima (Fabin 1996 and Fabin 1998).

In ℓ_1-optimal control problems, the minimization problem of the ℓ_1-gain of the closed loop system can be transformed to a linear programing (LP) problem with efficient numerical solution as discussed in Kammash (2000). However, these LP approaches result in high order controllers that limits their practical applications (Rieber *et al*., 2007). Therefore, in this study we decided to use a search-based optimization such as genetic algorithms (GAs). In ℓ_1-optimal control problem, the optimization objective function is a nonlinear function with variables from parameterization of matrices in the state-space realization of output-feedback controller. Using GAs we can numerically solve the optimization problems with nonlinear objective functions and large number of variables. Another advantage of using GAs for ℓ_1-optimal control problem is that we can arbitrarily choose the order of the output-feedback controller based on our desired control performance. Some works such as Abo-Hammour *et al.* (2011) are useful for the solution of optimal control problems using GAs.

As described in Goldberg (1989), Sakar and Modak (2004), Sim *et al.* (2000), Davidor (1991), and Abo-Hammour *et al.* (2002), Genetic Algorithms (GAs) can be distinguished from other calculus-based and enumerative methods for optimization. In GAs, a population of individuals are used for searching the optimal solution. This population –based nature of GAs has two main advantages. First, GAs can be implemented on parallel machines, which reduces

the CPU time required for finding the optimal solution. Second, information concerning different regions of the solution space is passed actively between individuals by crossover procedure that makes GA a robust optimization method for optimization of nonlinear functions with many variables. The memory space occupied is proportional to the size of population in GAs that is a drawback of GAs. In addition, because of the large computational effort that is required for some optimization problems using GAs, especially in sequential machines, these methods may be disadvantageous in real time applications. But in off-line solutions, such as the ℓ_1-optimal control of wind turbines that we are interested in, the accuracy of the solution is much more important than the time required for the solution.

1.5.3 Basic Description of Genetic Algorithm

Genetic algorithms (GAs) are inspired by natural evolution. The first step of many genetic algorithms starts with a set of solutions (chromosomes) called a population. Using GA operators (such as mutation and crossover), a new set of solutions (offspring) are generated. The new solutions are selected based on their fitness. Therefore, more suitable solutions have more chance to reproduce. This process is repeated until some condition (for example, number of generations or improvement of the best solution) is satisfied. The basic GA can be summarised in the following steps:

1. Generation of random population of n solutions (chromosomes). Often, a binary string is used for encoding of chromosomes. The whole string can represent a number or each bit can represent some characteristic of the solution.
2. Evaluation of the fitness, $f(x)$, of each chromosome x in the population.
3. A new population is created by repeating following steps 3.1 to 3.4 until the new population is complete.

3.1 Selection of two parent chromosomes from a population, so that the ones with better fitness have higher probability of being chosen. Roulette wheel selection and rank selection are two examples of many methods for selection of best chromosomes.

3.2 Crossing over the parent chromosomes to form a new offspring with a crossover probability. If no crossover was performed, the offspring is an exact copy of the parents. The simplest way to realize a crossover is to choose randomly some crossover point and copy from one parent everything before this point and then copy from the second parent everything after a crossover point. Also, there are multi-point crossover methods.

3.3 After a crossover is performed, mutation takes place. Mutation is made to prevent the GA from falling into a local extreme. With a chosen mutation probability, mutation randomly changes the new offspring. For binary encoding, we can switch a few randomly chosen bits from 1 to 0 or from 0 to 1.

3.4 Place the new offspring in the new population. There is a high chance of losing the best chromosome when creating a new population by crossover and mutation. In order to keep best solutions, the best chromosome (or a few best chromosomes) is first copied to the new population. (Elitism)

4 The new complete population is used for a further run of the algorithm.

5 If the termination condition is satisfied, the algorithm is stopped and the best solution of last generation is returned.

6 If the termination condition is not satisfied, go to step 2.

1.6 Contributions of Thesis

The main contributions of thesis are

- Introducing ℓ_1-optimal control approach to deal with the wind disturbances and turbulence profiles in control of large VS-VP wind turbines.
- Providing literature review of control design for wind turbines and ℓ_1-optimal control problem. (Chapter 1 and 2)
- A Presentation of linear matrix inequality (LMI) solution of the ℓ_1-optimal control problem and obtaining optimal control for state-feedback control case.(Chapter 2 and 3)
- Proposing a new computationally efficient method for calculation of ℓ_1-norm.(Chapter 2)
- Developing a LPV model of aerodynamic and drive-train dynamics of a VS-VP wind turbine in the transition region (Chapter 3).
- Derivation of the LMIs for ℓ_1 performance in theorem 4.2 and presentation of theorem 4.1 for discrete-time systems. (Chapter 4)

1.7 Organization of Thesis

- Chapter 1: A comprehensive overview of wind turbine systems and literature review of control design for wind turbines and also overview of ℓ_1-optimal control are presented.
- Chapter 2: Different approaches for solution of ℓ_1-optimal control problem in the literature are presented. Linear matrix inequality (LMI) solution of the ℓ_1-optimal control problem is explained. As an example of the LMI approach, ℓ_1-optimal PI gains for a state-feedback

controlled system is obtained. We proposed a new computationally efficient method for calculation of ℓ_1-norm.

- Chapter 3: A novel LPV model of aerodynamic and drive-train dynamics of a VS-VP wind turbine in the transition region is developed and the state-space realization of the control system is presented. A state-feedback controller is derived based on ℓ_1 performance by minimizing the upper bound problem on the ℓ_1-norm using a LMI approach.
- Chapter 4: The linear model of a wind turbine is derived at different operating points in Region III (the rated power region at high wind speeds). Next, we find local output feedback controllers at each operating point. The local controllers are optimized based on ℓ_1 performance using genetic algorithm method. Finally, a gain-scheduling technique with guaranteed stability is presented in order to interpolate the local controllers.
- Chapter 5: The proposed gain-scheduled ℓ_1-Optimal control is validated by implementing the controller on the FAST wind turbine simulation software and the ℓ_1 controller is compared with a well-tuned PI controller.
- Chapter 6: The summary of thesis and a few suggestions for future work are presented.

Chapter 2: ℓ_1-Optimal Control Synthesis

In this chapter, ℓ_1-optimal control is introduced and the linear matrix inequality (LMI) solution of the ℓ_1-optimal control problem is presented. As an example of the LMI approach, we obtain ℓ_1-optimal PI gains for a state-feedback controlled system. Then, methods found in the literature for calculation of the ℓ_1-norm and its upper and lower bounds are detailed. Next, we propose a computationally efficient method for calculation of ℓ_1-norm. Finally, using an aircraft model, we compared the accuracy and computation speed of our new method for calculation of ℓ_1-norm with some standard methods found in the literature. Also, in the aircraft example, we design optimal controllers for the system based on ℓ_1-performance, $\mathcal{H}_2$- performance, and $\mathcal{H}_\infty$-performance and then we simulate the closed-loop system responses.

2.1 Introduction to ℓ_1-Optimal Control

Consider an LTI discrete-time system, P, with state-space description

$$\begin{bmatrix} x(k+1) \\ z(k) \\ y(k) \end{bmatrix} = \begin{bmatrix} A & B_1 & B_2 \\ C_1 & D_{11} & D_{12} \\ C_2 & D_{21} & D_{22} \end{bmatrix} \begin{bmatrix} x(k) \\ w(k) \\ u(k) \end{bmatrix} \tag{2.1}$$

where $x \in \mathbb{R}^n$ denotes states and $w \in \mathbb{R}^{q_1}$ defines reference signals and disturbances. $u \in \mathbb{R}^{q_2}$ is the control input, $z \in \mathbb{R}^{p_1}$ is the performance output, and $y \in \mathbb{R}^{p_2}$ is the measurement. Assumptions in this description are stabilizability of the pair $(A\,, B_1)$ and detectability of the pair (C_2, A). The exogenous disturbances belong to ℓ_∞^n, which is the space of vector-valued bounded signals $s = \{s(k), k \geq 0\}$ with $s(k) = [s_1(k), \dots, s_n(k)]^T$ and the norm

$$\|s\|_\infty := max_{1\le i\le n} \sup_k |s_i(k)| \tag{2.2}$$

This means that the signals in this space have finite amplitude but not necessarily finite energy. Also, the space of matrix-valued right-sided absolutely summable real sequences is denoted by $\ell_1^{m\times n}$, with a norm

$$\|s\|_1 := \max_{1\le i\le m} \sum_{j=1}^{n} \sum_{k=0}^{\infty} \left|s_{ij}(k)\right| \tag{2.3}$$

To measure the worst-case signal amplification, the ℓ_∞-gain between input w and the output z of a system is introduced, which is the ℓ_∞-induced norm of the system operator $T : \ell_\infty^n \to \ell_\infty^m$, defined by

$$\|T\|_{\infty-ind} := \sup_{w\in\ell_\infty, w\neq 0} \frac{\|Tw\|_\infty}{\|w\|_\infty} \tag{2.4}$$

For an LTI operator or transfer function, the ℓ_∞-induced norm is the ℓ_1-norm of its impulse response matrix. The ultimate purpose of ℓ_1-optimal control is to find an LTI controller K, that stabilizes the closed-loop transfer function and minimizes the ℓ_∞-norm. K is the argument of the optimization objective function resulting in the smallest size of transfer function as

$$\gamma^* := \inf_K \|T(P,K)\|_1 \tag{2.5}$$

where $T(P,K)$ is the closed loop $p_1 \times q_1$ impulse response matrix.

2.2 LMI Solution of the ℓ_1-Optimal Control Problem

A well-known approach to ℓ_1-optimal control is using LMIs to find an upper bound on the ℓ_1-norm. Considering the system

$$\begin{cases} \dot{x} = Ax + Bw \\ z = Cx + Dw \end{cases} \tag{2.6}$$

where $x \in \mathbb{R}^n$ is the state, and $w \in \mathbb{R}^{q_1}$ is the input and $z \in \mathbb{R}^{p_1}$ is the output. Assuming T_{wz} is the transfer function that defines a mapping from bounded amplitude inputs $w \in \ell_\infty$ to the bounded amplitude outputs $z \in \ell_\infty$, then a relevant ℓ_1 performance criterion is the peak-to-peak or ℓ_∞-induced norm of this transfer function

$$\|T_{wz}\|_{\infty-ind} \coloneqq \sup_{0<\|w\|_\infty<\infty} \frac{\|z\|_\infty}{\|w\|_\infty} \tag{2.7}$$

An upper bound, γ, of the peak-to-peak gain is given in Scherer and Weiland (2004) and Khosravi and Jalali (2008). The matrix inequality constraints in the following theorem are used to find the upper bound γ for the system with state-space realization Eq. (2.6).

Theorem 2.1: *If there exists* $X > 0$, $\lambda > 0$, *and* $\mu > 0$ *such that*

$$\begin{bmatrix} A^T X + XA + \lambda X & XB \\ B^T X & -\mu I \end{bmatrix} < 0 \tag{2.8}$$

$$\begin{bmatrix} \lambda X & 0 & C^T \\ 0 & (\gamma - \mu) I & D^T \\ C & D & \gamma I \end{bmatrix} > 0 \tag{2.9}$$

then the peak-to-peak or ℓ_∞*-induced norm of the system is smaller than* γ, *i.e.* $\|T_{wz}\|_{\infty-ind} < \gamma$.

Because of conservatism, the inverse of the theorem is not true. λX is the only non-linear term in the matrix inequalities (2.8) and (2.9). To overcome this problem for a fixed $\lambda > 0$, we test whether the resulting LMIs are feasible; if yes, the bound γ on the peak-to-peak norm has been assured; if the LMIs are not feasible, we choose another $\lambda > 0$ and repeat the test (Scherer and Weiland, 2004).

It is advantageous to find the best possible (least conservative) upper bound on the peak-to-peak norm. For this purpose, a line-search over $\lambda > 0$ to minimize $\gamma^*(\lambda)$ (the minimum value of γ if $\lambda > 0$ is held fixed) is performed. Minimizing $\gamma^*(\lambda)$ subject to LMI constraints leads to a

convex optimization problem with extensive and efficient solutions. The line-search leads to the best achievable upper bound

$$\gamma^u = \inf_{\lambda>0} \gamma^*(\lambda) \tag{2.10}$$

A lower bound on the peak-to-peak norm is the $\mathcal{H}_\infty$-norm. The conservatism of the proposed LMI method can be estimated by calculating the $\mathcal{H}_\infty$-norm of the transfer function from w to z, *i.e.* $\|T_{wz}\|_\infty$. This minimal achievable $\mathcal{H}_\infty$-norm denoted by γ^l. The actual optimal peak-to-peak gain must be in the interval $[\gamma^l, \quad \gamma^u]$ and a small interval suggests that the upper bound is close to the actual peak-to-peak gain (Scherer and Weiland, 2004). In Sec. 2.3, we present an example of control design using the LMI approach. Also, in Ch. 3, we derive the state feedback controller for a wind turbine system using the LMI approach presented in this section.

2.3 Obtaining ℓ_1-Optimal PI Gains for a State-Feedback Controlled System Using the LMI Approach

We can derive the optimal proportional (P) and integral (I) gains for a state feedback controlled system to optimize the ℓ_1 performance of the closed-loop system using the LMIs of Theorem 2.1. In this section, we present a procedure to transform the optimal control design problem to an optimization problem with LMI constraints. Consider the system

$$\begin{cases} \dot{x} = Ax + B_1 w + B_2 u \\ z = C_1 x + D_{12} u \\ y = C_2 x + D_{21} w \end{cases} \tag{2.11}$$

In the realization (2.11), we assumed that $D_{11} = 0$ and $D_{22} = 0$.This assumption applies to many practical problems as it means that the performance measure is not subject to exogenous signals

(such as noise) and there is no direct feed through of the control inputs to the measured outputs. We consider a feedback control rule which composed of proportional and integral of states

$$u = K_P x + K_I \int x\, dt \tag{2.12}$$

where, u is the control input, x is the vector of states, K_P is the proportional gain, and K_I is the integral gain. We define a new state-space realization of the closed loop system with augmented states as expressed below

$$x_1 = x \quad , \quad x_2 = \int x\, dt \quad , \quad \Omega = \begin{bmatrix} x_1 \\ x_2 \end{bmatrix} \tag{2.13}$$

Closed loop system:

$$\begin{cases} \dot{\Omega} = \begin{bmatrix} A + B_2 K_P & B_2 K_I \\ I & 0 \end{bmatrix} \Omega + \begin{bmatrix} B_1 \\ 0 \end{bmatrix} w \\ z = [C_1 + D_{12} K_P \quad D_{12} K_I] \Omega \end{cases} \tag{2.14}$$

By substituting the closed-loop matrices in the LMIs of Theorem 2.1, the ℓ_1-optimal control problem for a system with PI control can be stated in terms of the matrix inequalities below

$$\begin{bmatrix} \begin{bmatrix} A + B_2 K_P & B_2 K_I \\ I & 0 \end{bmatrix}^T X + X \begin{bmatrix} A + B_2 K_P & B_2 K_I \\ I & 0 \end{bmatrix} + \lambda X & X \begin{bmatrix} B_1 \\ 0 \end{bmatrix} \\ \begin{bmatrix} B_1 \\ 0 \end{bmatrix}^T X & -\mu I \end{bmatrix} < 0 \tag{2.15}$$

$$\begin{bmatrix} \lambda X & 0 & [C_1 + D_{12} K_P \quad D_{12} K_I]^T \\ 0 & (\gamma - \mu) I & 0 \\ [C_1 + D_{12} K_P \quad D_{12} K_I] & 0 & \gamma I \end{bmatrix} > 0 \tag{2.16}$$

Assuming a matrix structure, $X = \begin{bmatrix} X_1 & 0 \\ 0 & X_1 \end{bmatrix}$, at the expense of some conservatism, we can simplify the inequalities (2.15) and (2.16) as

$$\begin{bmatrix} A^T X_1 + X_1 A + K_P^T B_2^T X_1 + X_1 B_2 K_P + \lambda X_1 & X_1 B_2 K_I + X_1 & X_1 B_1 \\ K_I^T B_2^T X_1 + X_1 & \lambda X_1 & 0 \\ B_1^T X_1 & 0 & -\mu I \end{bmatrix} < 0 \tag{2.17}$$

$$\begin{bmatrix} \lambda X_1 & 0 & 0 & C_1^T + K_P^T D_{12}^T \\ 0 & \lambda X_1 & 0 & K_I^T D_{12}^T \\ 0 & 0 & (\gamma - \mu)I & 0 \\ C_1 + D_{12}K_P & D_{12}K_I & 0 & \gamma I \end{bmatrix} > 0 \qquad (2.18)$$

The following Schur complement lemma is used to transform matrix inequalities (2.17) and (2.18) to LMIs.

Lemma 2.1: *The inequalities:*

$$R(x) > 0 \ (< 0) \ , Q(x) - S(x)R(x)^{-1}S(x)^T > 0 \qquad (< 0) \qquad (2.19)$$

are equivalent to the LMI:

$$\begin{bmatrix} Q(x) & S(x) \\ S(x)^T & R(x) \end{bmatrix} > 0 \qquad (< 0) \qquad (2.20)$$

Using Lemma 2.1, we can rewrite Eq.(2.17) in the form

$$\begin{bmatrix} A^T X_1 + X_1 A + K_P^T B_2^T X_1 + X_1 B_2 K_P + \lambda X_1 + \frac{1}{\mu} X_1 B_1 B_1^T X_1 & X_1 B_2 K_I + X_1 \\ K_I^T B_2^T X_1 + X_1 & \lambda X_1 \end{bmatrix} < 0 \quad (2.21)$$

Using the fact that if $\Phi > 0$ (positive definite), then $X\Phi X > 0$, and also assuming $X_1 > 0$, then multiplying the both sides of the inequality (2.21) by $\begin{bmatrix} X_1^{-1} & 0 \\ 0 & X_1^{-1} \end{bmatrix} > 0$, where $Y = X_1^{-1}$, we obtain

$$\begin{bmatrix} YA^T + AY + YK_P^T B_2^T + B_2 K_P Y + \lambda Y + \frac{1}{\mu} B_1 B_1^T & B_2 K_I Y + Y \\ YK_I^T B_2^T + Y & \lambda Y \end{bmatrix} < 0 \qquad (2.22)$$

Using the Schur complement Lemma 2.1 again, we can rewrite Eq. (2.22) as

$$\begin{bmatrix} YA^T + AY + YK_P^T B_2^T + B_2 K_P Y + \lambda Y & B_2 K_I Y + Y & B_1 \\ YK_I^T B_2^T + Y & \lambda Y & 0 \\ B_1^T & 0 & -\mu I \end{bmatrix} < 0 \qquad (2.23)$$

Using Schur complement Lemma 2.1, we can rewrite Eq. (2.18) as

$$\begin{bmatrix} \lambda X_1 - \frac{1}{\gamma}(C_1^T + K_P^T D_{12}^T)(C_1 + D_{12}K_P) & -\frac{1}{\gamma}(C_1^T + K_P^T D_{12}^T)(D_{12}K_I) \\ -\frac{1}{\gamma}(K_I^T D_{12}^T)(C_1 + D_{12}K_P) & \lambda X_1 - \frac{1}{\gamma}(K_I^T D_{12}^T)(D_{12}K_I) \end{bmatrix} > 0 \quad and\, \gamma > \mu \quad (2.24)$$

Multiplying both sides of the first inequality in Eq. (2.24) by $\begin{bmatrix} X_1^{-1} & 0 \\ 0 & X_1^{-1} \end{bmatrix} > 0$, where $Y = X_1^{-1}$, we obtain

$$\begin{bmatrix} \lambda Y - \frac{1}{\gamma}(YC_1^T + YK_P^T D_{12}^T)(C_1 Y + D_{12}K_P Y) & -\frac{1}{\gamma}(YC_1^T + YK_P^T D_{12}^T)(D_{12}K_I Y) \\ -\frac{1}{\gamma}(YK_I^T D_{12}^T)(C_1 Y + D_{12}K_P Y) & \lambda Y - \frac{1}{\gamma}(YK_I^T D_{12}^T)(D_{12}K_I Y) \end{bmatrix} > 0 \quad (2.25)$$

Using Lemma 2.1, we obtain

$$\begin{bmatrix} \lambda Y & 0 & 0 & YC_1^T + YK_P^T D_{12}^T \\ 0 & \lambda Y & 0 & YK_I^T D_{12}^T \\ 0 & 0 & (\gamma - \mu)I & 0 \\ C_1 Y + D_{12}K_P Y & D_{12}K_I Y & 0 & \gamma I \end{bmatrix} > 0 \quad (2.26)$$

Defining new variables $H = K_P Y$ and J=$K_I Y$, we can rewrite Eqs. (2.23) and (2.26) as given in Eqs. (2.27) and (2.28), respectively.

$$\begin{bmatrix} YA^T + AY + H^T B_2^T + B_2 H + \lambda X_1 & B_2 J + Y & B_1 \\ J^T B_2^T + Y & \lambda Y & 0 \\ B_1^T & 0 & -\mu I \end{bmatrix} < 0 \quad (2.27)$$

$$\begin{bmatrix} \lambda Y & 0 & 0 & YC_1^T + H^T D_{12}^T \\ 0 & \lambda Y & 0 & J^T D_{12}^T \\ 0 & 0 & (\gamma - \mu)I & 0 \\ C_1 Y + D_{12}H & D_{12}J & 0 & \gamma I \end{bmatrix} > 0 \quad (2.28)$$

The LMI minimization problem setup for obtaining a state-feedback PI-controller with ℓ_1-optimal criterion, is summarized in the following optimization problem

Optimization problem:

$$Find\ \min(\gamma)\ \ s.t.$$

$$Y > 0, \qquad \lambda > 0, \qquad \mu > 0, \qquad \gamma > \mu$$

$$\begin{bmatrix} YA^T + AY + H^T B_2^T + B_2 H + \lambda Y & B_2 J + Y & B_1 \\ J^T B_2^T + Y & \lambda Y & 0 \\ B_1^T & 0 & -\mu I \end{bmatrix} < 0$$

$$\begin{bmatrix} \lambda Y & 0 & 0 & YC_1^T + H^T D_{12}^T \\ 0 & \lambda Y & 0 & J^T D_{12}^T \\ 0 & 0 & (\gamma - \mu) I & 0 \\ C_1 Y + D_{12} H & D_{12} J & 0 & \gamma I \end{bmatrix} > 0 \qquad (2.29)$$

where, $X,\ \lambda,\ \mu,\ \gamma, H\ and\ J$ are variables and the PI gains can be obtained by the relations

$$K_P = HY^{-1}\ \ ,\ \ \ K_I = JY^{-1} \qquad (2.30)$$

The only term that has multiplication of two variables is λY. To solve this problem and having all the inequalities linear, we perform a line-search over $\lambda > 0$ to minimize $\gamma^*(\lambda)$, (the minimum value of γ) if $\lambda > 0$ is held fixed; Note that calculation of $\gamma^*(\lambda)$ indeed amounts to solving a LMI problem. The line-search leads to the best achievable upper bound.

2.4 Computing ℓ_1-Norm and its Upper and Lower Bounds for Discrete-Time Systems

Suppose a discrete-time LTI system of dimention $p_1 \times q_1$ without uncertainties has the impulse response $G = \{G(0), G(1), \dots\}$. From a state-space realization

$$\begin{bmatrix} x(k+1) \\ z(k) \end{bmatrix} = \begin{bmatrix} A & B \\ C & D \end{bmatrix} \begin{bmatrix} x(k) \\ w(k) \end{bmatrix} \qquad (2.31)$$

with $n_x = \dim(x)$, the Markov parameters of the impulse response are computed as

$$G(k) = \begin{cases} D & for\ k = 0 \\ CA^{k-1}B & for\ k \geq 1 \end{cases} \qquad (2.32)$$

Then, the ℓ_∞-gain is obtained as the ℓ_1-norm of G, *i.e.*

$$\|G\|_1 \coloneqq \max_{1\le i\le p_1} \sum_{j=1}^{q_1}\sum_{k=0}^{\infty}\left|G_{ij}(k)\right| =$$

$$\max_{1\le i\le p_1} \sum_{j=1}^{q_1}\sum_{k=0}^{N}\left|G_{ij}(k)\right| + \max_{1\le i\le p_1} \sum_{j=1}^{q_1}\sum_{k=N+1}^{\infty}\left|G_{ij}(k)\right| = \gamma^N + \gamma^{r,N} \qquad (2.33)$$

Due to the sub-additive property of the max-operator, where $G_{ij}(k)$ are the components of the matrix $G(k)$. By construction we can state that $\gamma^{r,N} > 0$ and

$$\gamma^N \le \|G\|_1 \le \gamma^N + \gamma^{r,N} \qquad (2.34)$$

The value of $\|G\|_1$ is approximated by truncation as $\|G\|_1 \approx \gamma^N$ provided that $\gamma^{r,N}$, which is the ℓ_1-norm of the truncated remainder is sufficiently small.

2.4.1 Star-Norm Performance

To compute the ℓ_∞-gain of the system G, one has to obtain the impulse response of G. Since getting the solution may be computationally expensive, another possibility is to use cheaper upper bounds. To this end, a linear matrix inequality condition is introduced to characterize the so-called star-norm and hence to determine an upper bound on the peak induced norm (Rieber *et al*., 2007).

Theorem 2.2*: Consider the system G with the realization above, and $x(k) = 0$. Suppose there exist $\mu > 0, 0 < \lambda < 1$, and $X = X^T$ satisfing*

$$\begin{bmatrix} A^TXA - \lambda X & A^TXB \\ B^TXA & B^TXB - \mu I \end{bmatrix} < 0, \qquad (2.35)$$

$$\begin{bmatrix} (\lambda-1)X + C^TC & C^TD \\ D^TC & (\mu-\gamma^2)I + D^TD \end{bmatrix} < 0 \qquad (2.36)$$

then

- $\|z\|_{peak} < \gamma$ *for* $\|w\|_{peak} \leq 1$, *and moreover* $\|G\|_{peak-ind} < \gamma$,
- $\|G\|_1 < \gamma\sqrt{q_1}$, *and*
- *A has all its eigenvalues in the open unit disk.*

The value γ appearing in Theorem 2.2 is an upper bound on the system's peak-induced norm. The smallest achievable γ is called the star norm $\|G\|_*$ of G. Mathematically speaking, $\|G\|_* \coloneqq \inf_{\mu,\gamma,X} \gamma$ such that $\mu > 0, 0 < \lambda < 1$, hold. Hence $\|G\|_{peak-ind} \leq \|G\|_*$ and

$$\|G\|_1 \leq \sqrt{q_1}\|G\|_{peak-ind} \leq \sqrt{q_1}\|G\|_* \tag{2.37}$$

2.4.2 Computing an Upper Bound on the ℓ_1-Norm of an Impulse Response Tail

In this section, we present the method in Rieber *et al*. (2007) for computing an upper bound on ℓ_1-norm. To compute an upper on $\gamma^{r,N}$, one can use Theorem 2.2. To this end, observe that the impulse response tail $G_{r,N} \coloneqq \{G(N+1), G(N+2), \dots\}$ is the impulse response of

$$\begin{bmatrix} x_r(k+1) \\ z_r(k) \end{bmatrix} = \begin{bmatrix} A & A^{N+1}B \\ C & CA^NB \end{bmatrix} \begin{bmatrix} x_r(k) \\ w_r(k) \end{bmatrix} \tag{2.38}$$

Hence $\gamma^{r,N} = \left\|G_{r,N}\right\|_1$ is the upper-bounded by using a star-norm computation as follows

Corollary 2.1*: Consider the system with the realization of Eq. (2.38) and* $x(0) = 0$. *Suppose there exist* $\mu > 0, 0 < \lambda < 1$, *and* $X = X^T$ *satisfing*

$$\begin{bmatrix} A^TXA - \lambda X & A^TXA^{N+1}B \\ (A^{N+1}B)^TXA & (A^{N+1}B)^TXA^{N+1}B - \mu I \end{bmatrix} < 0 \tag{2.39}$$

$$\begin{bmatrix} (\lambda-1)X + C^TC & C^TCA^NB \\ (CA^NB)^TC & (\mu - (\eta^N)^2)I + (CA^NB)^TCA^NB \end{bmatrix} < 0 \tag{2.40}$$

Then, $\gamma^{r,N} < \eta^N \sqrt{q_1}$, and A has its eigenvalues in the open unit disk.

2.5 A New Computationally Efficient Method for Computing ℓ_1-Norm

The following is a novel method for computing the ℓ_1-norm of a discrete time system which will be shown to be computationally efficient. Consider the discrete-time LTI system in Eq. (2.31). Using a linear matrix transformation, T, which is composed of the eigenvectors corresponding to the eigenvalues of matrix A , we can decouple the system so that

$$x = TX \tag{2.41}$$

$$\begin{cases} \dot{X} = (T^{-1}AT)X + (T^{-1}B)w \\ z = (CT)X + Dw \end{cases} \tag{2.42}$$

where, $A_t = (T^{-1}AT) = \begin{bmatrix} \lambda_1 & \cdots & 0 \\ \vdots & \ddots & \vdots \\ 0 & \cdots & \lambda_n \end{bmatrix}_{n\times n}$ is a diagonal matrix, $B_t = (T^{-1}B)|_{n\times q_1}$, $C_t = (CT)|_{p_1\times n}$, and $D_t = D|_{p_1\times q_1}$. Note that the eigenvalues and the transformation matrix, T, may have complex entries. We also assume that T is not singular and inverse matrix is available. Therefore, we should have non-repeating eigenvalues as the condition of using this method. The closed-loop system has impulse response $G_t(k) = \{G_t(0), G_t(1), \dots\}$. The Markov parameters of the impulse response are computed as

$$G_t(k) = \begin{cases} D_t & for\ k = 0 \\ C_t A_t^{k-1} B_t & for\ k \geq 1 \end{cases} \tag{2.43}$$

Then, the ℓ_1-norm of G_t is

$$\|G_t\|_1 \coloneqq \max_{1\leq i\leq p_1} \sum_{j=1}^{q_1} \sum_{k=0}^{\infty} \left| G_{t_{ij}}(k) \right| \tag{2.44}$$

for $k \geq 1$,

$$G_{t_{ij}}(k) = [C_{t_{i1}} \quad \cdots \quad C_{t_{in}}] \begin{bmatrix} \lambda_1 & \cdots & 0 \\ \vdots & \ddots & \vdots \\ 0 & \cdots & \lambda_n \end{bmatrix}^{k-1} \begin{bmatrix} B_{t_{1j}} \\ \vdots \\ B_{t_{nj}} \end{bmatrix} = C_{t_{i1}} \lambda_1^{k-1} B_{t_{1j}} + \cdots + C_{t_{in}} \lambda_n^{k-1} B_{t_{nj}} \quad (2.45)$$

Using the inequality $|a+b| \leq |a| + |b|$, we obtain

$$\sum_{k=0}^{\infty} \left| G_{t_{ij}}(k) \right| = \left| \mathrm{D}_{\mathrm{t_{ij}}} \right| + \left| C_{t_{i1}} B_{t_{1j}} + \cdots + C_{t_{in}} B_{t_{nj}} \right| + \left| C_{t_{i1}} \lambda_1^1 B_{t_{1j}} + \cdots + C_{t_{in}} \lambda_n^1 B_{t_{nj}} \right| + \cdots \leq$$

$$\left| \mathrm{D}_{\mathrm{t_{ij}}} \right| + \left| C_{t_{i1}} B_{t_{1j}} \right| + \cdots + \left| C_{t_{in}} B_{t_{nj}} \right| + \left| C_{t_{i1}} \lambda_1^1 B_{t_{1j}} \right| + \cdots + \left| C_{t_{in}} \lambda_n^1 B_{t_{nj}} \right| + \cdots \leq$$

$$\left| \mathrm{D}_{\mathrm{t_{ij}}} \right| + \left| C_{t_{i1}} B_{t_{1j}} \right| (1 + |\lambda_1|^1 + |\lambda_1|^2 \ldots) + \cdots + \left| C_{t_{in}} B_{t_{nj}} \right| (1 + |\lambda_n|^1 + |\lambda_n|^2 \ldots) \quad (2.46)$$

For a stable system, $|\lambda_i| \leq 1, i = 1, \ldots, n$. The sum of the geometric sequences with infinite terms, $1 + |\lambda_i| + |\lambda_i|^2 + \cdots = \frac{1}{1-|\lambda_i|}$ for $|\lambda_i| \leq 1, i = 1, \ldots, n$. Therefore

$$\|G_t\|_1 \coloneqq \max_{1 \leq \mathrm{i} \leq \mathrm{p}_1} \sum_{j=1}^{q_1} \sum_{k=0}^{\infty} \left| G_{t_{ij}}(k) \right|$$

$$\leq \max_{1 \leq \mathrm{i} \leq \mathrm{p}_1} \left\{ \begin{array}{r} \left(\left| \mathrm{D}_{\mathrm{t_{i1}}} \right| + \cdots + \left| \mathrm{D}_{\mathrm{t_{iq_1}}} \right| \right) + \frac{\left| C_{t_{i1}} \right|}{1-|\lambda_1|} \left(\left| B_{t_{11}} \right| + \cdots + \left| B_{t_{1q_1}} \right| \right) + \cdots \\ + \frac{\left| C_{t_{in}} \right|}{1-|\lambda_n|} \left(\left| B_{t_{n1}} \right| + \cdots + \left| B_{t_{nq_1}} \right| \right) \end{array} \right\}$$

(2.47)

The linear transformation does not change the transfer function, *i.e.* $G = G_t$. Therefore, $\|G_t\|_1 = \|G\|_1$. In fact, the relation (2.47) can be used for calculation of the upper bound on the ℓ_1-norm. In this new method, we can avoid the calculation of the series with infinite terms as in Eq. (2.33) to calculate the ℓ_1-norm of the system. The number of terms which should be calculated for a reasonable approximation of the ℓ_1-norm in Eq. (2.33) depends on the dynamics of the system and the sampling time of the discrete-time system. For high sampling rates, approximation of ℓ_1-norm requires a larger number of the series terms in the Eq. (2.33) to

be summed. Therefore, the Eq. (2.33) for calculation of ℓ_1-norm for high sampling rates is computationally expensive, whereas the upper bound which we proposed in relation (2.47), is independent of sampling rate and is computationally efficient. In the following example, we compare the accuracy and computation time of our proposed method and the truncated series for ℓ_1-norm computation.

Suppose that the state-space realization (2.31) represents a feedback controlled closed-loop system. Then, the system parameters $B_{t_{ij}}, C_{t_{ij}}, \mathrm{D_{t_{ij}}}, \lambda_i$ in the relation (2.47), are functions of feedback control parameters in K. In order to optimize the controller parameters (K) based on the ℓ_1 performance, the upper bound in Eq. (2.47) can be used as the objective function of optimization and the feedback control parameters are the variables of the optimization. The computationally efficient objective function allows us to use search-based optimization methods such as genetic algorithms (GAs). In Ch. 4, we use GAs to design ℓ_1-optimal control for a wind turbine system. Therefore, the minimization problem can be summarized below

Minimization Problem

$$\text{Find } \min_{K} \gamma(K) \quad \text{S.t. } |\lambda_i| \le 1 \ , \ i = 1, \dots, n \tag{2.48}$$

$$\gamma(K) = \max_{1 \le i \le p_1} \left\{ \begin{array}{r} \left(\left|\mathrm{D_{t_{i1}}}\right| + \cdots + \left|\mathrm{D_{t_{iq_1}}}\right|\right) + \frac{\left|C_{t_{i1}}\right|}{1-|\lambda_1|}\left(\left|B_{t_{11}}\right| + \cdots + \left|B_{t_{1q_1}}\right|\right) + \cdots \\ + \frac{\left|C_{t_{in}}\right|}{1-|\lambda_n|}\left(\left|B_{t_{n1}}\right| + \cdots + \left|B_{t_{nq_1}}\right|\right) \end{array} \right\} \tag{2.49}$$

$$\|G\|_1 \le \gamma(K) \tag{2.50}$$

This constrained optimization problem can be converted to an unconstrained problem using penalty methods, *e.g.*, adding a penalty term such as $W_i u(|\lambda_i| - 1)\ \ i = 1, \dots, n,$ where $u(t) = \begin{cases} 1 & t \geq 0 \\ 0 & t < 0 \end{cases}$ and W_i is the penalty weight, to the objective function in Eq. (2.49). Therefore, for the control parameters which the closed-loop system is unstable *i.e.* $|\lambda_i| \geq 1$, a large constant is added to the objective function as penalty.

2.6 Example: ℓ_1-Optimal Control Design for an Aircraft Model Using Genetic Algorithm

In this example, we use our proposed method of Sec. 2.5 for calculation of an upper bound on ℓ_1-norm. We consider an output feedback dynamic controller for the aircraft system and then we optimize the controller using GA method. We also use the truncated series, γ^N, in Eq. (2.33) to compute the ℓ_1-norm. We compared the accuracy and the computation speed for calculation of ℓ_1-norm. We obtained the first order, second order, and third order dynamic output feedback controllers for the aircraft model using the two methods .The results for the first-order controller are given in Figs. 2.1-2.3.

The discrete-time state space realization of the aircraft model is listed below

$$X = \begin{bmatrix} \alpha \\ \dot{\theta} \\ \gamma \end{bmatrix} = \begin{bmatrix} Angle\ of\ attack \\ Pitch\ rate \\ Flight\ path\ angle \end{bmatrix}, \qquad u = \begin{bmatrix} \delta_e \\ \delta_f \end{bmatrix} = \begin{bmatrix} Elevator \\ Flaperon \end{bmatrix}, \qquad w = \begin{bmatrix} w_\alpha \\ w_{\dot{\theta}} \\ w_\gamma \\ v_{x_1} \\ v_{x_2} \end{bmatrix}$$

$$A = \begin{bmatrix} 0.9866 & 0.0099 & 0 \\ 0.4322 & 0.913 & 0 \\ 0.013 & 0.0001 & 1 \end{bmatrix}, B_1 = \begin{bmatrix} 0.01 & 0 & 0 & 0 & 0 \\ 0 & 0.1 & 0 & 0 & 0 \\ 0 & 0 & 0.01 & 0 & 0 \end{bmatrix}, \qquad B_2 = \begin{bmatrix} -0.0017 & -0.0025 \\ -0.1725 & -0.0158 \\ 0.0017 & 0.0025 \end{bmatrix},$$

$$C_1 = \begin{bmatrix} 0 & 0 & 1 \\ 0 & 0 & 0 \\ 0 & 0 & 0 \end{bmatrix}, \quad D_{11} = \begin{bmatrix} 0 & 0 & 0 & 0 & 0 & 0 \\ 0 & 0 & 0 & 0 & 0 & 0 \\ 0 & 0 & 0 & 0 & 0 & 0 \end{bmatrix}, \quad D_{12} = \begin{bmatrix} 0 & 0 \\ 0.25 & 0 \\ 0 & 0.25 \end{bmatrix},$$

$$C_2 = \begin{bmatrix} 1 & 0 & 0 \\ 0 & 1 & 0 \\ 0 & 0 & 1 \end{bmatrix}, D_{21} = \begin{bmatrix} 0 & 0 & 0 & 0.2 & 0 & 0 \\ 0 & 0 & 0 & 0 & 0.1 & 0 \\ 0 & 0 & 0 & 0 & 0 & 0.2 \end{bmatrix}, \; D_{22} = \begin{bmatrix} 0 & 0 \\ 0 & 0 \\ 0 & 0 \end{bmatrix} \tag{2.51}$$

The sampling time for this discrete-time system is 0.01 seconds. Considering an output feedback dynamic controller $u(k) = Ky(k)$, where

$$K: \begin{cases} \varepsilon(k+1) = A_f \varepsilon(k) + B_f y(k) \\ u(k) = C_f \varepsilon(k) + D_f y(k) \end{cases} \tag{2.52}$$

The state-space realization of closed-loop system is

$$\begin{cases} \dot{X} = A_{cl} X + B_{cl} w \\ z = C_{cl} X + D_{cl} w \end{cases} \qquad X = \begin{bmatrix} x \\ \varepsilon \end{bmatrix} \tag{2.53}$$

$$A_{cl} = \begin{bmatrix} A + B_2 D_f C_2 & B_2 C_f \\ B_f C_2 & A_f \end{bmatrix}, \quad B_{cl} = \begin{bmatrix} B_1 + B_2 D_f D_{21} \\ B_f D_{21} \end{bmatrix}, \quad C_{cl} = [C_1 + D_{12} D_f C_2 \quad D_{12} C_f],$$

$$D_{cl} = D_{11} + D_{12} D_f D_{21} \tag{2.54}$$

Using GA method, we found the optimal values of A_f, B_f, C_f, and D_f in order to minimize the upper bound on ℓ_1-norm based on our calculation methods.

First order controller: *(Number of control variables: 12)*

$$A_f = [1.002], \quad B_f = [2.691 \quad 0.521 \quad 1.287], \quad C_f = \begin{bmatrix} 0.919 \\ -0.034 \end{bmatrix},$$

$$D_f = \begin{bmatrix} 4.633 & 3.469 & 2.513 \\ -0.496 & -0.148 & -3.886 \end{bmatrix} \tag{2.55}$$

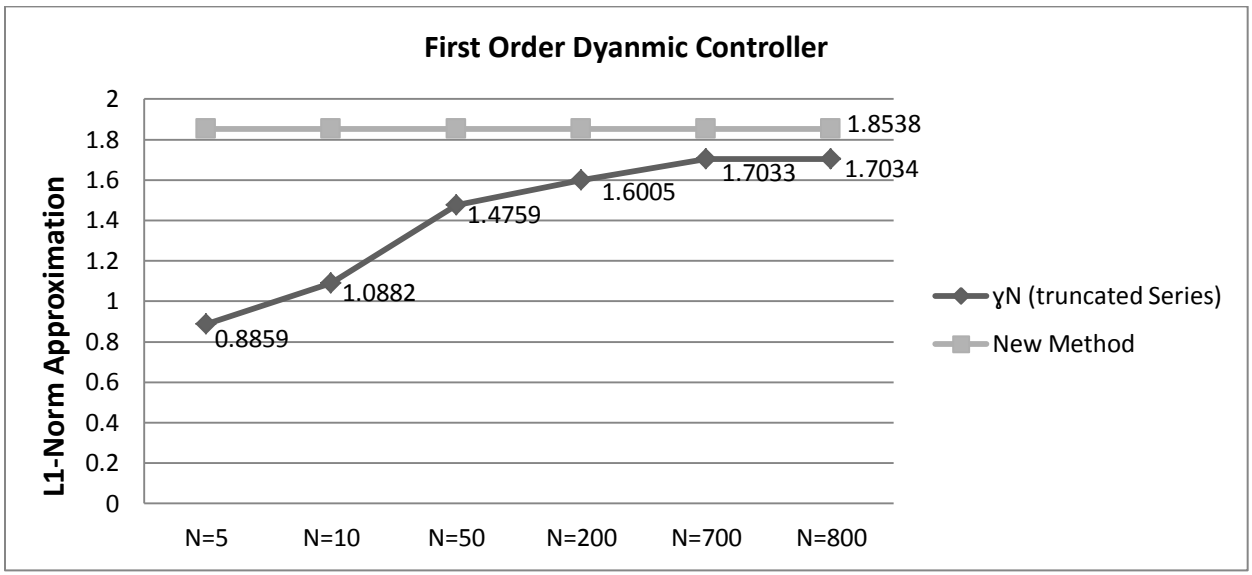

Figure 2.1 The accuracy of ℓ_1-norm computation is compared between the two methods. For the new method, the approximation error does not depend on N (truncation number), whereas for the truncated series, the accuracy increases with N.

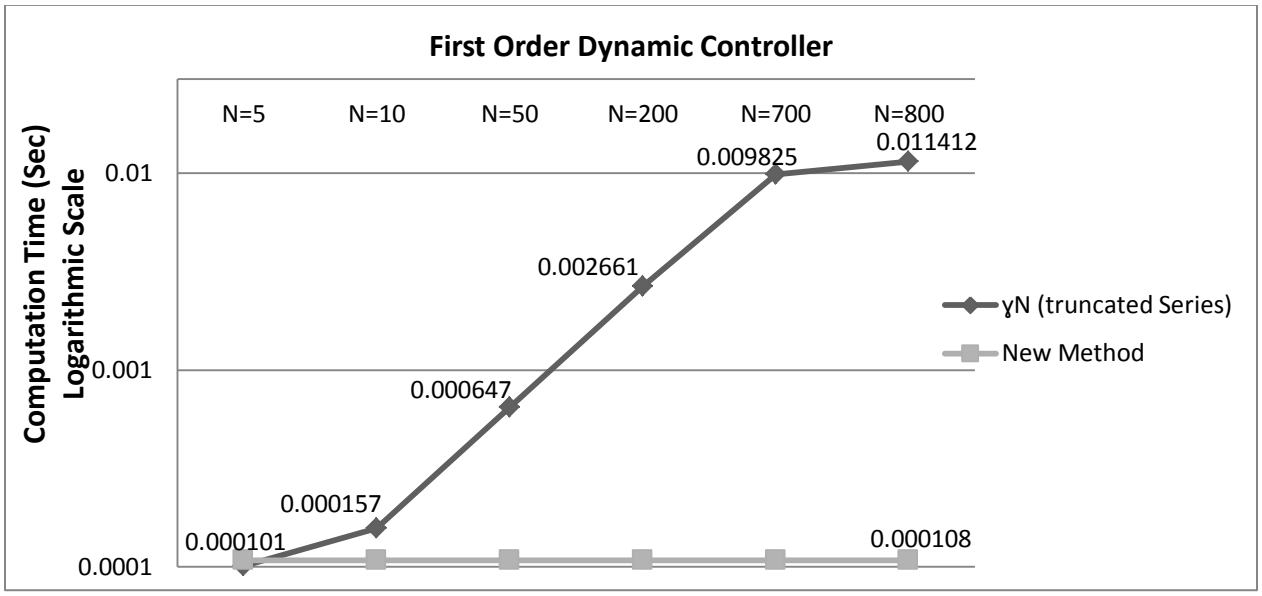

Figure 2.2 The ℓ_1-norm computation time for optimization purpose is compared between the two methods. For the new method, the computation time is independent of N (the truncation number), whereas the for the truncated series, the computation speed increases with N.

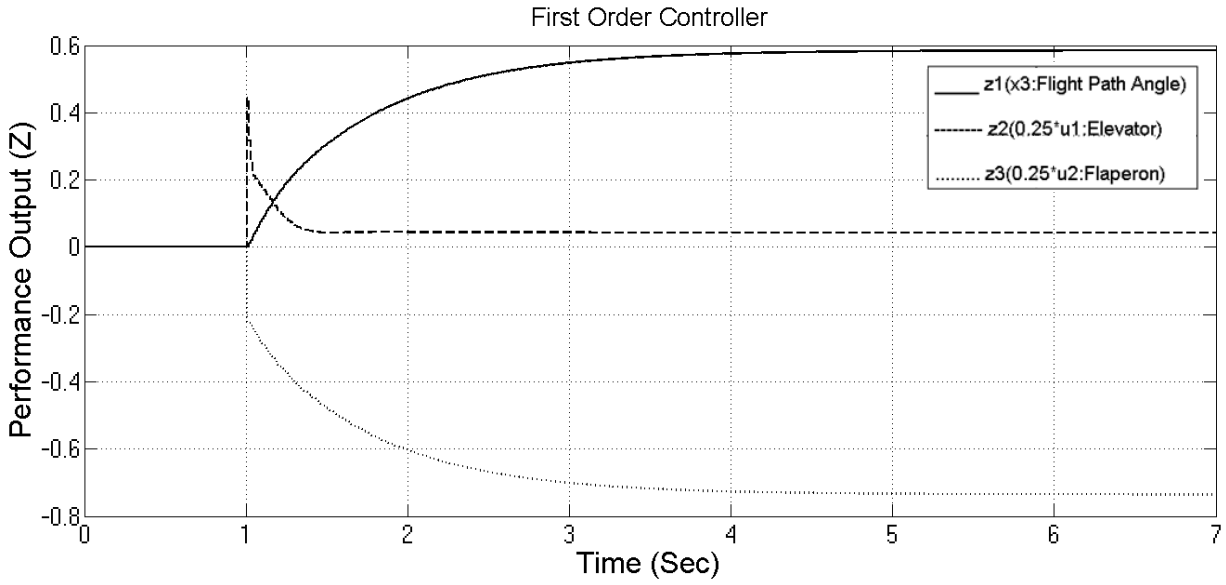

Figure 2.3 Unit step response of the feedback controlled aircraft system with first order dynamic controller.

We also obtained optimized higher order dynamic controllers. Similar results were obtained for second order and third order controllers. But, the higher order controllers have a higher number of variables and the ℓ_1-norm computation time was slightly longer.

Next, we synthesized ℓ_1-optimal state-feedback controllers for the aircraft system using optimization based on different ℓ_1-norm approximation methods. The results of optimization are summarized in the Tab. 2.1. Moreover, we optimized the state-feedback controller based on $\mathcal{H}_2$-norm, and $\mathcal{H}_\infty$-norm criteria and the results are presented in the following.

Table 2.1 The optimized state-feedback gains, the computation speed, and the accuracy of different methods for approximation of $\boldsymbol{\ell_1}$-norm are given.

ℓ_1-gain calculation method	New upper bound	ℓ_1-norm approximation (N=50)	ℓ_1-norm approximation (N=200)
Optimized feedback controller gains	$\begin{bmatrix} 18.373 & 1.51 & 13.824 \\ -0.955 & -0.043 & -4.980 \end{bmatrix}$	$\begin{bmatrix} 31.317 & 2.218 & 10.133 \\ -11.951 & -0.144 & -4.4559 \end{bmatrix}$	$\begin{bmatrix} 36.970 & 5.054 & 38.097 \\ 0.871 & 0.004 & -3.425 \end{bmatrix}$
Coomputation time per evaluation	0.000091 seconds	0.000602 seconds	0.002572 seconds
The optimal value	0.8005	0.4696	0.6529
Actual $\boldsymbol{\ell_1}$-norm (N=inf)	0.7800	1.6246	0.6548

In Tab. 2.1, we obtained the optimal feedback controller gains using three methods (our new upper bound and the truncated series with N=50 and N=200 terms) for approximation of ℓ_1-norm of closed-loop system. Tab. 2.1 suggests that the truncated series with N=50 does not provide an accurate approximation of ℓ_1-norm of the closed-loop system. For N=200, the approximation is closer to the actual value of the ℓ_1-norm. Compared to the new method, using truncated series with N=200, we obtained **19.1%** lower values for the ℓ_1-norm which means better result in terms of minimization. However, the computation speed is **28.3 times** higher using the new method.

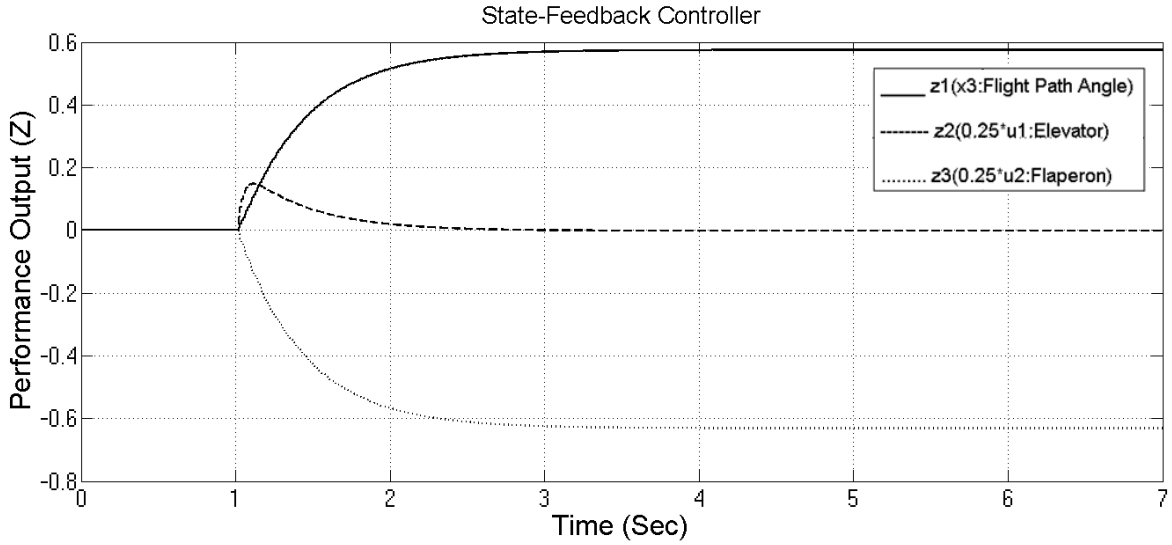

Figure 2.4 Unit step response of the closed-loop system.

In the following, we briefly introduce the $\mathcal{H}_2$-norm and $\mathcal{H}_\infty$-norm. In addition to ℓ_1-norm, we used the $\mathcal{H}_2$-norm and $\mathcal{H}_\infty$-norm to optimize the state-feedback gains of the aircraft system controller. In the Figs. (2.5) and (2.6), the impulse response and step response of the feedback controlled aircraft system which is optimized using different performance criteria, are simulated using SIMULINK software.

$\mathcal{H}_2$-norm

The $\mathcal{H}_2$-norm of a stable continuous system with transfer function $T(s)$, is the root-mean-square of its impulse response, or equivalently

$$\|T\|_2 = \sqrt{\frac{1}{2\pi}\int_{-\infty}^{+\infty} Trace\big(T(j\omega)^T T(j\omega)\big)d\omega} \tag{2.56}$$

This norm measures the steady-state covariance (or power) of the output response $y = Tw$ to unit white noise inputs w. Actually, for a unit intensity input, white noise process, the steady-state variance of output ,y, is $\|T\|_2$.

$$\|T\|_2^2 = \lim_{t\to\infty} E\{y(t)^T y(t)\}\ ,\ E(w(t)w(\tau)^T) = \delta(t-\tau)I \tag{2.57}$$

$\mathcal{H}_\infty$-norm

The infinity norm is the peak gain of the frequency response, that is,

$$\|T\|_\infty = \max_\omega |T(j\omega)| \quad \text{(SISO case)} \tag{2.58}$$

$$\|T\|_\infty = \max_\omega \sigma_{max}|T(j\omega)| \quad \text{(MIMO case)} \tag{2.59}$$

where $\sigma_{max}(.)$ denotes the largest singular value of a matrix. The ℓ_2 (or RMS) gain from $w \to y$, $\max_{w\neq 0} \frac{\|y\|_2}{\|w\|_2}$, is equal to $\|T\|_\infty$, where the ℓ_2-norm of a signal e, that is square integrable ($e \in \ell_2$), is defined as

$$\|e\|_2 \coloneqq \left(\int_{-\infty}^{+\infty} e^T(t)e(t)dt\right)^{\frac{1}{2}} \tag{2.60}$$

Note that the weighted $\mathcal{H}_\infty$-norm does not actually give element-by-element bounds on the components of performance output, y, based on element-by-element bounds on the components of input, u. The precise bound it gives is in terms of Euclidean norms of the components of y and u. Therefore, if realistic multivariable performance objectives are to be represented by a single MIMO $\mathcal{H}_\infty$-norm objective on a closed-loop transfer function, additional scalings are necessary. However, the ℓ_1-norm can provide element-by-element bounds on the maximum of components of input and output.

Table 2.2 The state-feedback control gains of the aircraft system are optimized based on $\boldsymbol{\ell_1}$-performance, $\boldsymbol{\mathcal{H}_2}$- performance, and $\boldsymbol{\mathcal{H}_\infty}$- performance. $\boldsymbol{\ell_1}$-norm, $\boldsymbol{\mathcal{H}_2}$-norm, and $\boldsymbol{\mathcal{H}_\infty}$-norm of the closed-loop system for different optimized feedback gains are given.

Performance Criterion	**Optimized State-Feedback Control Gains**	**ℓ_1-norm of System**	**$\mathcal{H}_2$-norm of System**	**$\mathcal{H}_\infty$-norm of System**
New Method	$\begin{bmatrix} 18.373 & 1.51 & 13.824 \\ -0.955 & -0.043 & -4.980 \end{bmatrix}$	0.7800	0.1361	0.8000
ℓ_1-Performance	$\begin{bmatrix} 36.970 & 5.054 & 38.097 \\ 0.871 & 0.004 & -3.425 \end{bmatrix}$	0.6548	0.2031	0.7067
$\mathcal{H}_2$- Performance	$\begin{bmatrix} 5.023 & 0.413 & 3.739 \\ 0.372 & 0.039 & -1.011 \end{bmatrix}$	1.0711	0.1004	0.7299
$\mathcal{H}_\infty$- Performance	$\begin{bmatrix} 21.134 & 1.469 & 29.762 \\ 0.482 & 0.104 & -1.053 \end{bmatrix}$	1.1885	0.1736	0.4766

Tab. 2.2 indicates that the various specific criteria do indeed minimize the closed loop system with respect to their slected norm measure. For example, using an $\ell_1$criteria, the minimum ℓ_1-norm of 0.6548 is found. When the closed loop is designed for a different criterion the norm is higher as seen looking down the column. The new method of computing the ℓ_1-norm, which does not guarantee optimality but rather only works with an upper bound, gives somewhat worse performance (0.7800 versus 0.6548). It is also noteworthy that using the new computationally efficient method gives good relative performance using the other standard norm measures looking across the top row of Tab. 2.2. In the following figures, we simulated the response of feedback controlled discrete-time model of aircraft for different feedback gains which were obtained based on different perforemance criteria. The impulse response and the step response of the closed-loop system is shown in the Figs. 2.5-2.6. The objective of optimization of the feedback gains is to minimize the system's gain between disturbance input and the performance output. Therefore, the responses with smaller peaks are more desirable when we apply impulse and step inputs.

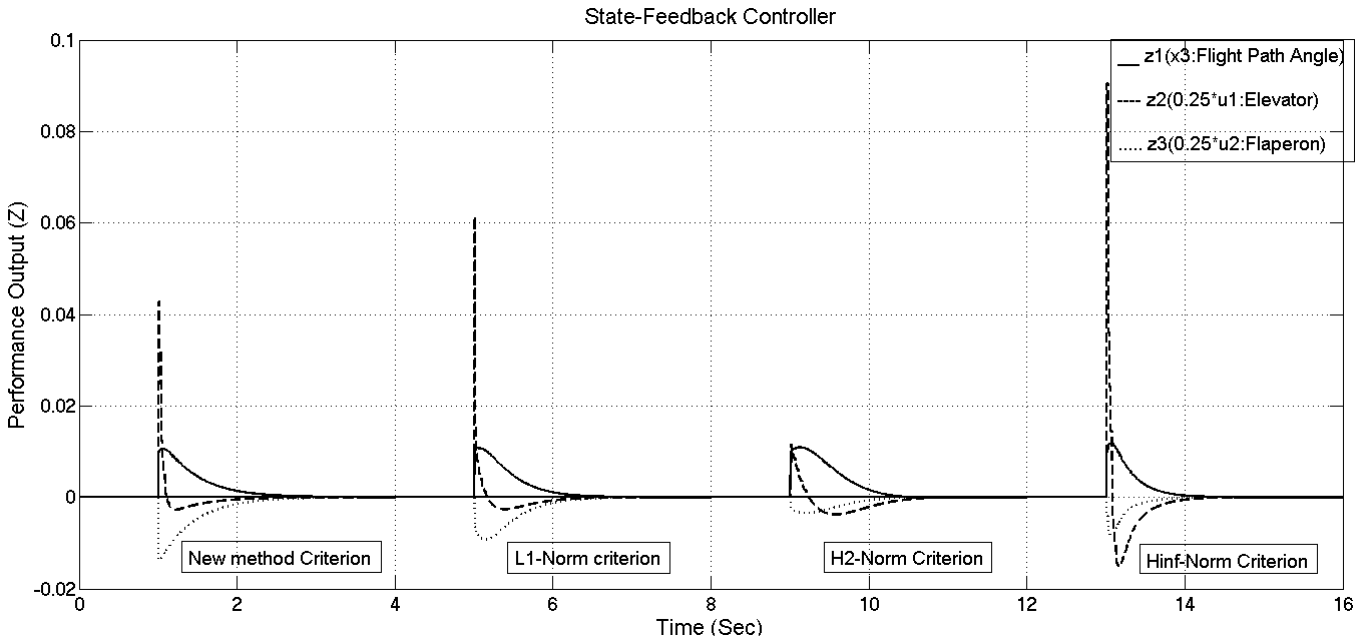

Figure 2.5 The unit impulse response of state-feedback controlled aircraft system. The feedback gains are optimazed based on $\boldsymbol{\ell_1}$-norm, $\boldsymbol{\mathcal{H}_2}$-norm, and $\boldsymbol{\mathcal{H}_\infty}$-norm criteria. The performance output vector (z) for each state-feedback controller is shown.

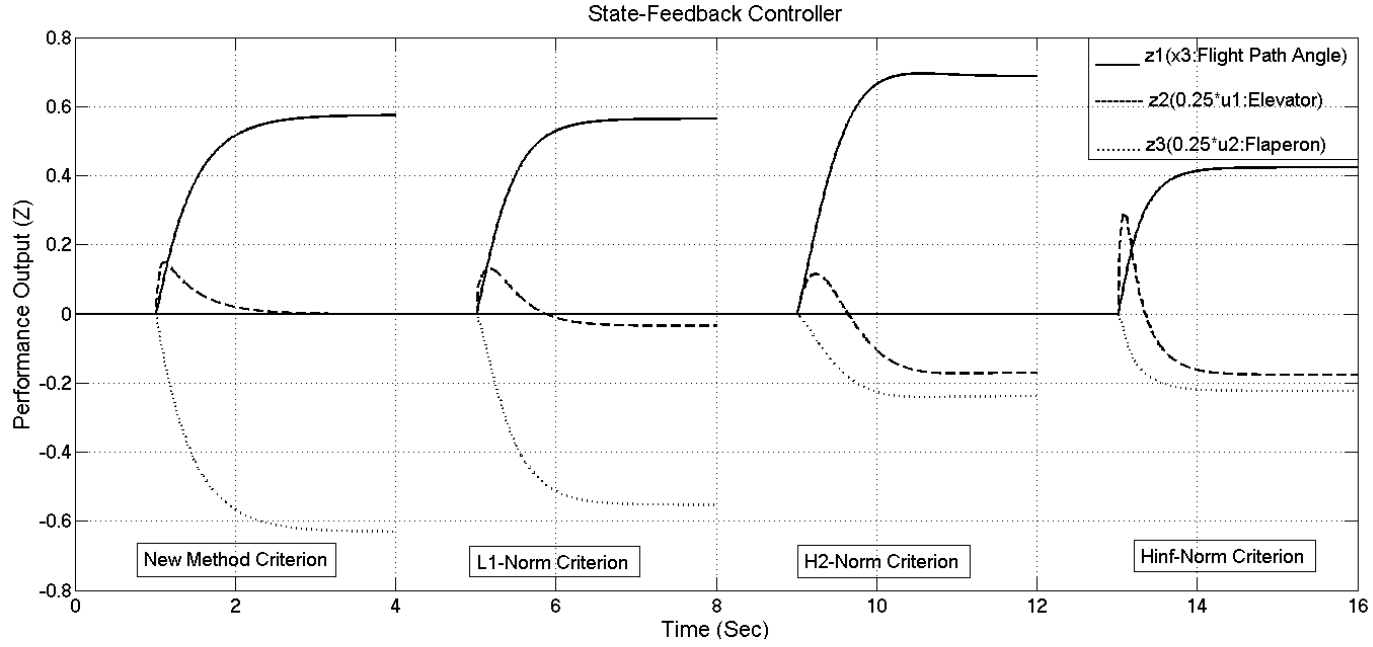

Figure 2.6 The unit step response of the state-feedback controlled aircraft system. The feedback gains are optimized based on $\boldsymbol{\ell_1}$-norm, $\boldsymbol{\mathcal{H}_2}$-norm, and $\boldsymbol{\mathcal{H}_\infty}$-norm. The performance output vector (z) for each state-feedback controller is shown.

Note that the impulse input has bounded energy or bounded ℓ_2-norm, whereas the step input has bounded magnitude or ℓ_∞-norm. As shown in Fig. 2.5, the impulse response of the feedback controlled system which is optimized based on an $\mathcal{H}_2$-norm criterion has smaller peaks. But the step response (Fig. 2.6) of the feedback controlled system which is optimize based on the ℓ_1-norm (or the new method) criterion has smaller peaks. In addition, as indicated in the Figs. 2.5-2.6, the response of the closed-loop systems which are optimized based on the new method and the accurate calculation of the ℓ_1-norm are very similar. These results validate our proposed method as a reliable approximation of the ℓ_1-norm.

Chapter 3: ℓ_1-Optimal Control of a LPV Model of VS-VP Wind Turbine in the Transition Region

This Chapter is organized as follows: a novel LPV model of aerodynamic and drive-train dynamics of a VS-VP wind turbine in the transition region is developed and the state-space realization of the control system is presented. Then, a state feedback controller based on ℓ_1 performance is derived by minimizing the upper bound problem on the ℓ_1-norm using an LMI approach. Next, the LPV control strategy is presented and the controller is implemented on the LPV model and simulation results are given.

3.1 LPV Model of Wind Turbine in the Transition Region

The developed wind turbine control structure consists of

1) *electrical subsystem (inner loop) with fast time response including the generator and pitch actuator*
2) *mechanical subsystem (outer loop) with much slower time response including aerodynamics and drive-train.*

This defines a cascaded structure (Boukhezzar and Siguerdidjane, 2009). Our concern in this study is the outer loop that provides the reference inputs of the inner loop. The main equation expressing the aerodynamic and rotor speed is given by

$$J\dot{\Omega} = f(\Omega, V, \beta) - T_{el} \tag{3.1}$$

where, Ω is the rotor speed, V is the wind speed, and β is the blade pitch angle. f is the aerodynamic torque induced in the blades. T_{el} is the electrical torque applied in the generator. f is given by

$$f(\Omega, V, \beta) = \frac{1}{2}\rho\pi R^3 \frac{C_p(\lambda,\beta)}{\lambda} V^2 \tag{3.2}$$

where λ, the so-called tip-speed ratio is given by

$$\lambda = \frac{\Omega R}{V} \tag{3.3}$$

C_p is the power coefficient. C_p is a function of tip-speed ratio and pitch angle. The following relation is a mathematical model for C_p given by Hui and Bakhshai (2008)

$$C_p(\lambda, \beta) = c_1\left(\frac{c_2}{\lambda_i} - c_3\beta - c_4\right)e^{\frac{-c_5}{\lambda_i}} + c_6\lambda \tag{3.4}$$

$$\frac{1}{\lambda_i} = \frac{1}{\lambda+0.02\beta} - \frac{0.035}{(\beta/4)^3+1} \tag{3.5}$$

$$c_1 = 0.5176, c_2 = 116, c_3 = 0.1, c_4 = 5, c_5 = 21, c_6 = 0.0068$$

To develop the LPV model, we utilize the second order Taylor expansion of nonlinear term, f, near the vicinity of a mid-operating point in the transition region, as presented in the following

$$\hat{\Omega} = \Omega - \bar{\Omega} \ , \ \hat{V} = V - \bar{V} \ , \ \hat{\beta} = \beta - \bar{\beta} \ , \hat{T}_{el} = T_{el} - \bar{T}_{el} \tag{3.6}$$

$$f(\Omega, V, \beta) = f\left(\bar{\Omega}, \bar{V}, \bar{\beta}\right) + f\left(\hat{\Omega}, \hat{V}, \hat{\beta}\right), \ \bar{T}_{el} = f\left(\bar{\Omega}, \bar{V}, \bar{\beta}\right) \tag{3.7}$$

$$J\dot{\hat{\Omega}} = f\left(\hat{\Omega}, \hat{V}, \hat{\beta}\right) - \hat{T}_{el} \tag{3.8}$$

$$f\left(\hat{\Omega}, \hat{V}, \hat{\beta}\right) = f_\Omega\hat{\Omega} + f_V\hat{V} + f_\beta\hat{\beta} + \frac{1}{2}f_{\Omega\Omega}\hat{\Omega}^2 + \frac{1}{2}f_{VV}\hat{V}^2 + \frac{1}{2}f_{\beta\beta}\hat{\beta}^2 + f_{V\beta}\hat{V}\hat{\beta} + f_{\Omega\beta}\hat{\Omega}\hat{\beta} + f_{\Omega V}\hat{\Omega}\hat{V} + \cdots \tag{3.9}$$

where $f_\Omega, f_V, f_{\Omega\Omega}, \ldots$ are partial derivatives that are evaluated at the point $\left(\bar{\Omega}, \bar{V}, \bar{\beta}\right)$ and $\hat{V}, \hat{\Omega},$ and $\hat{\beta}$ are deviations from $\bar{V}, \bar{\Omega},$and $\bar{\beta}$. We define $\hat{\Omega} \equiv \theta_1$ and $\hat{\beta} \equiv \theta_2$ as the scheduling parameters of

the LPV model. This introduces a quasi-LPV model, because $\hat{\Omega}$ is a state variable and a LPV parameter. Rotor speed and pitch angle can be accurately measured online. In this model, wind speed is viewed as exogenous disturbance. By rearranging (3.9)

$$f(\hat{\Omega}, \hat{V}, \hat{\beta}) \approx F_{\Omega}(\theta)\hat{\Omega} + F_{\beta}(\theta)\hat{\beta} + F_{V}(\theta)\hat{V} + \frac{1}{2} f_{VV}\hat{V}^2 \tag{3.10}$$

where $\theta = \{\theta_1, \theta_2\}$ and

$$\begin{aligned} F_{\Omega}(\theta) &= f_{\Omega} + \frac{1}{2} f_{\Omega\Omega}\theta_1 + \frac{1}{2} f_{\Omega\beta}\theta_2 \\ F_{\beta}(\theta) &= f_{\beta} + \frac{1}{2} f_{\Omega\beta}\theta_1 + \frac{1}{2} f_{\beta\beta}\theta_2 \\ F_{V}(\theta) &= f_{V} + f_{\Omega V}\theta_1 + f_{V\beta}\theta_2 \end{aligned} \tag{3.11}$$

The VS-VP control strategy for capturing maximum power is illustrated in Fig. 3.1. According to this strategy, the reference rotor speed for optimum power tracking is

$$\hat{\Omega}_r = \begin{cases} \frac{\lambda_{opt}\hat{V}_F}{R} & \hat{V}_F < \hat{V}_{\Omega_N} \\ \hat{\Omega}_N & \hat{V}_F \geq \hat{V}_{\Omega_N} \end{cases} \tag{3.12}$$

where, $\hat{\Omega}_N$ is the rated rotor speed and $\hat{V}_{\Omega_N}$ is the wind speed that the optimal rotor speed first hits the rated rotor speed. $\hat{V}_F$ is the filtered wind speed. A low-pass filter $F(s) = 1/(\tau s + 1)$ with time constant τ, eliminates high frequency noise in the wind speed measurement. Moreover, the derivative of the reference rotor speed, $\dot{\hat{\Omega}}_r$, will be kept bounded in the fast wind speed variations, because $\left|\dot{\hat{V}}_F\right| \leq |\Delta V|_{max}/\tau$. In the transition region, two inputs are acting; generator torque and pitch angle are the control inputs that are acting independently. Therefore, for better controllability and optimum power tracking in the transition region, we can define the reference input torque of Eq. (3.13) for generator to track the ideal torque curve as shown in Fig. 3.1(c).

$$\hat{T}_r = \begin{cases} CV_F^2 & CV_F^2 < \hat{T}_N \\ \hat{T}_N & CV_F^2 \geq \hat{T}_N \end{cases} \qquad \left(C = \frac{1}{2}\rho\pi R^3 \frac{C_p|max}{\lambda_{opt}}\right) \tag{3.13}$$

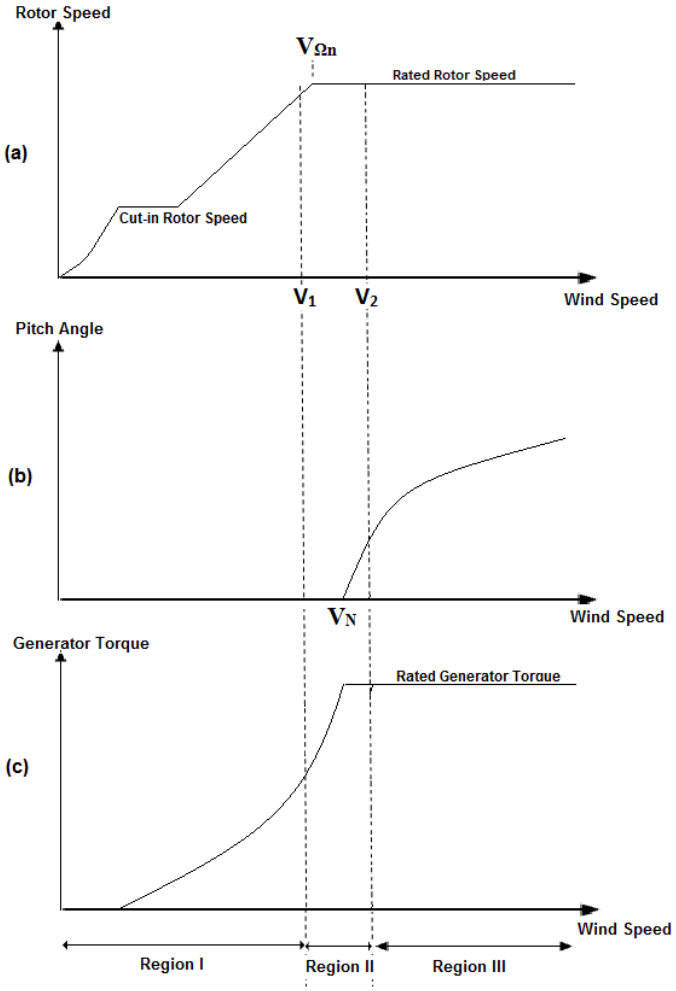

Figure 3.1 The control strategy at transition region. (a) The ideal rotor speed curve. Control inputs, pitch angle (b) and generator torque (c) at different wind speeds.

Defining $\tilde{\Omega} = \hat{\Omega} - \hat{\Omega}_r$ and $\tilde{T}_{el} = \hat{T}_{el} - \hat{T}_r$ as the tracking errors and using Eq. (3.10), we can rewrite Eq. (3.8) as

$$J\left(\dot{\hat{\Omega}}_r + \dot{\tilde{\Omega}}\right) = F_\Omega(\theta)\left(\tilde{\Omega} + \hat{\Omega}_r\right) + F_\beta(\theta)\hat{\beta} + F_V(\theta)\hat{V} + \frac{1}{2}f_{VV}\hat{V}^2 - \left(\tilde{T}_{el} + \hat{T}_r\right) \qquad (3.14)$$

The state-space realization of the LPV wind turbine model is

$$\begin{cases} \dot{x} = A(\theta)x + B_1(\theta)w + B_2(\theta)u \\ z = C_1(\theta)x + D_{12}(\theta)u \\ y = C_2(\theta)x + D_{21}(\theta)w \end{cases} \qquad (3.15)$$

where

$$A = \left[\frac{F_{\Omega}(\theta)}{J}\right]$$

$$B_1 = \left[\frac{F_V(\theta)\left|\hat{V}\right|_{max}}{J} \quad \frac{f_{VV}\left|\hat{V}^2\right|_{max}}{2J} \quad \frac{F_{\Omega}(\theta)\left|\hat{\Omega}_r\right|_{max}}{J} \quad -\frac{\lambda_{opt}|\Delta V|_{max}}{R\tau} \quad -\frac{\left|\hat{T}_r\right|_{max}}{J}\right]$$

$$B_2 = \left[\frac{F_{\beta}(\theta)}{J} \quad -\frac{1}{J}\right], \qquad C_1 = \begin{bmatrix} \frac{1}{\left|\tilde{\Omega}\right|_{max}} \\ 0 \\ 0 \end{bmatrix}, \qquad D_{12} = \begin{bmatrix} 0 & 0 \\ 0 & \frac{1}{\left|\tilde{T}_{el}\right|_{max}} \\ \frac{1}{\left|\hat{\beta}\right|_{max}} & 0 \end{bmatrix}$$

$$C_2 = [1],\ x \equiv \tilde{\Omega}\ ,\quad u \equiv \begin{bmatrix} \hat{\beta} \\ \tilde{T}_{el} \end{bmatrix} \tag{3.16}$$

Disturbances and reference inputs vector, w, and performance output vector, z, are normalized based on their maximum values so that for $\|w\|_{\infty} \leq 1$ in the transition region, the optimal control objective is $\|z\|_{\infty} \leq 1$.

3.2 Controller Design

3.2.1 LMI Approach to ℓ_1-Optimal Control

A well-known approach to ℓ_1-optimal control is using LMIs to find an upper bound on the ℓ_1-norm. Considering the system below

$$\begin{cases} \dot{x} = Ax + Bw \\ z = Cx + Dw \end{cases} \tag{3.17}$$

where $x \in \mathbb{R}^n$ is the state, and $w \in \mathbb{R}^m$ is the input and $z \in \mathbb{R}^q$ is the output. Assuming T_{wz} is the transfer function that defines a mapping from bounded amplitude inputs $w \in \ell_{\infty}$ to the

bounded amplitude outputs $z \in \ell_\infty$, then a relevant ℓ_1 performance criterion is the peak-to-peak or ℓ_∞-induced norm of this transfer function

$$\|T_{wz}\|_{\infty-ind} \coloneqq \sup_{0<\|w\|_\infty<\infty} \frac{\|z\|_\infty}{\|w\|_\infty} \tag{3.18}$$

An upper bound, γ, of the peak-to-peak gain is given in Scherer and Weiland (2004) and Khosravi and Jalali (2008). The matrix inequality constraints in the following theorem are used to find the upper bound γ for the system with state-space realization Eq. (3.17).

Theorem 3.1*: If there exists $X > 0$, $\lambda > 0$, and $\mu > 0$ such that*

$$\begin{bmatrix} A^T X + XA + \lambda X & XB \\ B^T X & -\mu I \end{bmatrix} < 0 \tag{3.19}$$

$$\begin{bmatrix} \lambda X & 0 & C^T \\ 0 & (\gamma - \mu) I & D^T \\ C & D & \gamma I \end{bmatrix} > 0 \tag{3.20}$$

Then the peak-to-peak (or ℓ_∞-induced) norm of the system is smaller than γ, i.e. $\|T_{wz}\|_{\infty-ind} < \gamma$.

Because of conservatism, the inverse of the theorem is not true. λX is the only non-linear term in the matrix inequalities (3.19) and (3.20). To overcome this problem for a fixed > 0 , we test whether the resulting LMIs are feasible; if yes, the bound γ on the peak-to-peak norm has been assured; if the LMIs are not feasible, we choose another $\lambda > 0$ and repeat the test (Scherer and Weiland, 2004).

It is advantageous to find the best possible (least conservative) upper bound on the peak-to-peak norm. For this purpose, A line-search over $\lambda > 0$ to minimize $\gamma^*(\lambda)$ (the minimum value of γ if $\lambda > 0$ is held fixed) is performed. Minimizing $\gamma^*(\lambda)$ subject to LMI constrains leads to a

convex optimization problem with extensive and efficient solutions. The line-search leads to the best achievable upper bound

$$\gamma^u = \inf_{\lambda>0} \gamma^*(\lambda) \tag{3.21}$$

A lower bound on peak-to-peak norm is the H_∞-norm. The conservatism of the proposed LMI method can be estimated by calculating the H_∞-norm of the transfer function from w to z, *i.e.* $\|T_{wz}\|_\infty$. This minimal achievable H_∞-norm denoted by γ^l. The actual optimal peak-to-peak gain must be in the interval $[\gamma^l \quad \gamma^u]$ and a small interval suggests that the upper bound is close to the actual peak-to-peak gain (Scherer and Weiland, 2004).

3.2.2 Derivation of State-Feedback Controller

Now, we can derive a state-feedback controller $(u = Kx)$ for the general system

$$\begin{bmatrix} \dot{x} \\ z \\ y \end{bmatrix} = \begin{bmatrix} A & B_1 & B_2 \\ C_1 & D_{11} & D_{12} \\ C_2 & D_{21} & D_{22} \end{bmatrix} \begin{bmatrix} x \\ w \\ u \end{bmatrix} \tag{3.22}$$

where $x \in \mathbb{R}^n$ denotes states and $w \in \mathbb{R}^{q_1}$ defines reference signals and disturbances. $u \in \mathbb{R}^{q_2}$ is the control input, $z \in \mathbb{R}^{p_1}$ is the performance output and $y \in \mathbb{R}^{p_2}$ is the measurement. The matrix K is the feedback gain. In this work, we use the assumption that the system is srictly proper, *i.e.* $D_{11} = 0$ and $D_{22} = 0$. In addition to simplifying the manipulation, the assumption is valid for the typical wind turbine models. In the following, to derive the feedback controller for the closed loop system, we use some techniques to transform matrix inequalities into a suitable LMI-format for solution. The closed loop system is given by

$$\begin{cases} \dot{x} = (A + B_2K)x + B_1w \\ z = (C_1 + D_{12}K)x \end{cases} \tag{3.23}$$

We substitute the closed loop system matrices in Eqs. (3.19) and (3.20) as

$$\begin{bmatrix} (A+B_2K)^T X + X(A+B_2K) + \lambda X & XB_1 \\ {B_1}^T X & -\mu I \end{bmatrix} < 0 \tag{3.24}$$

$$\begin{bmatrix} \lambda X & 0 & (C_1+D_{12}K)^T \\ 0 & (\gamma-\mu)I & 0 \\ (C_1+D_{12}K) & 0 & \gamma I \end{bmatrix} > 0 \tag{3.25}$$

The following lemma is used to transform matrix inequalities (3.24) and (3.25) to LMIs. According to Schur complement lemma,

Lemma 3.1*:* *The inequalities:*

$$R(x) > 0 \ \ (< 0) \ \ , Q(x) - S(x)R(x)^{-1}S(x)^T > 0 \qquad (< 0) \tag{3.26}$$

Are equivalent to LMI:

$$\begin{bmatrix} Q(x) & S(x) \\ S(x)^T & R(x) \end{bmatrix} > 0 \qquad (< 0) \tag{3.27}$$

Using Lemma 3.1, we can rewrite (3.24) in the following form. It is assumed that $\lambda > 0$ and $X > 0$.

$$(A+B_2K)^T X + X(A+B_2K) + \lambda X + \frac{1}{\mu} X B_1 {B_1}^T X < 0 \tag{3.28}$$

Therefore, we can multiply both sides of inequality (3.28) by $Y = X^{-1} > 0$ as given below

$$(AY+B_2KY)^T + (AY+B_2KY) + \lambda Y + \frac{1}{\mu} B_1 {B_1}^T < 0 \tag{3.29}$$

We define new variable $H = KY$ and use Lemma 3.1 to obtain

$$\begin{bmatrix} (AY+B_2H)^T + (AY+B_2H) + \lambda Y & B_1 \\ {B_1}^T & -\mu I \end{bmatrix} < 0 \ , \qquad \mu > 0 \tag{3.30}$$

λY is the only nonlinear term in matrix inequality (3.30), This problem can be treated as discussed before. Therefore, the matrix inequality (3.30) is suitable for LMI minimization

problem with ℓ_1-norm performance. Note that, the feedback gain can be obtained by the relation $K = HY^{-1}$.

Using the same procedure, we can obtain the LMI equivalent to the matrix inequality (3.25). Using the Schur complement lemma for Eq. (3.25), we obtain

$$\begin{bmatrix} \lambda X - \frac{1}{\gamma}(C_1 + D_{12}K)^T(C_1 + D_{12}K) & 0 \\ 0 & (\gamma - \mu)I \end{bmatrix} > 0 \quad , \gamma > 0 \tag{3.31}$$

Because of diagonal elements, the inequality (3.31) is equivalent to

$$I)\ \lambda X - \frac{1}{\gamma}(C_1 + D_{12}K)^T(C_1 + D_{12}K) > 0 \qquad and \qquad II)\ \gamma > \mu \tag{3.32}$$

Multiplying both sides of the first inequality in Eq. (3.32) by $Y = X^{-1} > 0$ and using the new variable $H = KY$, we obtain

$$\lambda Y - \frac{1}{\gamma}(C_1 Y + D_{12}H)^T(C_1 Y + D_{12}H) > 0 \tag{3.33}$$

or

$$\begin{bmatrix} \lambda Y & (C_1 Y + D_{12}H)^T \\ (C_1 Y + D_{12}H) & \gamma I \end{bmatrix} > 0 \tag{3.34}$$

The LMI minimization problem setup for obtaining a state-feedback controller with ℓ_1-optimal criterion, is summarized in the following optimization problem

Optimization Problem:

$$Find\ \min(\gamma)\ \ s.t.$$

$$Y > 0, \qquad \lambda > 0, \qquad \mu > 0, \qquad \gamma > \mu,$$

$$\begin{bmatrix} (AY + B_2H)^T + (AY + B_2H) + \lambda Y & B_1 \\ {B_1}^T & -\mu I \end{bmatrix} < 0,$$

$$\begin{bmatrix} \lambda Y & (C_1 Y + D_{12}H)^T \\ (C_1 Y + D_{12}H) & \gamma I \end{bmatrix} > 0 \tag{3.35}$$

where $Y,\ \lambda,\ \mu,\ \gamma$, and H are variables and the feedback gain can be obtained by relation

$$K = HY^{-1} \tag{3.36}$$

3.2.3 Derivation of LPV State-Feedback Controller

Application of matrix inequalities for LPV system will result in parameterized LMIs (PLMIs). Therefore, the LPV problem solution involves infinitely many LMIs associated with each value of the parameter θ. PLMIs are still very complex and the general solutions are open research problems. However, there are some relaxation techniques to transform (potentially conservatively) PLMIs to standard LMIs. By enforcing some constraints of a geometric nature on the functional dependence in θ, it is, however, possible to reduce the problem to solving a finite number of LMIs. As the system matrices in LPV models have linear parameter dependence, we can assume an affine form for the PLMI decision variables, so that the resulting PLMIs have quadratic parameter dependence. The following proposition in Apkarian and Tuan (1998), can be utilized for this class of PLMIs.

Proposition 3.1 *(Multi-convexity Property): Consider the function*

$$F(x,\theta) = F_0(x) + \sum_{i=1}^{m} \theta_i F_i(x) + \sum_{i<j}^{m} \theta_i\theta_j F_{i,j}(x) + \sum_{i}^{m} \theta_i^2 F_{i,i}(x) < 0 \tag{3.37}$$

where $\in \Theta \subset \mathbb{R}^m$, $\Theta = Co\{\theta_{v_1}, \dots, \theta_{v_r},\}$ *is a convex polytope of r vertices and* $F_i(x)$, $F_{i,j}(x)$ *and* $F_{i,i}(x)$ *are symmetric affine functions of the decision variable x. Then,*

$$F(x,\theta) > 0 \quad (< respectively) \quad \forall\theta \in \Theta \tag{3.38}$$

whenever the following finite set of LMIs

$$F\left(x,\theta_{v_j}\right) > 0\ (< respectively)\ \ j = 1,\dots,r \tag{3.39}$$

$$F_{i,i}(x) < 0\ (> respectively)\ \ i = 1,\dots,m \tag{3.40}$$

holds.

In the wind turbine LPV model, system matrices A, B_1, and B_2 are linearly dependent on the scheduling parameters $\theta = \{\theta_1 , \theta_2\}$. As presented below, the decision matrix variables of LMIs in Eq. (3.35) are assumed to be in affine form as in Eq. (3.41). Although, imposing the constraint on the decision variable to be a linear function of scheduling parameters causes conservatism, the resulting PLMIs for ℓ_1 criterion have quadratic parameter dependence as in Eq. (3.37).

$$
\begin{aligned}
Y &= Y_0 + \theta_1 Y_1 + \theta_2 Y_2 \\
H &= H_0 + \theta_1 H_1 + \theta_2 H_2 \\
\gamma &= \gamma_0 + \theta_1 \gamma_1 + \theta_2 \gamma_2 \\
\mu &= \mu_0 + \theta_1 \mu_1 + \theta_2 \mu_2 \\
\lambda &= \lambda_0 + \theta_1 \lambda_1 + \theta_2 \lambda_2 \\
K(\theta) &= H(\theta)\big(Y(\theta)\big)^{-1}
\end{aligned}
\tag{3.41}
$$

The ideal pitch angle-rotor speed diagram is illustrated in Fig. 3.2. At low wind speeds (Region I), the pitch angle is constant ($\beta = \beta_1$). At high wind speeds (Region III), the rotor speed is kept constant at Ω_N while the pitch angle increases to limit the aerodynamic torque. As shown in the Fig. 3.2, to specify a convex domain of variation of system parameters in LPV model of wind turbine at transition region (Region II), we need a polytope with at least three vertices.

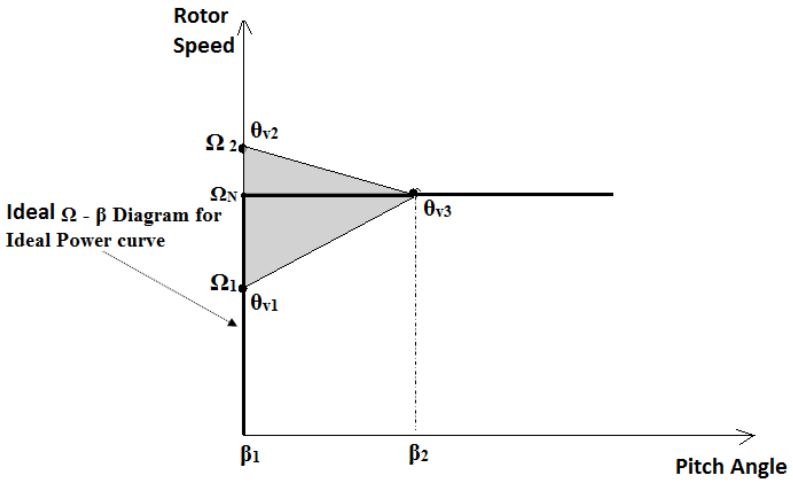

Figure 3.2 Ideal pitch angle ($\boldsymbol{\beta \equiv \theta_2}$)-rotor speed ($\boldsymbol{\Omega \equiv \theta_1}$) diagram. A convex polytope specifies the parameter-variation domain for LPV model of wind turbine.

3.3 Simulation Results

In this section, results of simulation of implementing the LPV state-feedback controller on a simplified nonlinear model of wind turbine introduced earlier in this chapter. A step wind speed input (from 10 to 11 m/s) as exogenous disturbance is applied to the wind turbine model and the performance of the LPV state-feedback controller is shown in the Fig. 3.3. In this chapter, we did not use the FAST wind turbine simulation software, as our simplified non-linear wind turbine model with limited DOF, provides a more clear results in terms of validation of the mathematical development in this chapter. In the following chapter, we extensively present the simulation results using the FAST software to validate the peformance of the gain-scheduled ℓ_1 controller which we develop in the next chapter.

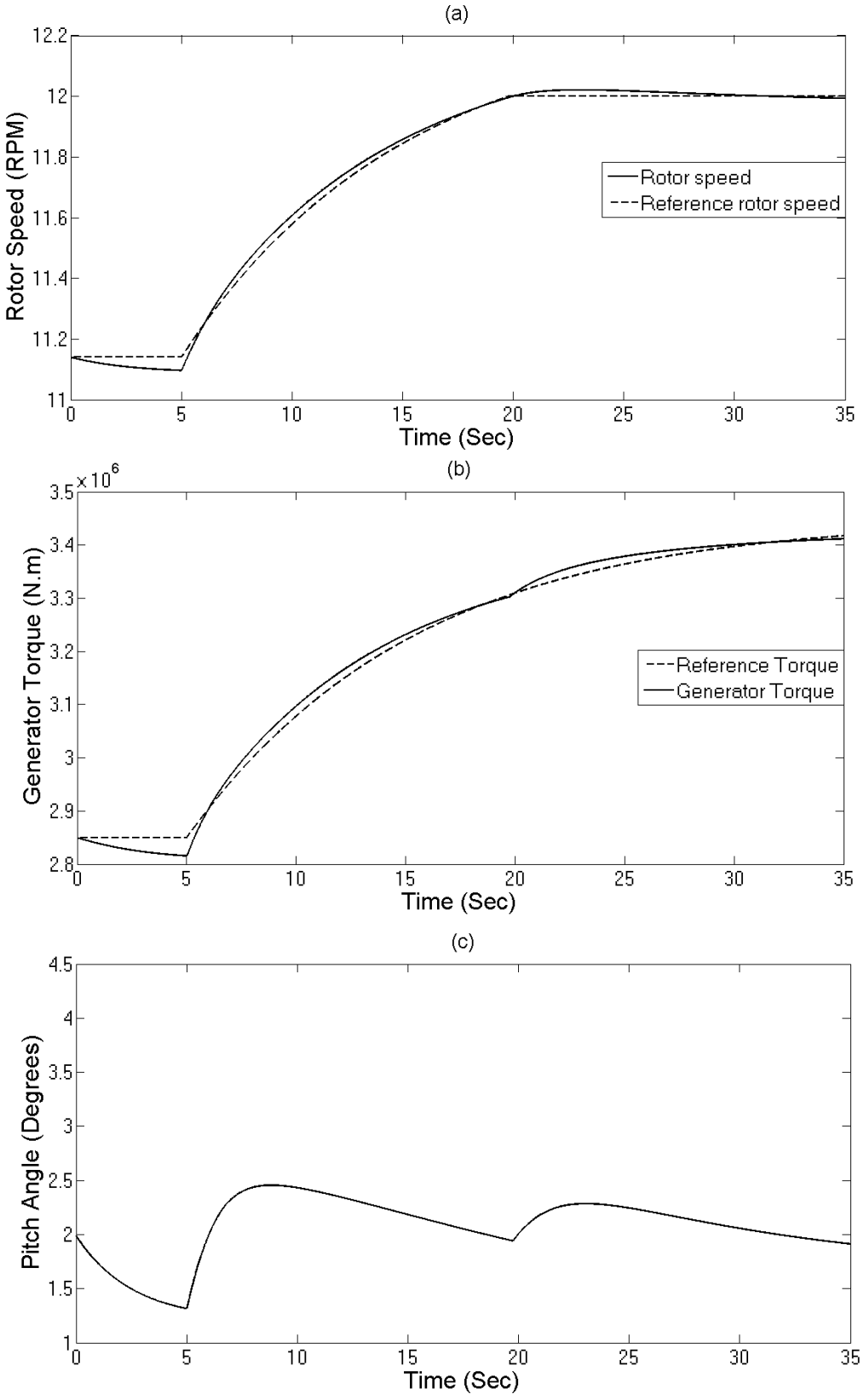
(a)
Rotor Speed (RPM)
Time (Sec)
Rotor speed
Reference rotor speed
(b)
x10^6
Generator Torque (N.m)
Time (Sec)
Reference Torque
Generator Torque
(c)
Pitch Angle (Degrees)
Time (Sec)

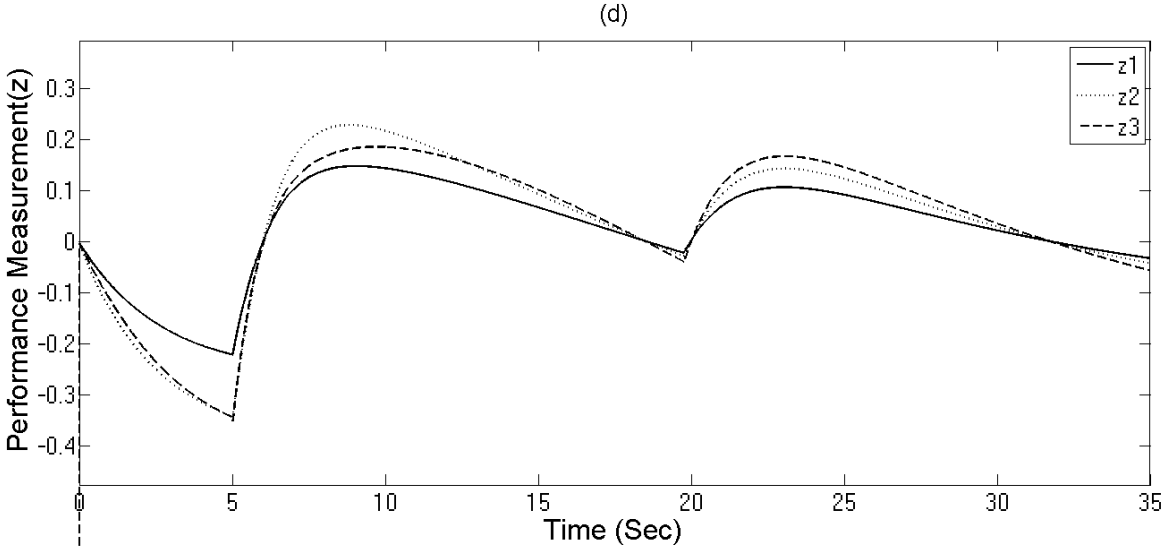

Figure 3.3 Response of wind turbine control system to a step wind speed input. (a) rotor speed vs. time. (b) Generator torque input vs. time. (c) Pitch angle vs. time. (d) Normalized performance output vs. time.

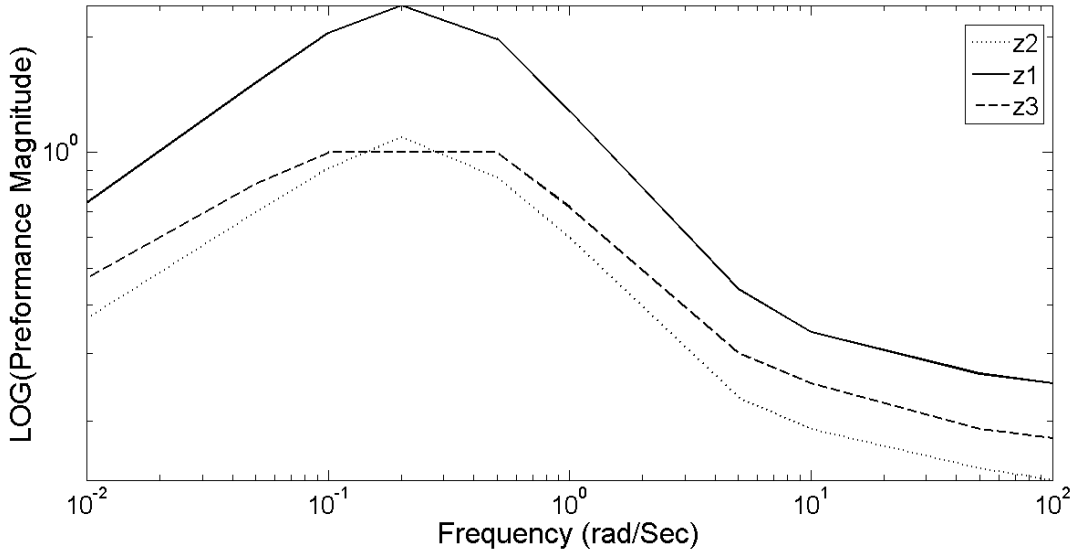

Figure 3.4 Peak magnitude of output performance at different input frequencies $\left(\widehat{\boldsymbol{V}} = \mathbf{0.5}\,\mathbf{sin}(\boldsymbol{\omega t})\right)$ in the logarithmic scale.

As shown, the normalized performance output is small($\|z\|_\infty < 1$). Therefore, we can conclude that the tracking errors do not exceed their specified maximum value. The frequency response of the control system to wind speed disturbance $\left(\hat{V} = .5\sin(\omega t)\right)$ is shown in Fig. 3.4, as the peak magnitude of performance output is plotted. The largest induced gain in the system is observed in the torques response with a peak amplification of 2.5 near a frequency 0.2 rad/s.

3.4 Conclusion

In this chapter, an LPV wind turbine model is developed for control synthesis over the transition region. An LPV and ℓ_1 -optimal state-feedback controller is proposed for VS-VP wind turbines in the transition region. The parameter-varying feedback gains of the controller are designed so that the ℓ_1 -based time-domain performance measures are optimized. As the results suggest, in presence of different persistent disturbances, the performance output shows small tracking errors. In addition to disturbance rejection and guaranteed stability over the transition region, the multivariable ℓ_1-optimal control of pitch actuation and generator torque, results in a smooth and consistent transition between the maximum power region and the rated power region.

Chapter 4: Gain-Scheduled ℓ_1-Optimal Control Design for a Wind Turbine at High Wind Speeds

In this chapter, we first derive the linear model of a wind turbine at different operating points in Region III (the rated power region at high wind speeds). Next, we find local output feedback controllers at each operating point. The local controllers are optimized based on ℓ_1 performance using genetic algorithm method. Then, we present a gain-scheduling technique with guaranteed stability in order to interpolate the local controllers.

4.1 A Linear Model of Wind Turbine at Different Operating Points

Linear models for a wind turbine system can be expressed as

$$\dot{x} = Ax + B_1 u + B_2 w \tag{4.1}$$

$$y = Cx + D_1 u + D_2 w \tag{4.2}$$

In the model which is used in this study, the first drive-train torsion mode as well as the rotor and the generator speeds are being considered. Higher order state-space models of wind turbines include more degree of freedoms (DOFs). In this study, we modeled a limited number of dynamical equations in the wind turbine systems. However, the control design procedure we proposed in this chapter can be easily used for higher order wind turbine models. For this model, it is assumed that the control input is perturbation in blade pitch angle $\delta\beta$ (the pitch angles of all blades are identical). The disturbance input is the perturbation in the uniform component of wind speed over the rotor disk, δV. It is also assumed that generator speed is the measured control signal.

In the standard state-space realization of the wind turbine model, wind speed is the exogenous disturbance and the performance output consists of the deviation of rotor speed from the rated rotor speed, variation of pitch angle, and the rate of change of the pitch angle. The purpose of control optimization is to regulate power generation while less control effort is applied on the system. Therefore, variation of pitch angle which is a control input and its rate of change were considered in the performance output. We use constant power strategy in Region III operation. The pitch angle is the control input and the generator torque varies so that the electrical power output remains constant *i.e.* $T_g = \frac{P_{nom}}{\Omega_g}$, in which, P_{nom} is the nominal power capacity of the generator in the rated power region, Ω_g is the generator speed and T_g is the generator torque. Therefore, the generator torque variation which is another control input is also considered in the performance output by choosing the deviation of rotor speed from the rated rotor speed as a performance output. In addition, the power output is maintained constant.

Using ℓ_1-optimal control we can minimize the closed-loop system gain between the disturbance input and the performance output. Also, the performance output can be easily normalized based on the maximum allowable value of the performance variables in the presence of bounded-magnitude disturbances. In ℓ_1-optimal control the ℓ_∞-norm of the input and outputs are measured. In fact, one of advantages of the ℓ_1-optimal control is that we can address the maximum of errors and rates of changes using ℓ_∞-norm of the inputs and the outputs. The state-space realization which we used for the control design is given by

$$\begin{bmatrix}\dot{x}_1\\ \dot{x}_2\\ \dot{x}_3\\ \dot{x}_4\\ \dot{x}_5\end{bmatrix}=\begin{bmatrix}0 & 0 & 1 & 0 & 0\\ K_d/I_g & \epsilon & C_d/I_g & 0 & 0\\ -K_d/I & \gamma/I_r-\epsilon & -C_d/I+\gamma/I_r & \zeta/I_r & 0\\ 0 & 0 & 0 & -1/\tau_1 & 0\\ 0 & 0 & 0 & -1/\tau_1\tau_2 & -1/\tau_2\end{bmatrix}\begin{bmatrix}x_1\\ x_2\\ x_3\\ x_4\\ x_5\end{bmatrix}+\begin{bmatrix}0\\ 0\\ \alpha\delta V_{max}/I_r\\ 0\\ 0\end{bmatrix}\frac{\delta V}{\delta V_{max}}+$$

$$\begin{bmatrix}0\\ 0\\ 0\\ 1/\tau_1\\ 1/\tau_1\tau_2\end{bmatrix}[\delta\beta]$$

$$y=[0\quad c_1\quad 0\quad 0\quad 0]\begin{bmatrix}x_1\\ x_2\\ x_3\\ x_4\\ x_5\end{bmatrix}+[0]\frac{\delta V}{\delta V_{max}}+[0][\delta\beta]$$

$$z=\begin{bmatrix}0 & 1/\delta\Omega_{max} & 0 & 0 & 0\\ 0 & 0 & 0 & 0 & 0\\ 0 & 0 & 0 & 0 & 1/\dot{\beta}_{max}\end{bmatrix}\begin{bmatrix}x_1\\ x_2\\ x_3\\ x_4\\ x_5\end{bmatrix}+\begin{bmatrix}0\\ 0\\ 0\end{bmatrix}\frac{\delta w}{\delta w_{max}}+\begin{bmatrix}0\\ 1/\delta\beta_{max}\\ 0\end{bmatrix}[\delta\beta]\quad (4.3)$$

The states in the realization of Eq. 4.3 are:

x_1 : drive-train torsion $(\theta_r-\theta_g)$,

x_2 : generator speed variation $(\delta\Omega_{\mathrm{g}})$,

x_3 : drive-train torsion rate $\left(\Omega_r-\Omega_g\right)\equiv(\dot{\theta}_r-\dot{\theta}_g)$,

x_4: pitch angle variation

x_5: rate of change of pitch angle

I_r and $I_g$represent the rotational inertia of the rotor and generator about the spin axis, respectively and $\frac{1}{I}=\frac{1}{I_r}+\frac{1}{I_g}$. The parameter γ is the partial derivative of the aerodynamic torque (T_a) with respect to rotor speed (Ω_{r}), $(\frac{\partial T_a}{\partial\Omega_{\mathrm{r}}}).\frac{\zeta}{I_r}$ is the pitch control input gain, in which ζ is the partial derivative of the aerodynamic torque with respect to the pitch angle(β), $(\frac{\partial T_a}{\partial\beta}).\frac{\alpha}{I_r}$ is the

disturbance input gain, in which α represents the partial derivative of rotor aerodynamic torque with respect to the wind speed (V) , $\frac{\partial T_a}{\partial V}$. K_d is the drive-train torsional spring constant and C_d is the torsional damping constant. The constant $\epsilon = \frac{P_{nom}}{\Omega_{g_r}^2 I_g}$, is the approximation of the partial derivative of the generator torque with respect to the generator speed in the vicinity of the rated generator speed (Ω_{g_r}). In fact, the constant ϵ represents the effect of the constant power strategy in the linearized model of wind turbine.

In order to provide a reasonable pitch activity with low rate of change at high wind speeds in Region III of wind turbine operation, we augmented the pitch angle variation and the rate of pitch angle change to the state-space model of wind turbine. We used first-order filters for measurement of the pitch angle variation and its rate of change to add these variables in the state-space model of wind turbine as given in the following

$$\dot{x}_4 = -\frac{1}{\tau_1} x_4 + \frac{1}{\tau_1} \delta\beta \tag{4.4}$$

$$\dot{x}_5 = -\frac{1}{\tau_2} x_5 + \frac{1}{\tau_2} x_4 \tag{4.5}$$

where, τ_1 and τ_2 are the time constants of the first order filters. Moreover, $\delta\Omega_{max}$, $\delta\beta_{max}$, $\dot{\beta}_{max}$, and δV_{max} are the maximum values of rotor speed variation, pitch angle variation, pitch angle rate of change, and wind speed variations, respectively. These constants are used to normalize the performance output and disturbance input vectors. The parameters of the NREL-Offshore-Baseline-5MW wind turbine which can be found in Jonkman *et al.* (2009) are used for simulation. NREL-Offshore-Baseline-5MW is a variable-speed variable-pitch (VS-VP) wind turbine with a nominal power rating of 5 MW, hub height of 90 m, and has three blades with rotor diameter of 126 m. The main parameters of the wind turbine are summarized in Tab. 4.1.

We used the FAST software to obtain the linear model of wind turbine at three different operating points at wind speeds of 12, 18, and 24 m/s. The numerical values of the state-space realization above at three different wind speeds in the rated power region (Region III) and also the constants, which we used to design a controller for our particular model of wind turbine (NREL-Offshore-Baseline-5MW) are given in the following list.

$$\tau_1 = 0.1sec\ ,\ \tau_2 = 0.1\ sec,\quad \delta\Omega_{max} = 0.0262\frac{rad}{sec},\quad \delta\beta_{max} = 0.1\ rad,\ \delta V_{max} = 3\frac{m}{s},$$

$$\dot{\beta}_{max} = 1\ rad/Sec \tag{4.6}$$

$$B_2 = \begin{bmatrix} 0 \\ 0 \\ 0 \\ 10 \\ 100 \end{bmatrix},\ C_{1,i} = \begin{bmatrix} 0 & 38.2 & 0 & 0 & 0 \\ 0 & 0 & 0 & 0 & 0 \\ 0 & 0 & 0 & 0 & 1 \end{bmatrix},\ D_{11,i} = \begin{bmatrix} 0 \\ 0 \\ 0 \end{bmatrix},\ D_{12} = \begin{bmatrix} 0 \\ 10 \\ 0 \end{bmatrix} \tag{4.7}$$

$$C_2 = [0 \quad 926.3 \quad 0 \quad 0 \quad 0],\qquad D_{21} = [0]\quad ,\qquad i = \{1,2,3\}$$

$$\Omega_{\mathrm{g_r}} = 1174\ rpm = 122.94\frac{rad}{sec},\ T_r = 43.09\ kN.m = 43094\ N.m \tag{4.8}$$

Operating point i=1: 12 m/s wind speed

$$A_1 = \begin{bmatrix} 0 & 0 & 1 & 0 & 0 \\ 172.6 & 0.6564 & 1.237 & 0 & 0 \\ -195 & -0.7232 & -1.464 & -0.4404 & 0 \\ 0 & 0 & 0 & -10 & 0 \\ 0 & 0 & 0 & -100 & -10 \end{bmatrix},\qquad B_{1,1} = \begin{bmatrix} 0 \\ 0 \\ 0.075 \\ 0 \\ 0 \end{bmatrix},$$

$$\beta_{op} = 3.968^o = 0.06925\ rad \tag{4.9}$$

Operating point i=2: 18 m/s wind speed

$$A_2 = \begin{bmatrix} 0 & 0 & 1 & 0 & 0 \\ 172.6 & 0.6564 & 1.237 & 0 & 0 \\ -195 & -0.9302 & -1.671 & -1.3362 & 0 \\ 0 & 0 & 0 & -10 & 0 \\ 0 & 0 & 0 & -100 & -10 \end{bmatrix},\qquad B_{1,2} = \begin{bmatrix} 0 \\ 0 \\ 0.0939 \\ 0 \\ 0 \end{bmatrix},$$

$$\beta_{op} = 14.9^o = 0.26005\ rad \tag{4.10}$$

Operating point i=3 : 24 m/s wind speed

$$A_3 = \begin{bmatrix} 0 & 0 & 1 & 0 & 0 \\ 172.6 & 0.6564 & 1.237 & 0 & 0 \\ -195 & -1.2155 & -1.9562 & -2.0571 & 0 \\ 0 & 0 & 0 & -10 & 0 \\ 0 & 0 & 0 & -100 & -10 \end{bmatrix}, \quad B_{1,3} = \begin{bmatrix} 0 \\ 0 \\ 0.1158 \\ 0 \\ 0 \end{bmatrix},$$

$$\beta_{op} = 22.05^o = 0.38485\, rad \tag{4.11}$$

Table 4.1 NREL-Offshore-Baseline-5MW wind turbine characteristics.

Rating	5 MW
Rotor Orientation, Configuration	Upwind, 3 Blades
Control	Variable Speed, Variable Pitch
Rotor, Hub Diameter	126 m, 3 m
Hub Height	90 m
Cut-In, Rated, Cut-Out Wind Speed	3 m/s, 11m/s, 25 m/s
Cut-In, Rated Rotor Speed	6.9 rpm, 12.1 rpm
Rotor Mass	110,000 kg
Optimal Tip-Speed-Ratio	7.55
Rated Generator Torque	43,100 Nm
Maximum Generator Torque	47,400 Nm
Rated Generator Speed	1174 RPM

The value of pitch angle at different steady operating points (β_{op}) is interpolated as a function of wind speed, V as given below

$$\beta_{op}(V) = aV^2 + bV + c \tag{4.12}$$

$$a = -0.000917,\ b = 0.05930,\ c = -0.51035 \tag{4.13}$$

In Ch. 2, we developed the ℓ_1-optimal control design for discrete-time systems. In order use our proposed procedure for wind turbine system, we need to transform the state-space realizations above to discrete-time. We can develop the discrete-time state-space realization of the wind turbine by a first order approximation of the equations. The new discrete-time system matrices can be related to the continues-time matrices as follows

$$A_d = I + \Delta t \times A \ , \quad B_{1,d} = \Delta t \times B_1, \ B_{2,d} = \Delta t \times B_2 \tag{4.14}$$

where, A_d, $B_{1,d}$, and $B_{2,d}$ are the discrete-time system matrices, I is the identity matrix same size as A, and Δt is the sampling time which can be arbitrarily chosen a small value for more accurate approximation. The order of error in the approximation is proportional with Δt^1. The other system matrices are exactly the same for discrete-time and continue –time systems.

4.2 Gain-Scheduled ℓ_1-Optimal Control

In this study we used the gain-scheduling technique proposed in Bianchi and Sanchez-Pena (2011) for interpolation of individually optimized local controllers. This approach provides guaranteed stability and its advantage over LPV approach is that we can design local controllers for each operating point individually for optimized performance. Also LPV method results in high-order controllers and derivation of the optimal controller demands a high computational effort. As discussed in Ch. 2, we proposed a new computationally efficient method for approximation of the ℓ_1-norm of discrete-time system. We used this new method to derive the ℓ_1-optimal controller using genetic algorithm (GA). Therefore, we found the discrete-time equivalent of the theory presented in Bianchi and Sanchez-Pena (2011) for interpolation of gain-scheduled controllers. In the following, we present the theory for discrete-time systems.

The nonlinear dynamics of a system can be discribed by a set of linear models at each operating point as

$$G_i: \begin{cases} x(k+1) = A_i x(k) + B_{1,i} w(k) + B_2 u(k) \\ z(k) = C_{1,i} x(k) + D_{11,i} w(k) + D_{12} u(k) \\ y(k) = C_2 x(k) + D_{21} w(k) \end{cases} \tag{4.15}$$

The operation region is parameterized by a set of points $\rho_i \in \{\rho_1, \dots, \rho_{n_p}\}$, that divides the region $\mathcal{P}$ into a set of sub-regions $\mathcal{P}_j$ defined by the vertices $\nu_j \subseteq \{\rho_1, \dots, \rho_{n_p}\}$. Any point $\rho \in \mathcal{P}_j$ can be expressed as a convex combination of vertices ν_j, *i.e.*,

$$\rho = \sum_{i=1}^{n_p} \alpha_i \rho_i \tag{4.16}$$

where, $\sum_{i=1}^{n_p} \alpha_i = 1$ and $\alpha_i \geq 0,\ \forall \rho_i \in \nu_j,\ \alpha_i = 0,\ \forall \rho_i \notin \nu_j$. The parameterized model of the system can be described by a linear combination of state-space realizations corresponding to the vertices ν_j

$$G(\rho): \begin{cases} x(k+1) = A(\rho)x(k) + B_1(\rho)w(k) + B_2 u(k) \\ z(k) = C_1(\rho)x(k) + D_{11}(\rho)w(k) + D_{12}u(k) \\ y(k) = C_2 x(k) + D_{21} w(k) \end{cases} \tag{4.17}$$

where

$$\begin{bmatrix} A(\rho) & B_1(\rho) \\ C_1(\rho) & D_{11}(\rho) \end{bmatrix} = \sum_{i=1}^{n_p} \alpha_i(\rho) \begin{bmatrix} A_i & B_{1,i} \\ C_{1,i} & D_{11,i} \end{bmatrix} \tag{4.18}$$

$\alpha_i(\rho)$ is the coordinate corresponding to ρ_i. In this model, B_2, D_{12}, C_2, D_{21} are assumed to be constant. However, when they are parameter time-varying, a method to enforce these requirements consists of filtering the control input and the output through low-pass filters having sufficiently large bandwidths. By this technique, the parameter trajectory is shifted into the state matrix $A(\rho)$ (Bianchi and Sanchez-Pena, 2011). Stabilizing controllers with optimized performance can be designed independently at each plant G_i

$$C_i: \begin{cases} x_c(k+1) = A_c(\rho)x_c(k) + B_c(\rho)y(k) \\ u = C_c(\rho)x_c + D_c(\rho)y \end{cases} \tag{4.19}$$

$$C_i: \begin{cases} x_c(k+1) = A_{c,i}x_c(k) + B_{c,i}y(k) \\ u(k) = C_{c,i}x_c(k) + D_{c,i}y(k) \end{cases} \qquad i = 1, \dots, n_p \tag{4.20}$$

Then, the objective is to formulate an interpolation for local state-space realization such that the gain-scheduled controller

$$C(\rho):\begin{cases} x_c(k+1) = A_c(\rho)x_c(k) + B_c(\rho)y(k) \\ u(k) = C_c(\rho)x_c(k) + D_c(\rho)y(k) \end{cases} \tag{4.21}$$

stabilizes the plant $G(\rho)$ at any point $\rho \in \mathcal{P}$. Note that the order of $C(\rho)$ is different from order of local controllers.

In the following, a systematic method to find the interpolation of the local controllers is presented. The gain-scheduled controller stabilizes the system $G(\rho)$ at any point $\rho \in \mathcal{P}$. This interpolation improves the performance at design points while the stability and performance level are guaranteed during the transition between controllers. Also, an LMI method is used to optimize the ℓ_1 performance at intermediate points that guarantees certain performance level at intermediate points. The following theorem gives the gain-scheduled controller that stabilizes system at all points. The proof of this theorem can be found in Appendix A.

Theorem 4.1: *Given a set of linear plants and a set of stabilizing controllers, if there exists positive definite matrices X_1, $X_{2,i}$, and X_3, and matrices V_i and W_i, such that*

$$\begin{bmatrix} X_1 & X_1A_i + W_iC_2 \\ (X_1A_i + W_iC_2)^T & X_1 \end{bmatrix} > 0 \tag{4.22}$$

$$\begin{bmatrix} X_{2,i} & A_{q,i} \\ A_{q,i}^T & X_{2,i} \end{bmatrix} > 0 \tag{4.23}$$

$$\begin{bmatrix} X_3 & (A_iX_3 + B_2V_i) \\ (A_iX_3 + B_2V_i)^T & X_3 \end{bmatrix} > 0 \tag{4.24}$$

for all $i = 1, \dots, n_p$

$$A_{q,i} = \begin{bmatrix} A_i + B_2D_{c,i}C_2 & B_2C_{c,i} \\ -B_{c,i}C_2 & A_{c,i} \end{bmatrix} \tag{4.25}$$

then, the following gain-scheduled controller stabilizes plant for all $\rho \in \mathcal{P}$, and its state-space matrices are

$$A_C(\rho) = \sum_{i=1}^{n_p} \alpha_i(\rho) \begin{bmatrix} A_i + B_2 F_i + H_i C_2 - B_2 D_{c,i} C_2 & B_2 \tilde{C}_{q,i} \\ -\tilde{B}_{q,i} C_2 & A_{q,i} \end{bmatrix}$$

$$B_C(\rho) = \sum_{i=1}^{n_p} \alpha_i(\rho) \begin{bmatrix} B_2 D_{c,i} - H_i \\ \tilde{B}_{q,i} \end{bmatrix}$$

$$C_C(\rho) = \sum_{i=1}^{n_p} \alpha_i(\rho) \begin{bmatrix} F_i - D_{c,i} C_2 & \tilde{C}_{q,i} \end{bmatrix}$$

$$D_C(\rho) = \textstyle\sum_{i=1}^{n_p} \alpha_i(\rho) D_{c,i} \tag{4.26}$$

$$\tilde{A}_{q,i} = T_i A_{q,i} T_i^{-1}, \qquad \tilde{B}_{q,i} = T_i \begin{bmatrix} B_2 D_{c,i} - H_i \\ B_{c,i} \end{bmatrix}, \qquad \tilde{C}_{q,i} = \begin{bmatrix} D_{c,i} C_2 - F_i & C_{c,i} \end{bmatrix} T_i^{-1}$$

$$T_i = X_{2,i}^{1/2}\ ,\ F_i = V_i X_3^{-1},\ H_i = X_1^{-1} W_i\ ,\ (i = 1, \dots, n_p) \tag{4.27}$$

The gain-scheduling technique suggested in Bianchi and Sanchez-Pena (2011), can address the performance level at intermediate points in addition to guaranteed stability.

In the following, the problem setup for optimization of the gain-scheduled controller is addressed using LMI approach. It results in achieving the best ℓ_1 performance possible in the intermediate points without degrading the performance at the design points. For the $\mathcal{H}_\infty$ performance case, the LMIs constraints were derived in Bianchi and Sanchez-Pena (2011). We used the same procedure to drive the LMIs for ℓ_1 performance. In the following theorem, the LMI constraints for ℓ_1 performance optimization are discussed. Imposing a block-diagonal structure on X_{cl}, at the expense of certain conservatism, the research for realization reduces to the following result.

Theorem 4.2: *Given a set of plants and a set of controllers,* $\left\|\mathcal{F}_l\left(G_i(s), C_i(s)\right)\right\|_1 \leq \gamma_i$. *If there exist positive definite matrices* $X_1, X_{2,i}$, *and* X_3, *real parameters* $\lambda > 0$ *and* $\mu > 0$, *matrices* F_i *and* H_i $(i = 1, \dots, n_p)$, *such that* n_p *matrix inequalities below are satisfied, then the controller with the state-space presented in theorem 4.1, quadratically stabilizes the plant for any point* $\rho \in \mathcal{P}$, *and guaranties a performance level* $\|z\|_1 \leq \sqrt{q}\gamma\|w\|_1$, *with* $\gamma_i \leq \sqrt{q}\gamma$, $(i = 1, \dots, n_p)$, *and* q *is the number of control inputs.*

$$\begin{bmatrix} \left(X_1 A_{H,i}\right)^T + X_1 A_{H,i} + \lambda X_1 & \left(B_{q,i} C_2\right)^T X_2 & C_2 B_{H,i}^T & X_1 B_{1,i} + X_1 H_i D_{21} \\ X_{2,i} B_{q,i} C_2 & \left(X_{2,i} A_{q,i}\right)^T + X_2 A_{q,i} + \lambda X_{2,i} & \left(B_2 C_{q,i}\right)^T & X_{2,i} B_{q,i} D_{21} \\ B_{H,i} C_2 & B_2 C_{q,i} & \left(A_{F,i} X_3\right)^T + A_{F,i} X_3 + \lambda X_3 & B_{H,i} D_{21} \\ \left(X_1 B_{1,i} + X_1 H_i D_{21}\right)^T & \left(X_{2,i} B_{q,i} D_{21}\right)^T & \left(B_{H,i} D_{21}\right)^T & -\mu I \end{bmatrix} < 0 \quad (4.28)$$

$$\begin{bmatrix} \lambda X_1 & 0 & 0 & 0 & \left(C_{1,i} + D_{12} D_{c,i} C_2\right)^T \\ 0 & \lambda X_{2,i} & 0 & 0 & \left(D_{12} C_{q,i}\right)^T \\ 0 & 0 & \lambda X_3 & 0 & \left(C_{F,i} X_3\right)^T \\ 0 & 0 & 0 & (\gamma - \mu) I & \left(D_{11,i} + D_{12} D_{c,i} D_{21}\right)^T \\ C_{1,i} + D_{12} D_{c,i} C_2 & D_{12} C_{q,i} & C_{F,i} X_3 & D_{11,i} + D_{12} D_{c,i} D_{21} & \gamma I \end{bmatrix} < 0 \quad (4.29)$$

where

$$A_{q,i} = \begin{bmatrix} A_i + B_2 D_{c,i} C_2 & B_2 C_{c,i} \\ -B_{c,i} C_2 & A_{c,i} \end{bmatrix}, \quad B_{q,i} = \begin{bmatrix} B_2 D_{c,i} - H_i \\ B_{c,i} \end{bmatrix}, \quad C_{q,i} = \begin{bmatrix} D_{c,i} C_2 - F_i & C_{c,i} \end{bmatrix}$$

$$A_{H,i} = A_i + H_i C_2,\ A_{F,i} = A_i + B_2 F_i,\ B_{H,i} = B_2 D_{q,i} - H_i,\ C_{F,i} = C_{1,i} + D_{12} F_i \quad (4.30)$$

Note that Theorem 4.2 is presented for continuous-time systems. Also, the matrix inequalities above produce a non-convex problem, because some terms in the inequalities in Eqs.

4.28-4.29 involve multiplication of matrix variables. Therefore, the variables cannot be found simultaneously using an LMI approach. Nevertheless, note that I/O behavior at all vertices are unaffected by particular selection of H_i and F_i based on Youla parameterization results. Therefore, it is sensible to replace the matrices obtained from the stabilization problem in Theorem 4.1 (Bianchi and Sanchez-Pena, 2011). Moreover, the terms λX_j $(j = \{1, 2, 3\})$ are non-linear. However, the problem can be solved as follows:

1) Given the controllers $C_i(s)$, find X_1, X_3, and the n_p variables V_i and W_i satisfying the LMIs in theorem 4.1, and compute $F_i = V_i X_3^{-1}$ and $H_i = X_1^{-1} W_i$ $(i = 1, \dots, n_p)$.

2) Assign the previous computed F_i and H_i in the LMIs in theorem 4.2 and find X_1, X_3, and the n_p variables $X_{2,i}$.

3) For fixed $\lambda > 0$, solve the obtained linear matrix inequalities, if the LMIs are infeasible, one has to pick another. If the LMIs are feasible, the bound γ on the peak-to-peak norm has been assured.

4) To find the best possible upper bound on the peak-to-peak norm, perform a line-search over $\lambda > 0$ under the LMI constraints to minimize $\gamma^*(\lambda)$, the minimal value of γ if $\lambda > 0$ is held fixed. The line search leads to the best upper bound

$$\gamma^u = \inf_{\lambda > 0} \gamma^*(\lambda) \tag{4.31}$$

4.3 Obtaining the ℓ_1-Optimal Controllers Using Genetic Algorithms

In order to derive the optimized local controllers at each operating point (at wind speeds of 12, 18, and 24 m/s), we used the Matlab optimization toolbox to find the matrices of output feedback controller. We used the genetic algorithm (GA) method to search for optimal parameters. The ℓ_1 norm of the output feedback controlled closed-loop system is the objective function for optimization. The number of optimization parameters (the value of matrices in the state-space model of output feedback controller) depends on the order of the output feedback controller. In the GA optimization, in each evaluation, some values are assigned to the control parameters, and the value of ℓ_1 norm of the closed-loop system is calculated. The new method which was suggested in Ch. 2, decreases the computation time for evaluation of ℓ_1 norm, so that the time and calculations required for GA optimization decreases significantly.

Some details regarding the options for genetic algorithm solver in MATLAB optimization toolbox are given in the following. The population type is set to be double vector. Population type specifies the type of the input to the fitness function. The population size can change in a wide range. For this problem, population size of 100 to 500 was chosen. Uniform function was used to create the initial population. Uniform function creates a random initial population with a uniform distribution. We can specify the initial score and initial range of variables. However we used default for these options. The scaling function specifies the function that performs the scaling. We chose rank function which scales the row scores based on the rank of each individual rather than its score. The rank of an individual is its position in the sorted scores. The selection function chooses parents for the next generation based on their scaled values from the fitness scaling function. We chose stochastic uniform selection function which

lays out a line in which each parent corresponds to a section of the line of length proportional to its expectation. Elite count was set to 2. It specifies the number of individuals that are guaranteed to survive to the next generation. 0.8 was chosen for crossover fraction which specifies the fraction of the next generation that crossover produces. Mutation produces the remaining individuals in the next generation. The Gaussian mutation function chosen for the problem in this study. Mutation functions make small random changes in the individuals in the population, which provide genetic diversity and enable the genetic algorithm to search a broader space. Gaussian adds a random number to each vector entry of an individual. This random number is taken from a Gaussian distribution centered on zero. Crossover combines two individuals, or parents, to form a new individual, or child, for the next generation. We chose scattered crossover function which creates a random binary vector. Then selects the genes where the vector is a 1 from the first parent, and the genes where the vector is a 0 from the second parent, and combines the genes to form the child. Stopping criteria determines what causes the algorithm to terminate. Number of generations and stall generation were set to 1000. Generations specifies the maximum number of iterations the genetic algorithm performs. If the weighted average change in the fitness function value over stall generations is less than function tolerance, the algorithm stops. The function tolerance was set to e-6. The time limit was set to infinity.

We found the first order and the second order output feedback ℓ_1-optimal controllers for each operating point. As the higher order controllers did not improve the ℓ_1 performance, it is preferred to use lower order controllers (first order in this case). Note that, although the local controllers are first order, the interpolated gain-scheduled controller has higher order (in the wind turbine case, the order of controller is 11) as expressed in Theorem 4.1. The system matrices of the first-order controllers which we obtained and also the best value of ℓ_1-norm at each operating

point are given in the following. In the next chapter, we present the simulation results of implementing the gain-scheduled ℓ_1-optimal controller on the non-linear model of wind turbine using FAST software.

Operating point i=1 : 12 m/s wind speed

$$A_{c,1} = [0.7087], \quad B_{c,1} = [0.2417], \quad C_{c,1} = [0.0382], \quad D_{c,1} = [-0.0310],$$
$$\gamma_1 = 13.1855 \tag{4.32}$$

Operating point i=2: 18 m/s wind speed

$$A_{c,2} = [0.7107], \quad B_{c,2} = [0.2091], \quad C_{c,2} = [0.0176], \quad D_{c,2} = [-0.0113],$$
$$\gamma_2 = 6.2164 \tag{4.33}$$

Operating point i=3 : 24 m/s wind speed

$$A_{c,3} = [0.7113], \quad B_{c,3} = [0.0867], \quad C_{c,3} = [0.0292], \quad D_{c,3} = [-0.0077],$$
$$\gamma_3 = 7.1099 \tag{4.34}$$

where, $A_{c,i}$, $B_{c,i}$, $C_{c,i}$, and $D_{c,i}$ $i = \{1,2,3\}$ are system matrices of optimized local controllers and γ_i is the ℓ_1-norm of the closed loop system. Now, having the linear model of wind turbine at each operating point and the corresponding optimized local controllers, we can use Theorem 4.1, to find the stabilizing gain-scheduled controller for wind turbine system. We used Matlab software to find feasible solutions for LMI constrains in Theorem 4.1. Then, LMI variables can be used to derive the interpolation for local controllers with guaranteed stability as presented in Theorem 4.1.

Chapter 5: Result of Simulation of Gain-Scheduled ℓ_1-Optimal Control on a 5MW Wind Turbine at High Wind Speeds

In this chapter, we present the simulation results. The proposed gain-scheduled ℓ_1-Optimal control is implemented on the model using a SIMULINK interface provided in the FAST software. The results are shown in the following figures. The specification of the 5MW wind turbine model we use for simulation was given in Tab. 4.1. Wind inputs to these simulations are TurbSim-generated (Jonkman and Buhl, 2006) 24×24 grids of IEC Class A Kaimal-spectrum turbulence, sampled every 50ms, with a logarithmic vertical wind profile corresponding to a roughness length of 3 cm. Each simulation is 600 seconds in length; results are computed based on the final 500s of each simulation in order to eliminate the effect of initial conditions.

We performed the simulation for 6 different fully turbulent wind profiles with average speeds of 14, 16, 18, 20, 22, 24 m/s (in region III). We compared the performance of our proposed controller with a well-tuned PI controller. This PI-controller is developed by Jonkman *et al.* (2009) for the NREL-Offshore-Baseline-5MW model of wind turbine which we used for our simulation study. To quantify the power quality, rotor speed and generator torque fluctuations we used statistical standard deviations in order to compare the PI and ℓ_1 controls. Finally, the conclusion for this simulation study is presented at the end of this chapter.

5.1 Simulation results at Different Wind Speeds

Figs. 5.1-5.6 show the wind speed input (effectively a disturbance input to this system relative to a constant wind speed at the chosen operating condition), the rotor speed, the

generator torque (one control input), electrical power output and the blade pitch angle (second control input) for each of the following nominal wind speeds: 14, 16, 18, 20, 22 and 24 m/s. In all cases, both the ℓ_1 and PI control results are shown.

Simulation results for average wind speed of 14 m/s:

(a)

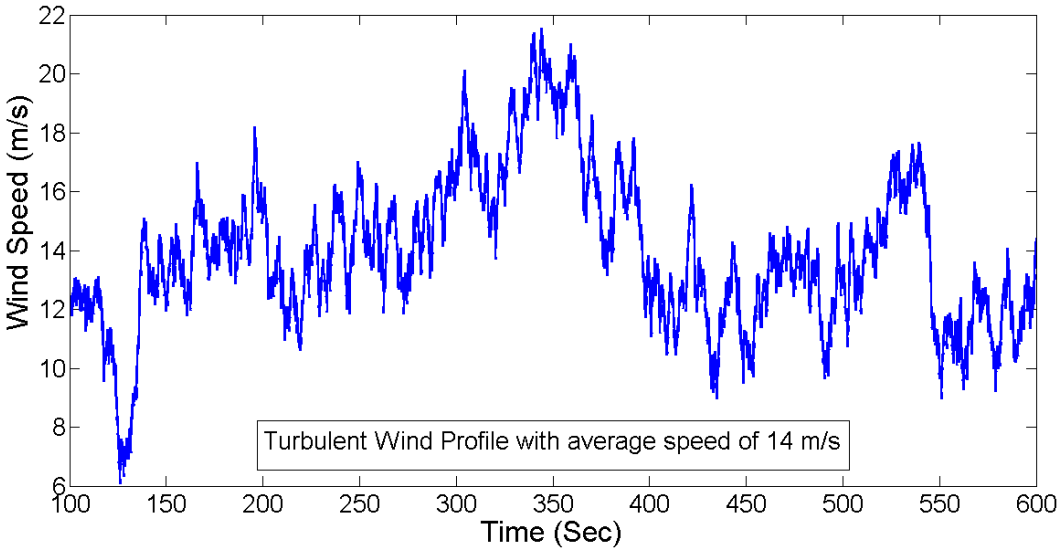

(b)

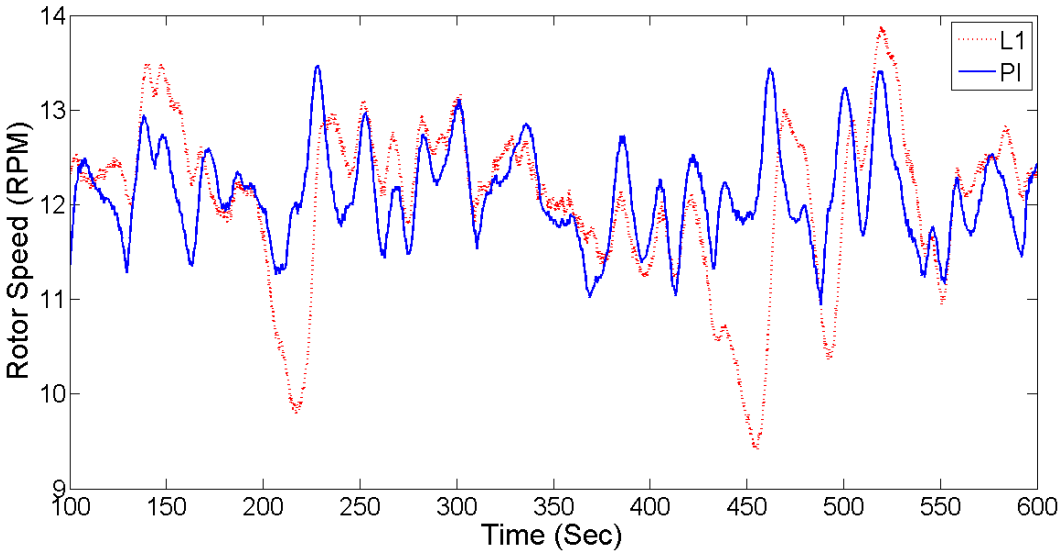

(c)

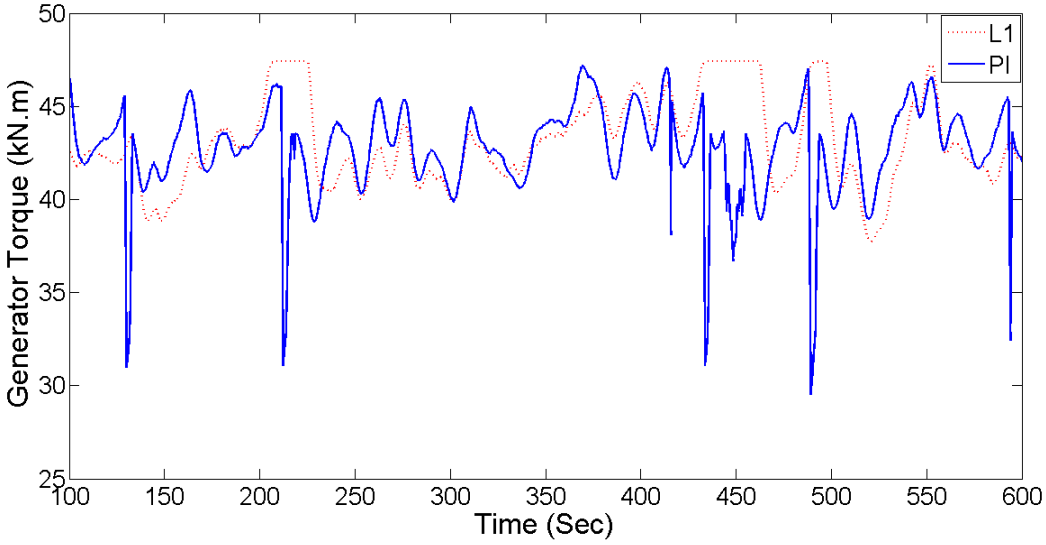
Generator Torque (kN.m)
Time (Sec)
L1
PI
50
45
40
35
30
25
100
150
200
250
300
350
400
450
500
550
600

(d)

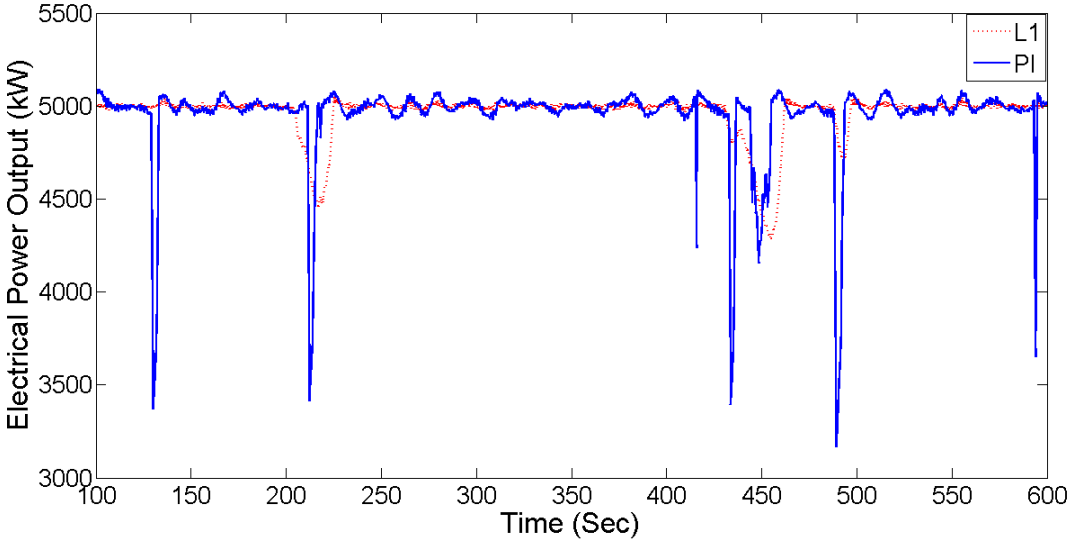
Electrical Power Output (kW)
Time (Sec)
L1
PI
5500
5000
4500
4000
3500
3000
100
150
200
250
300
350
400
450
500
550
600

(e)

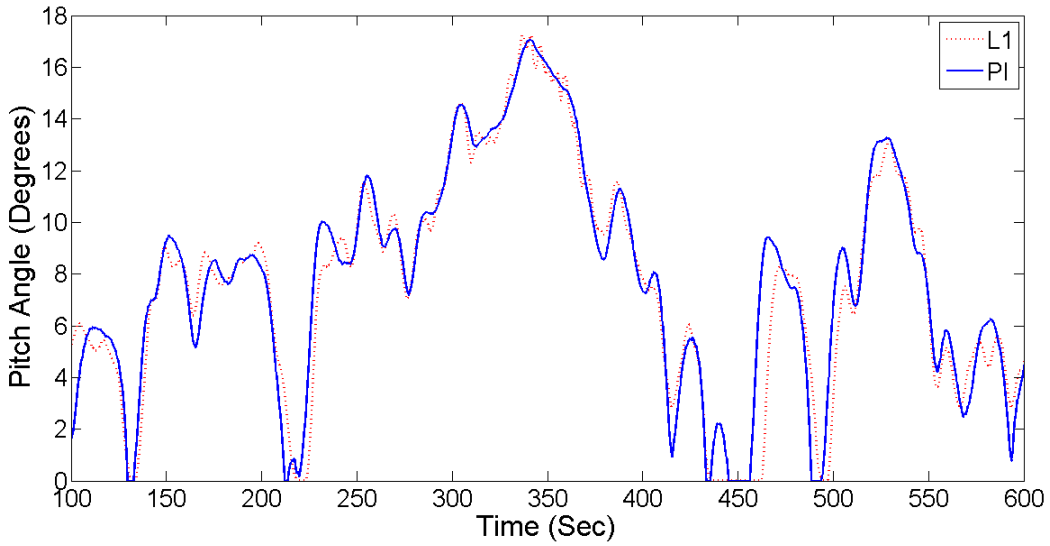

Figure 5.1 ℓ_1 and PI control of NREL-Offshore-Baseline-5 MW wind turbine in the rated power area (Region III) are compared at average wind speed of 14 m/s. (a) Wind speed profile, (b) Rotor speed, (c) Generator torque, (d) Electrical power output, and (e) Pitch angle are shown in a time interval of 10 minutes.

Simulation results for average wind speed of 16 m/s:

(a)

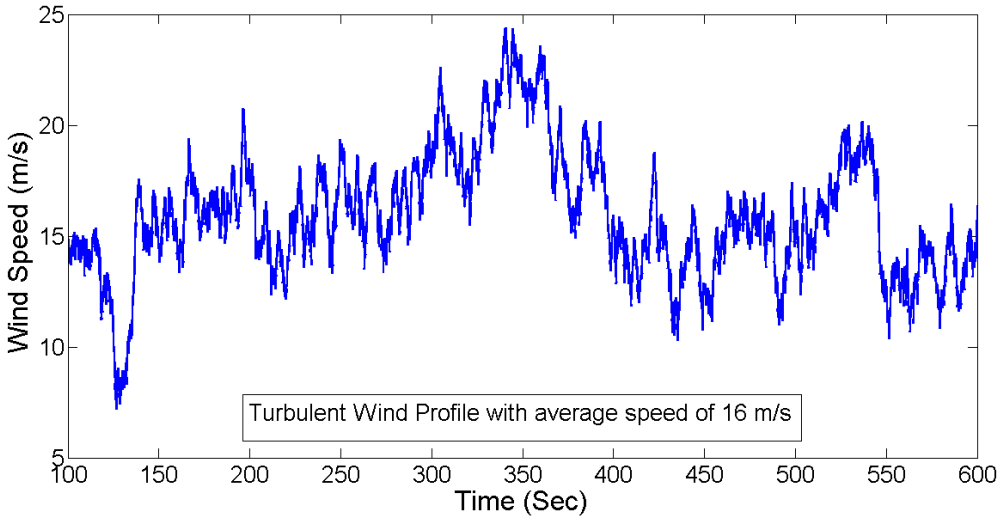

(b)

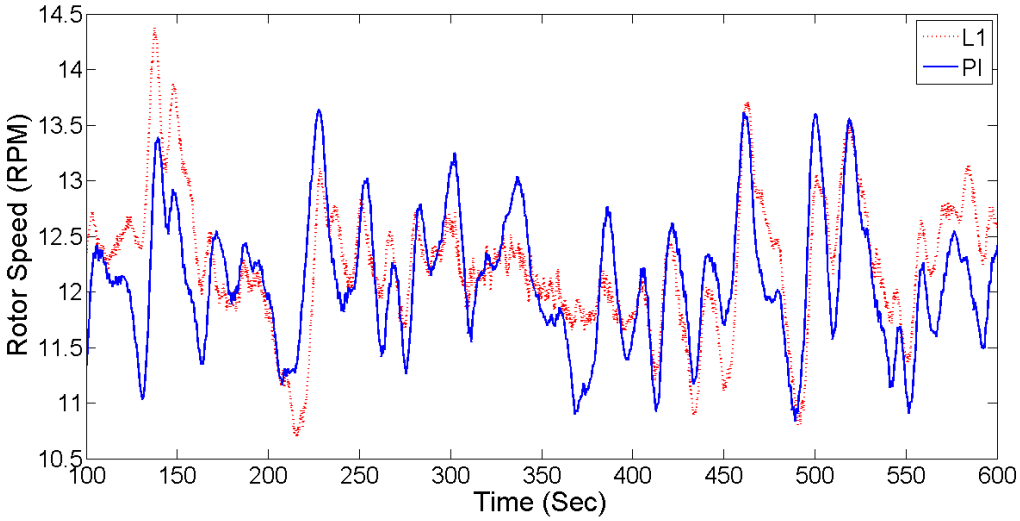
Rotor Speed (RPM)
Time (Sec)
L1
PI
14.5
14
13.5
13
12.5
12
11.5
11
10.5
100
150
200
250
300
350
400
450
500
550
600

(c)

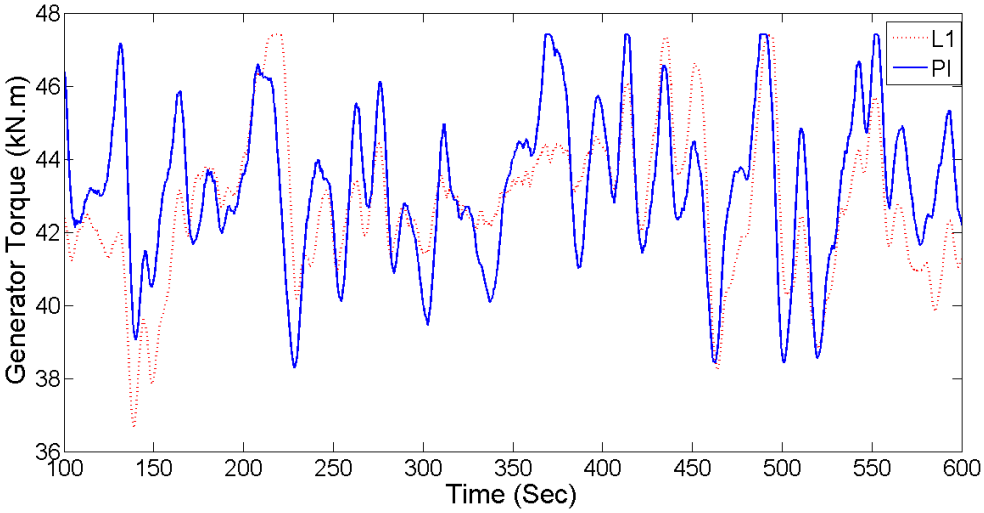
Generator Torque (kN.m)
Time (Sec)
L1
PI
48
46
44
42
40
38
36
100
150
200
250
300
350
400
450
500
550
600

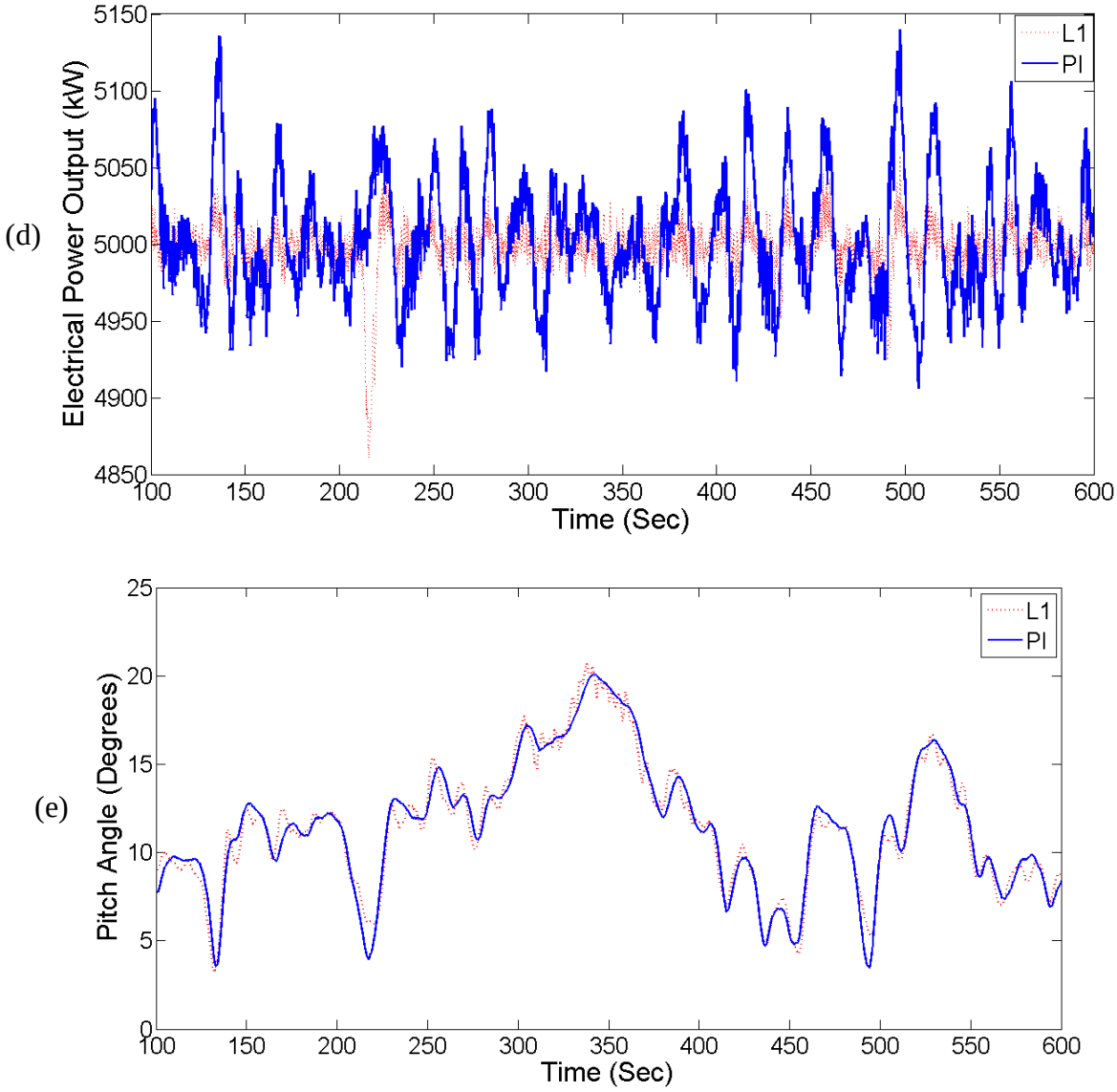

Figure 5.2 ℓ_1 and PI control of NREL-Offshore-Baseline-5 MW wind turbine in the rated power area (Region III) are compared at average wind speed of 16 m/s. (a) Wind speed profile, (b) Rotor speed, (c) Generator torque, (d) Electrical power output, and (e) Pitch angle are shown in a time interval of 10 minutes.

Simulation results for average wind speed of 18 m/s:

(a)

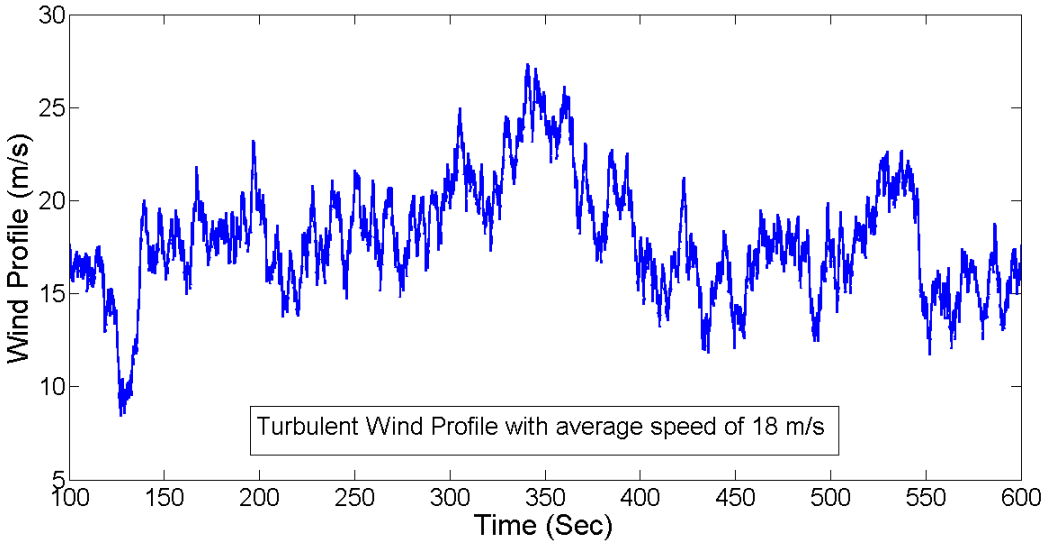

(b)

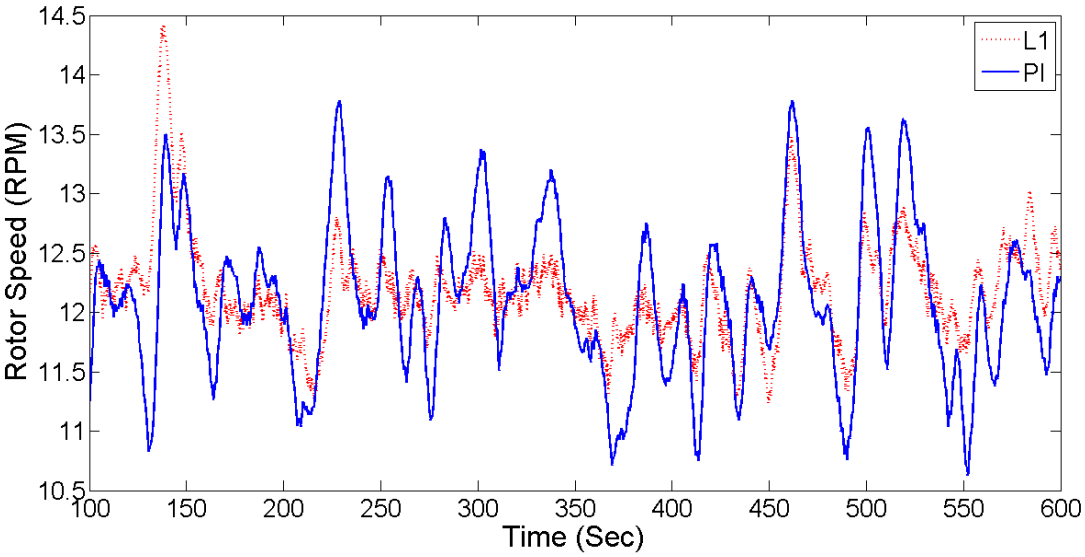

(c)

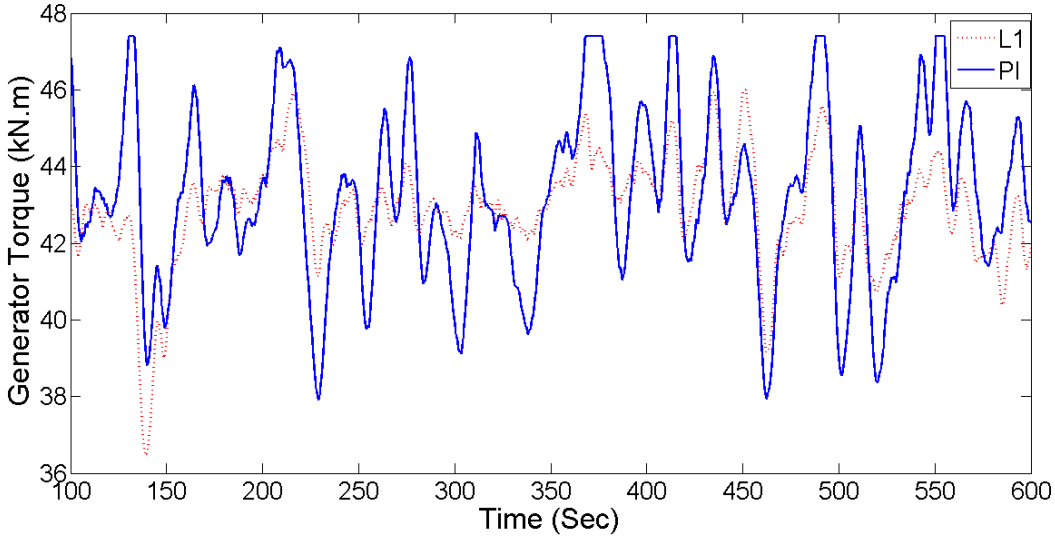
Generator Torque (kN.m)
Time (Sec)
L1
PI
48
46
44
42
40
38
36
100
150
200
250
300
350
400
450
500
550
600

(d)

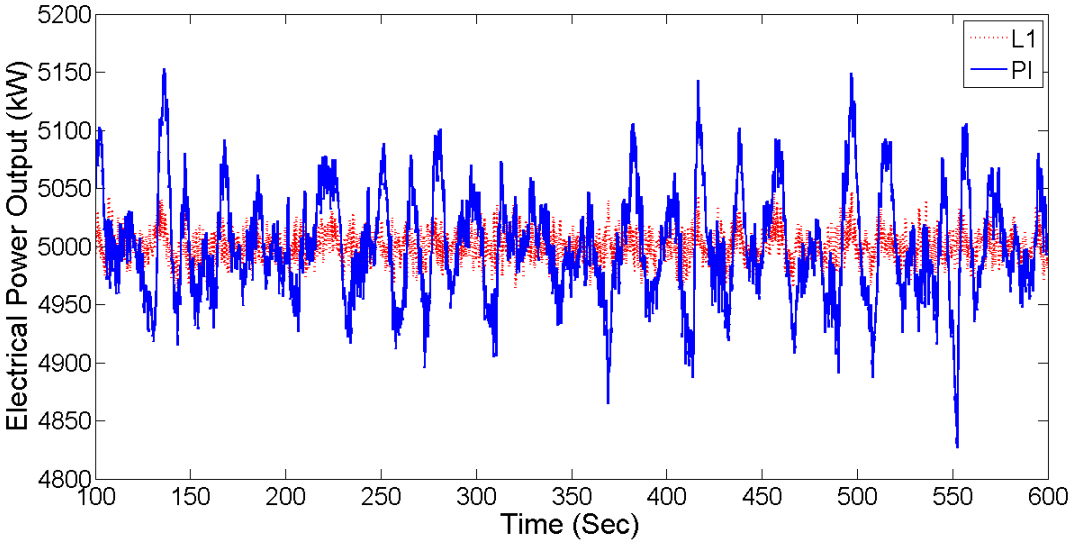
Electrical Power Output (kW)
Time (Sec)
L1
PI
5200
5150
5100
5050
5000
4950
4900
4850
4800
100
150
200
250
300
350
400
450
500
550
600

(e)

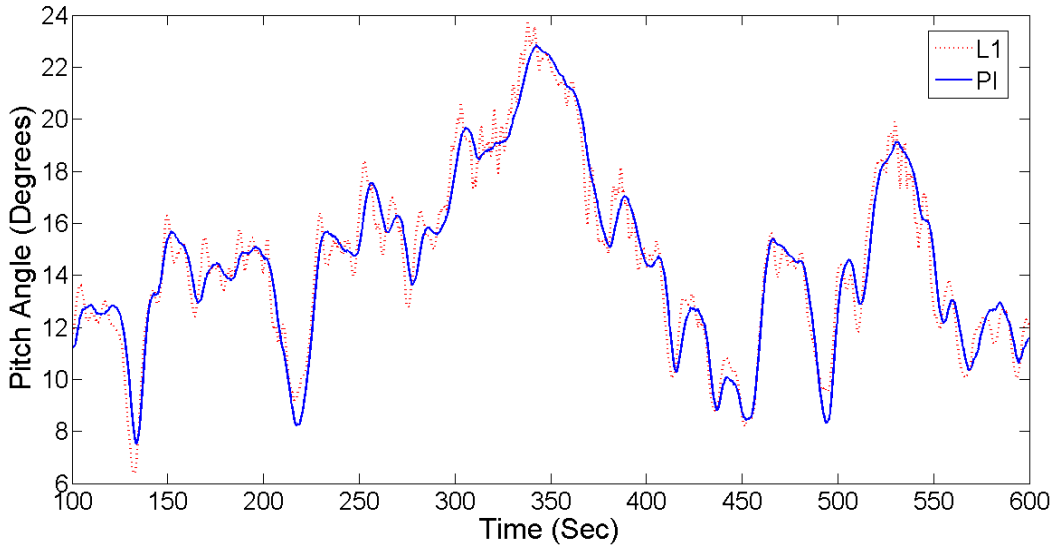

Figure 5.3 ℓ_1 and PI control of NREL-Offshore-Baseline-5 MW wind turbine in the rated power area (Region III) are compared at average wind speed of 18 m/s. (a) Wind speed profile, (b) Rotor speed, (c) Generator torque, (d) Electrical power output, and (e) Pitch angle are shown in a time interval of 10 minutes.

Simulation results for average wind speed of 20 m/s:

(a)

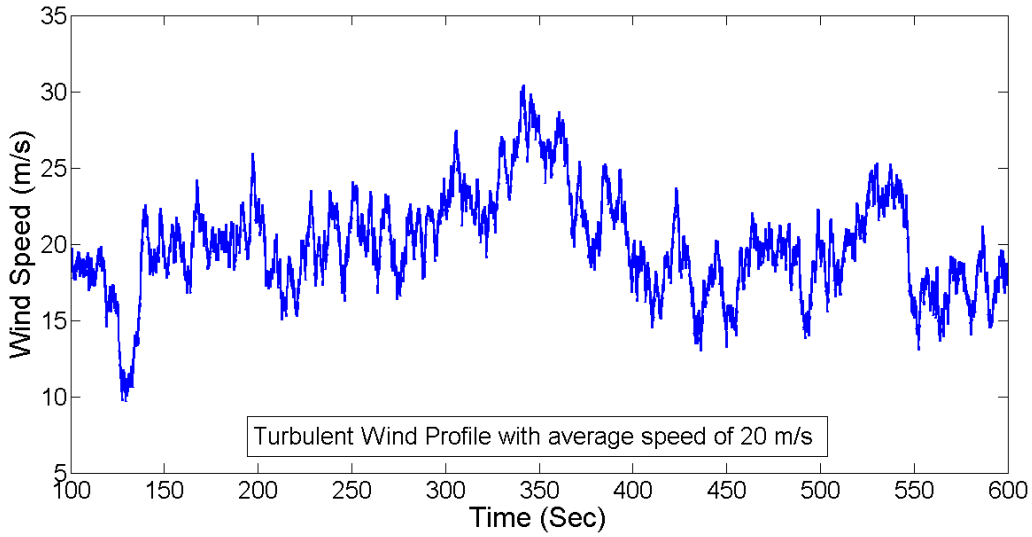

(b)

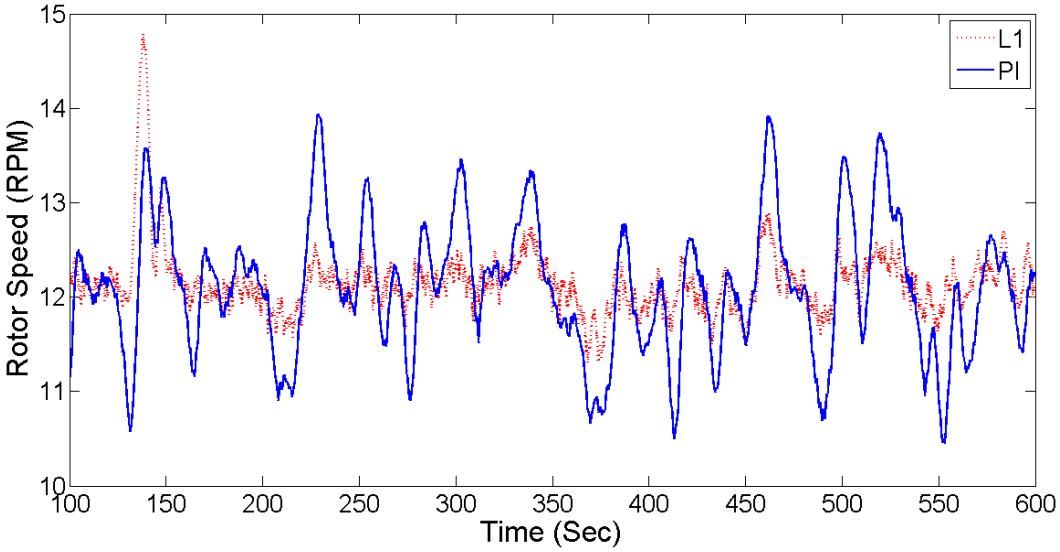
Rotor Speed (RPM)
Time (Sec)
L1
PI
15
14
13
12
11
10
100
150
200
250
300
350
400
450
500
550
600

(c)

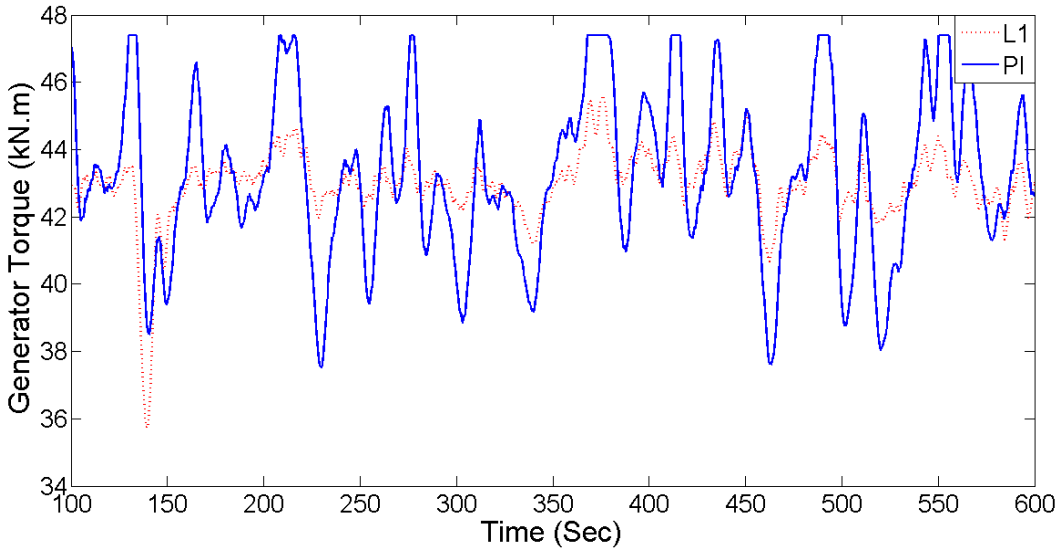
Generator Torque (kN.m)
Time (Sec)
L1
PI
48
46
44
42
40
38
36
34
100
150
200
250
300
350
400
450
500
550
600

(d)

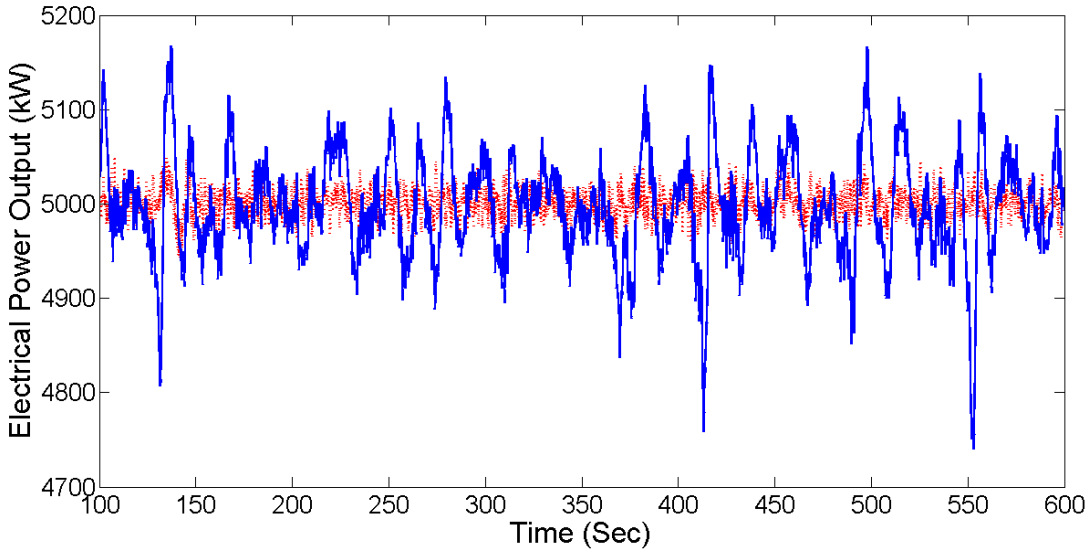

(e)

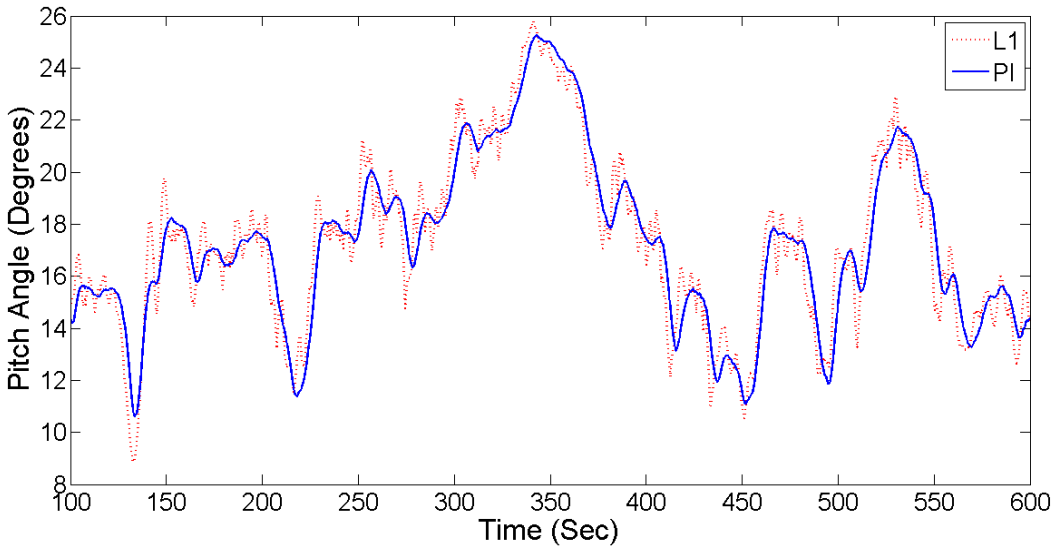

Figure 5.4 ℓ_1 and PI control of NREL-Offshore-Baseline-5 MW wind turbine in the rated power area (Region III) are compared at average wind speed of 20 m/s. (a) Wind speed profile, (b) Rotor speed, (c) Generator torque, (d) Electrical power output, and (e) Pitch angle are shown in a time interval of 10 minutes.

Simulation results for average wind speed of 22 m/s:

(a)

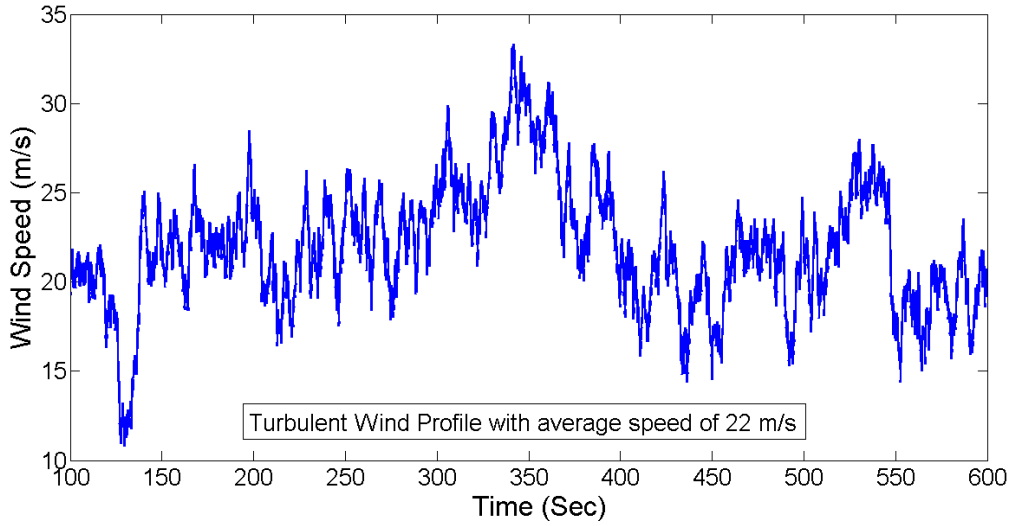

(b)

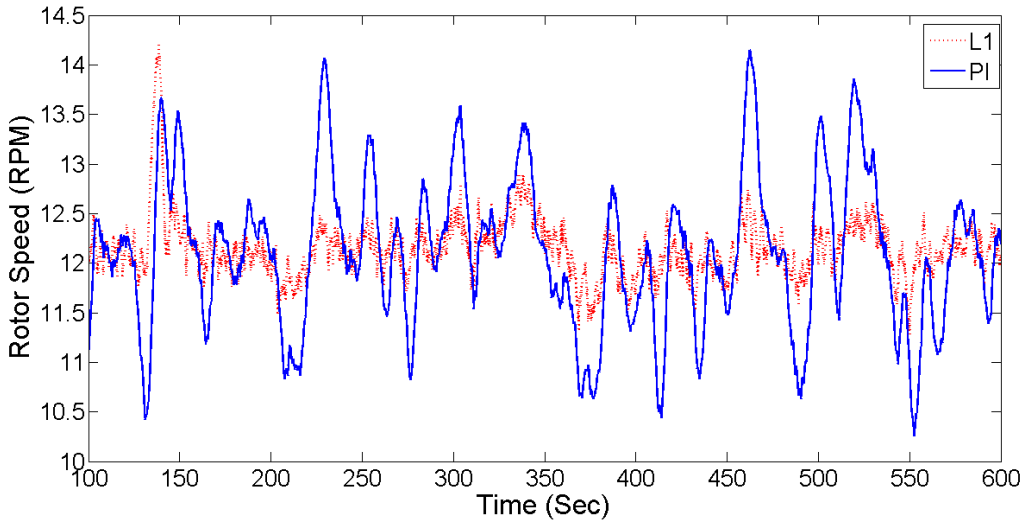

(c)

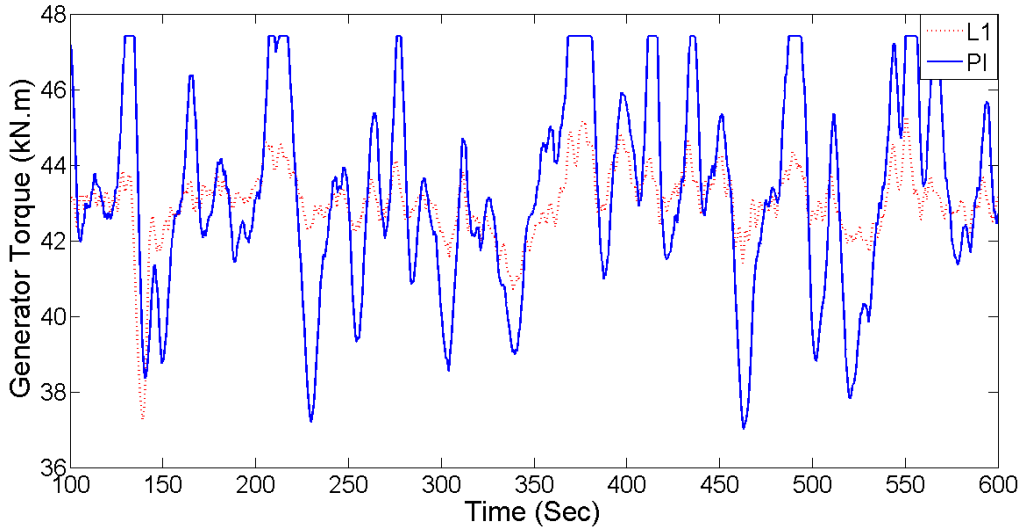
Generator Torque (kN.m)
Time (Sec)
L1
PI
48
46
44
42
40
38
36
100
150
200
250
300
350
400
450
500
550
600

(d)

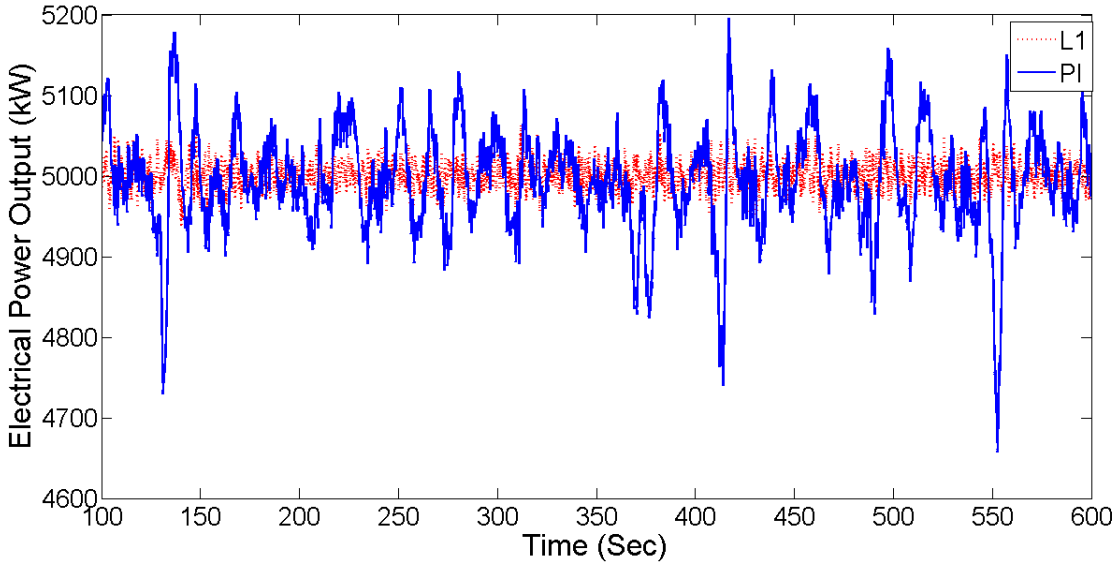
Electrical Power Output (kW)
Time (Sec)
L1
PI
5200
5100
5000
4900
4800
4700
4600
100
150
200
250
300
350
400
450
500
550
600

(e)

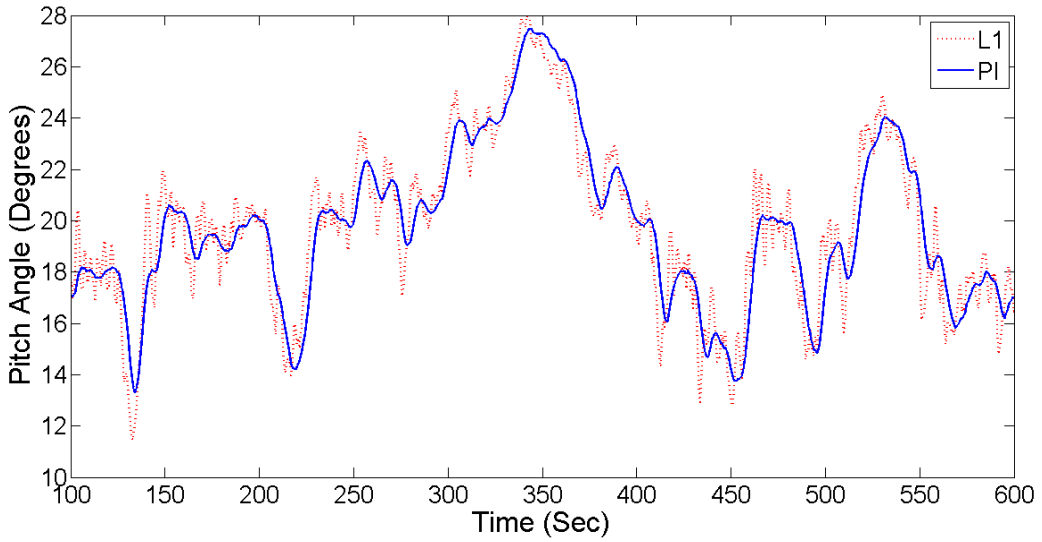

Figure 5.5 ℓ_1 and PI control of NREL-Offshore-Baseline-5 MW wind turbine in the rated power area (Region III) are compared at average wind speed of 22 m/s. (a) Wind speed profile, (b) Rotor speed, (c) Generator torque, (d) Electrical power output, and (e) Pitch angle are shown in a time interval of 10 minutes.

Simulation results for average wind speed of 24 m/s:

(a)

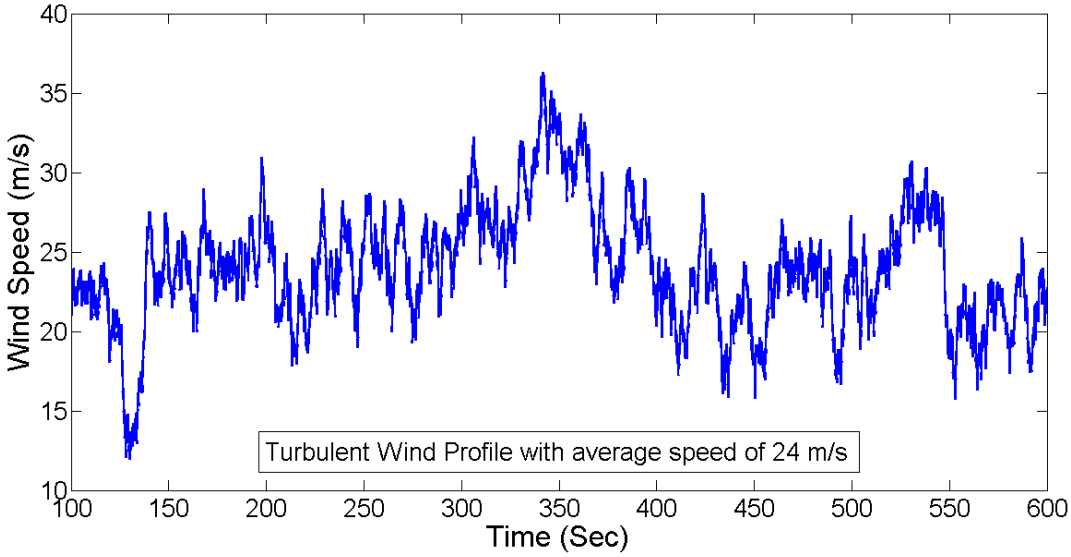

(b)

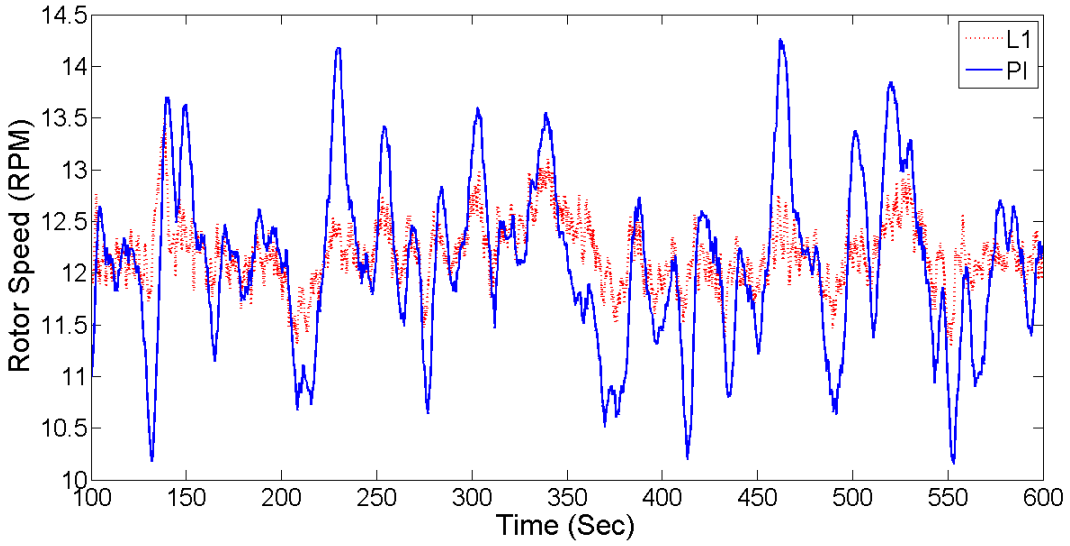
Rotor Speed (RPM)
Time (Sec)
L1
PI
14.5
14
13.5
13
12.5
12
11.5
11
10.5
10
100
150
200
250
300
350
400
450
500
550
600

(c)

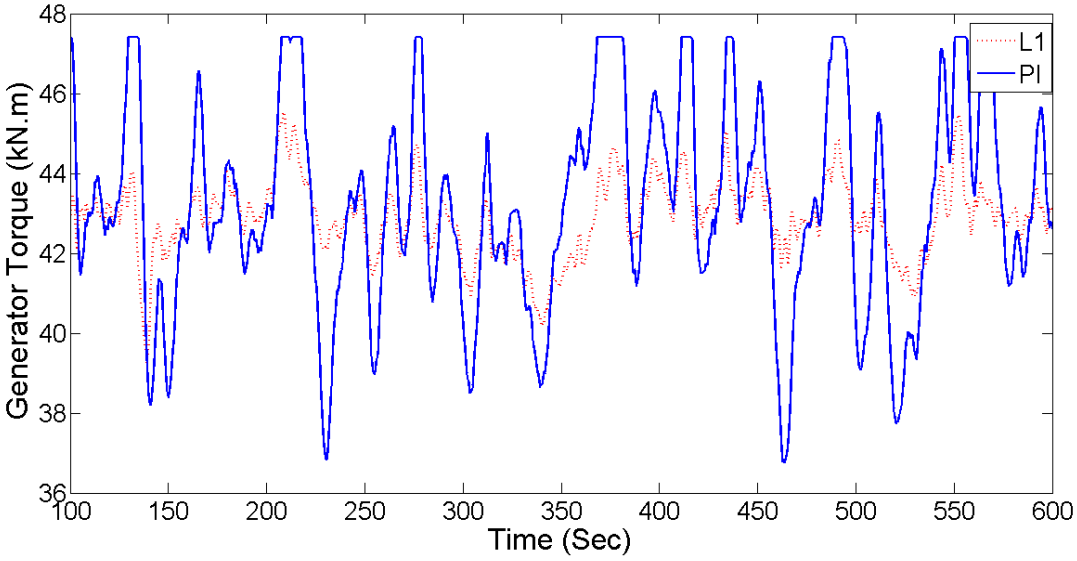
Generator Torque (kN.m)
Time (Sec)
L1
PI
48
46
44
42
40
38
36
100
150
200
250
300
350
400
450
500
550
600

(d)

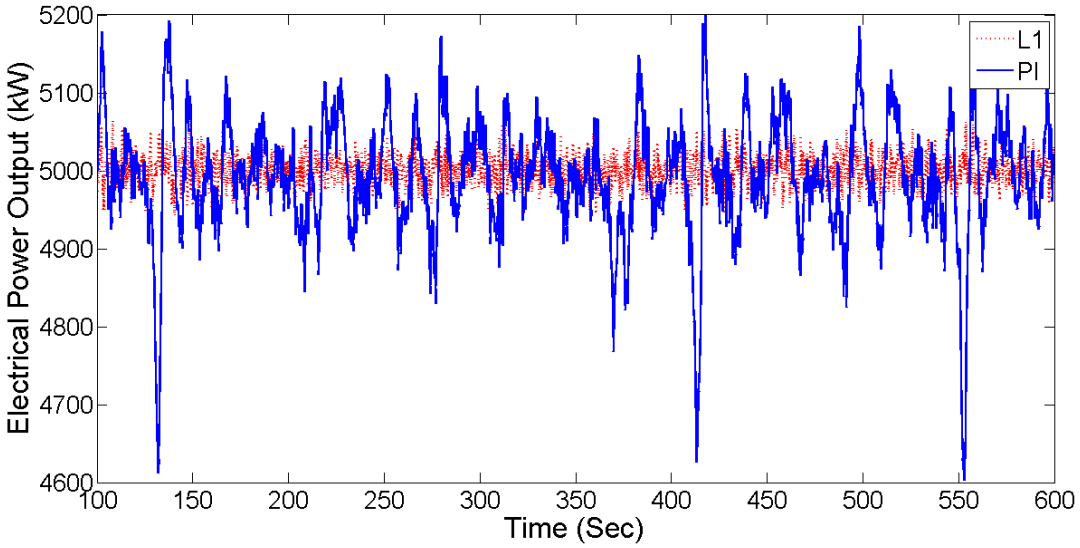

(e)

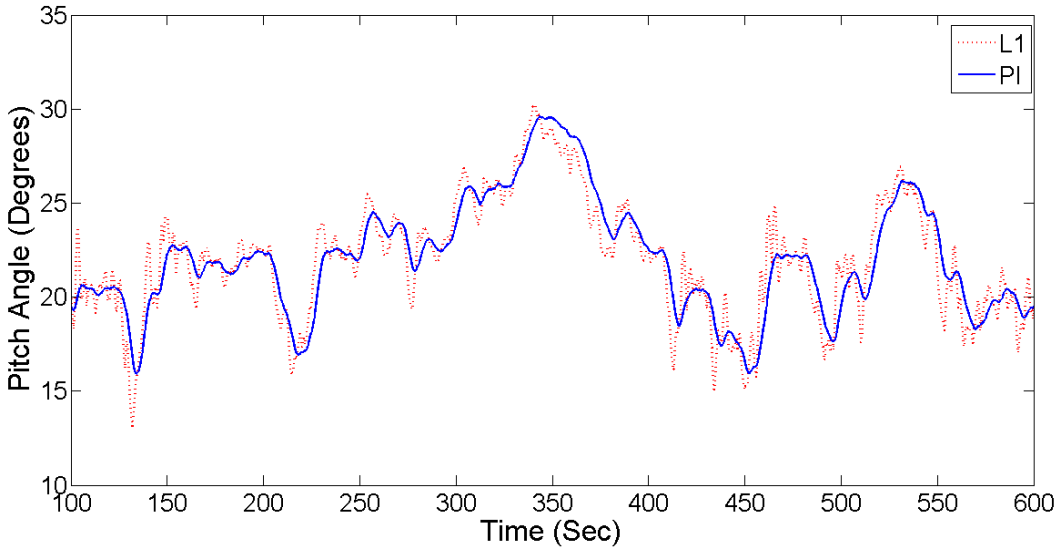

Figure 5.6 ℓ_1 and PI control of NREL-Offshore-Baseline-5 MW wind turbine in the rated power area (Region III) are compared at average wind speed of 24 m/s. (a) Wind speed profile, (b) Rotor speed, (c) Generator torque, (d) Electrical power output, and (e) Pitch angle are shown in a time interval of 10 minutes.

We can observe the advantages of the gain scheduled ℓ_1-optimal control over the PI control, especially at higher wind speeds. As shown in the figures, the fluctuation in the rotor speed and generator torque has significantly reduced by our proposed controller (as shown in

Tab. 5.1). Therefore, the ℓ_1 controller alleviates the mechanical loads induced in the drive-train and the turbine structure, so that it enhances the useful life of the wind turbine. In addition, the generator torque-time figures indicate that the generator torque reaches the maximum torque several times using PI control, but the torque saturation rarely happens under ℓ_1 control (it only occurs in the case of the average wind speed of 14 m/s). Frequent operation at maximum generator torque induces high stresses in the mechanical components and may cause overheating in the electric circuits. As shown in the pitch angle-time figures, the ℓ_1 control has slightly more pitch activity than the PI control. However, the difference in pitch activities are negligible as the pitch rate is always less than 2 degree/sec under both controllers which is safely less that the allowed pitch rate (for large wind turbines the maximum pitch rate is about 5 degrees/sec). Moreover, as shown in the electrical power output-time figures, implementing the ℓ_1 control, has significantly improved the power quality compared with the PI control. These results meet the main purpose of this research which is the application of ℓ_1 control to minimize the effect of persistent disturbances in the control systems such as turbulent wind in wind turbine systems.

5.2 Analysis of Simulation Results Using Statistical Tools

We used the standard deviation and the average of the data from simulation to compare the performance of the PI and ℓ_1 controls. The standard deviation is commonly used to measure the spread or dispersion of data around the mean. The mean and standard deviation for a set of n data x_i are

$$\text{Mean:} \quad \bar{x} = \frac{\sum x_i}{n} \tag{5.1}$$

$$\text{Standard deviation:} \quad \sigma = \sqrt{\frac{\sum(\bar{x}-x_i)^2}{n-1}} \tag{5.2}$$

In the Tab. 5.1, we calculated the standard deviation and the average of rotor speed, generator torque, and the power output for six different simulations for average wind speeds of 14, 16, 18, 20, 22, and 24 m/s.

Table 5.1 The average and standard deviation of the rotor speed, power output, and the generator torque at different wind speeds.

Average Wind Speed (m/s)	**Average and Standard Deviation of Rotor Speed (RPM)**		**Average and Standard Deviation of Power Output (kW)**		**Average and Standard Deviation of Generator Torque (kN.m)**	
	ℓ_1-Control	**PI-Control**	**ℓ_1-Control**	**PI-Control**	**ℓ_1-Control**	**PI-Control**
14	Ave=12.0484 STD=0.8536	Ave=12.0946 STD=0.5027	Ave=4960.3 STD=126.1512	Ave=4944.4 STD=241.5105	Ave=43.1035 STD=2.3866	Ave=42.6875 STD=2.4785
16	Ave=12.2323 STD=0.6000	Ave=12.0951 STD=0.5934	Ave=4998.3 STD=16.6186	Ave=5000.2 STD=39.4159	Ave=42.7162 STD=2.0049	Ave=43.2130 STD=2.0696
18	Ave=12.1777 STD=0.4350	Ave=12.0945 STD=0.6510	Ave=5000.0 STD=12.2776	Ave=4998.0 STD=45.9396	Ave=42.8714 STD=1.4101	Ave=43.2147 STD=2.2391
20	Ave=12.1438 STD=0.3562	Ave=12.0929 STD=0.7094	Ave=5000.0 STD=14.2666	Ave=4994.6 STD=56.0099	Ave=42.9751 STD=1.0911	Ave=43.2098 STD=2.3927
22	Ave=12.1378 STD=0.3034	Ave=12.0919 STD=0.7593	Ave=5000.0 STD=15.7840	Ave=4991.1 STD=65.0365	Ave=42.9824 STD=0.9275	Ave=43.2005 STD=2.5119
24	Ave=12.1723 STD=0.3056	Ave=43.1873 STD=2.6010	Ave=4999.9 STD=17.2607	Ave=4988.1 STD=74.9502	Ave=42.8638 STD=0.9600	Ave=43.1873 STD=2.6010

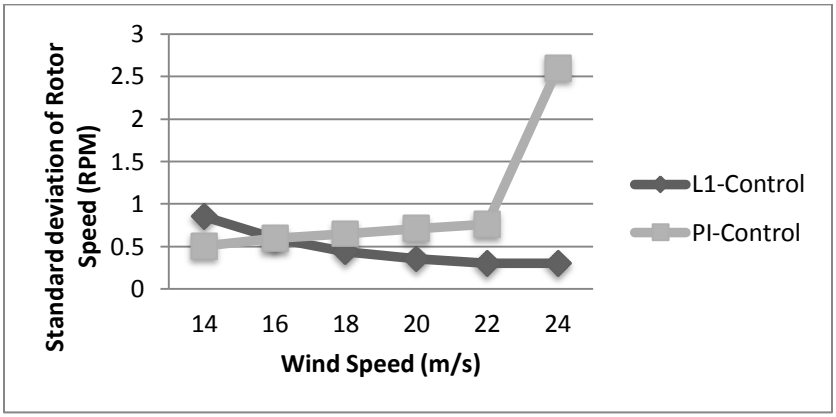

Figure 5.7 The standard deviation of rotor speed fluctuations around the rated rotor speed under ℓ_1 and PI controls is shown at different wind speeds.

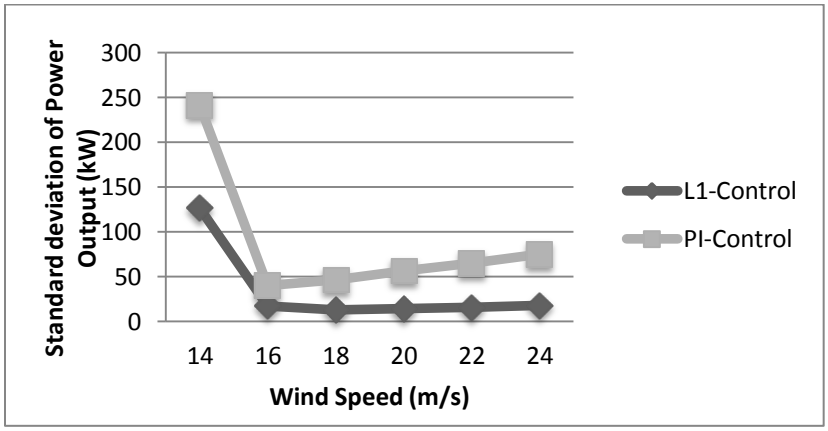

Figure 5.8 The standard deviation of power output fluctuations around the rated power under ℓ_1 and PI controls is shown at different wind speeds.

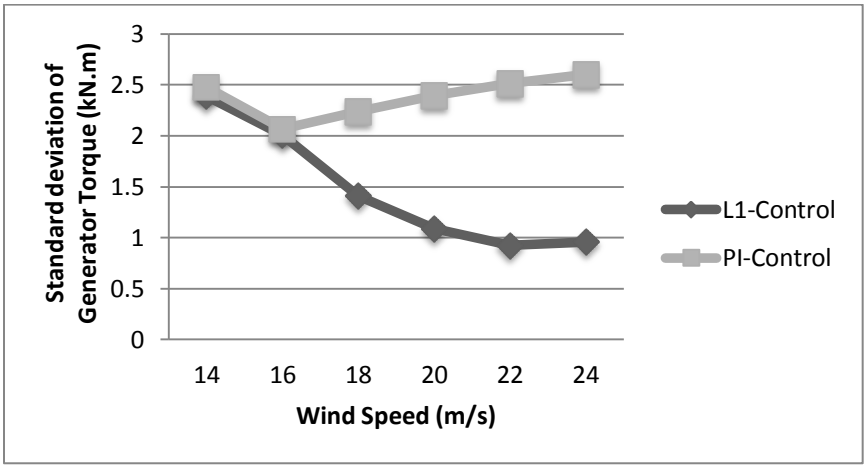

Figure 5.9 The standard deviation of generator torque fluctuations around the rated generator torque under ℓ_1 and PI controls is shown at different wind speeds.

As shown in Figs. 5.7-5.9, our proposed gain-scheduled ℓ_1-optimal controller has better performance compared to the well-tuned PI controller in reducing the standard deviations. The decrease in the standard deviations means that the fluctuations in the rotor speed, the generator torque, and the power output has been reduced. Therefore, the gain-scheduled ℓ_1-optimal controller can alleviate the mechanical loads induced in the wind turbine components by minimizing the effect of turbulent wind disturbances. Also, values of the rotor speed, power output, and generator torque are very close to the rated values in the Region III, 12.1 RPM, 5MW, and 43kN.m, respectively.

As shown in the Figs. 5.7-5.9, at lower wind speeds with the average of 14 m/s, the performance of our proposed controller is not much better than the PI-controller. These ranges of wind speeds are close to the rated wind speed (11.5 m/s) in the transition region and the wind turbine may enter Region I. As we designed our controller to operate at high wind speeds in Region III, the controller performance is lower at wind speeds close to the rated wind speed. However, as our controller is designed based on gain scheduling, we can easily extend the range of operation of the controller to the lower wind speeds in the region I and the transition region (region II).

Chapter 6: Summary and Suggestions

6.1 Summary

The fast-growing technology of large scale wind turbines demands control systems capable of enhancing both the efficiency of capturing wind power, and the useful life of the turbines. Control based on ℓ_1 performance is an approach to deal with persistent exogenous disturbances which have bounded magnitude (ℓ_1-norm) such as realistic wind disturbances and turbulence profiles. In Ch. 1, a comprehensive overview of wind turbine systems and literature review of control design for wind turbines and also overview of ℓ_1-optimal control were presented.

In Ch. 2, ℓ_1-optimal control was introduced and the linear matrix inequality (LMI) solution of the ℓ_1-optimal control problem was presented. As an example of the LMI approach, we obtained ℓ_1-optimal PI gains for a state-feedback controlled system. Then, methods found in the literature for calculation of the ℓ_1-norm and its upper and lower bounds were detailed. Next, we proposed a computationally efficient method for calculation of ℓ_1-norm. Finally, using an aircraft model, we compared the accuracy and computation speed of our new method for calculation of ℓ_1-norm with some standard methods found in the literature. Also, in the aircraft example, we designed optimal controllers for the system based on ℓ_1-performance, $\mathcal{H}_2$-performance, and $\mathcal{H}_\infty$- performance and then we simulated the closed-loop system responses.

In Ch. 3, a novel LPV model of aerodynamic and drive-train dynamics of a VS-VP wind turbine in the transition region was developed and the state-space realization of the control system was presented. Then, a state feedback controller based on ℓ_1 performance was derived by

minimizing the upper bound problem on the ℓ_1-norm using an LMI approach. Next, the LPV control strategy was presented and the controller implemented on the LPV model and simulation results are given.

In Ch. 4, we first derived the linear model of a wind turbine at different operating points in Region III (the rated power region at high wind speeds). Next, we found local output feedback controllers at each operating point. The local controllers were optimized based on ℓ_1 performance using genetic algorithm method. Then, we presented a gain-scheduling technique with guaranteed stability in order to interpolate the local controllers.

In Ch. 5, we presented the simulation results. The proposed gain-scheduled ℓ_1-Optimal control was implemented on the model using a SIMULINK interface provided in the FAST software. We performed the simulation for 6 different fully turbulent wind profiles with average speeds of 14, 16, 18, 20, 22, 24 m/s (in region III). We compared the performance of our proposed controller with a well-tuned PI controller. The results show improved power quality, and decrease in the fluctuations of generator torque and rotor speed. These results meet the main purpose of this research which is the application of ℓ_1 control to minimize the effect of persistent disturbances in the control systems such as turbulent wind in wind turbine systems.

6.2 Suggestions

- In this work, we used genetic algorithms to obtain all the matrix entries of an output feedback controller. For higher order of controllers, the number of optimization variables increases. Therefore, searching for stabilising controllers becomes computationally

expensive. For future work, an algorithm which improves the optimization of output-feedback controllers using methods such as genetic algorithm is useful.

- In this study, we obtained the gain-scheduled ℓ_1-optimal control for Region III (high wind speeds). Extending the LPV model of wind turbine and the optimal gain-scheduled control for the full range of operation of wind turbine including Regions I, II, and III is recommended for future work.
- The theorem (4.2) allows us to optimize the performance level of gain scheduled controller at interpolating points. In this work, we obtained the LMI constraints of ℓ_1 performance for continues-time systems which cannot be used for discrete-time systems. Therefore, we suggested that an equivalent of LMIs in Theorem (4.2) is obtained for discrete-time systems.
- Higher order model of wind turbine which includes more DOFs, can be considered for optimal control design in future work. Large wind turbines are flexible structures with many moving components. Consideration of some of these dynamic equations in the wind turbine model is very important for designing optimal control.

Bibliography

1. Abedor, J., Nagpal, K., and Poolla, K., (1996). A linear matrix inequality approach to peak-to-peak gain minimization, *International Journal of Robust and Nonlinear Control,* Vol. 6, 899-927.
2. Abo-Hammour, Z.S., Asasfeh, A.G., Al-Smadi, A.M., and Alsmadi, O.M.K., (2011). A novel continuous genetic algourithm for the solution of optimal control problems, *Optimal Control Application and Methods,* 32, 414–432.
3. Abo-Hammour, Z.S., Mirza, N.M., Mirza, S.M., and Arif, M., (2002). Cartesian path generation of robot manipulators using continuous genetic algorithms. Robotics and Autonomous Systems; 41(40):179–223.
4. Ackermann, T., and Soder, L., (2002). An overview of wind energy-status. *Renewable and Sustainable Energy Reviews,* 6(1-2), 67–127.
5. Ackermann, T., editor (2005). *Wind Power in Power Systems*. John Wiley & Sons Ltd, Chichester, UK.
6. Apkarian, P., and Tuan, H.D., (1998). Parameterized LMIs in control theory. *Proceedings of 37th Conference on Decision and Control*, Vol. 1, pp. 152-157.
7. Apkarian, P., and Tuan, H.D., (2000). Parameterized LMIs in control theory. *SIAMJ. Control and Optimization* 38(4), 1241-1264.
8. Apkarian, P., Gahinet, P., and Beck, G., (1995). Self-scheduling H_∞ control of linear parameter varying systems: A design example. *Automatica*, 31, (9), pp. 1251-1261.
9. Barabanov, A.E., and Granichin, O.N., (1984). Optimal controller for linear plant with bounded noise, *Automation and Remote Control*, 45(5), 578-584.

10. Bianchi, F., and Sanchez Pena, R.S., (2011). Interpolation for gain-scheduled control with guarantees, *Automatica* 47, pp. 239-243.
11. Bianchi, F., De Battista, H., and Mantz, R. J. (Eds.). (2007). *Wind Turbine Control Systems, principles, Modeling, and Gain Scheduling Design*, Springer, London, U.K.
12. Blanchini, F., Miani, S., and Mesquine, F., (2009). A separation principle for linear switching systems and parametrization of all stabilizing controllers. *IEEE Transactions on Automatic Control*, 54, 279–292.
13. Bossanyi, E., (2000). The design of closed loop controllers for wind turbines. *Wind Energy* 3(3), 149–163.
14. Bossanyi, E.A, (1987). Adaptive pitch control for a 250 kW wind turbine. *Proceedings of the 9th BWEA Wind Energy Conference*. Edinburgh, Scotland, pp. 85-92.
15. Boukhezzar, B., and Siguerdidjane, H., (2009). Nonlinear control with wind estimation of a DFIG variables wind turbine for power capture optimization. *Elsevier Energy Conversion and Management*, Vol. 50, pp. 885-892.
16. Burton, T., Sharpe, D., Jenkins, N., and Bossanyi, E. (2001). *Wind Energy Handbook*. John Wiley & Sons, Ltd., Chichester, UK.
17. Chang, Y. J.,and Rasmussen, B., (2008). Stable controller interpolation for LPV systems. In: *Proceedings of American Control Conference*, pp. 3082–3087.
18. Dahleh, M.A., and Diaz-Bobillo, I.J., (1995). *Control of Uncertain Systems: A Linear Programming Approach.* Prentice-Hall, Englewood Cliffs, NJ.
19. Dahleh, M.A., and Kammash, M.H., (1993). Controller design for plants with structured uncertainty. *Automatica*, 29(1), 37-56.

20. Dahleh, M.A., and Pearson, J.B., (1987b). ℓ_1-optimal feedback controllers for MIMO discrete-time systems. *IEEE Transactions on Automatic Control,* 32(4), 314-322.

21. Dahleh, M.A., Pearson, J.B., (1987). ℓ_1 optimal feedback controller for discrete-time system. *IEEE Transactions on Automatic Contol,* 32 314–322.

22. Davidor, Y., (2004). Genetic *Algorithms and Robotics: A Heuristic Strategy for Optimization*. World Scientific, Singapore.

23. De Battista, H., Mantz, R., and Christiansen, C. (2000). Dynamical sliding mode power control of wind driven induction generators. *IEEE Transactions on Energy Conversion* 15(4), 451–457.

24. Diaz-bobillo, I.J., and Dahleh, M.A., (1993). Minimization of the maximum peak-to peak gain: the general multiblock program. *IEEE Transactions on Automatic Control,* 38(10), 1459-1482.

25. Dorea, C.E.T., and Hennet, J.C., (1997). A Geometric approach to the ℓ_1 linear control problem. In: *Proceedings of 36thIEEE Conference of Decision and Control,* San Diego, CA, pp. 1552-1557.

26. Doyle, J.C., and stein, G., (1981). Multivariable feedback design: concepts for a classical/modern synthesis. *IEEE Transactions on Automatic Control,* 26(1), 4-16.

27. Ehlers, J., Diop, A., and Bindner, H., (2007). Sensor selection and state estimation for wind turbine controls. *Proceedings of the 45th AIAA Aerospace Sciences Meeting and Exhibit*, Reno, Nevada.

28. Fabian, B.C., (1996). Numerical solution of constrained optimal control problems with parameters. *Applied Mathematics and Computation*, 80, 43–62.

29. Fabian, B.C., (1998). Some tools for the direct solution of optimal control problems. *Advances in Engineering Software*, 29(1), 45–61.

30. Freeman, J.B., and Balas, M.J., (1999). An investigation of variables horizontal-axis wind Turbines using direct model-reference adaptive control. *Proceedings of the 37th AIAA Aerospace Sciences Meeting and Exhibit*. Reno, Nevada, pp. 66-76.

31. Gahinet, P., (1996). Explicit controller formulas for LMI-based H_∞ synthesis. *Automatica*, 32(7), 1007-1014.

32. Gardner, P., Garrad, A., Jamieson, P., Snodin, H., and Tindal, A., (2003). *Wind Energy. The facts*. Technical report, European Wind Energy Association (EWEA), Brussels, Belgium.

33. Goldberg, D.E., (1989). Genetic algorithms in search, *Optimization and Machine Learning*. Addison-Wesley, Reading, MA.

34. Hansen, M., Hansen, A., Larsen, T., Øye, S., Sørensen, P., and Fuglsang, P. (2005). *Control design for a pitch-regulated, variable speed wind turbine*. Technical Report RISO-R-1500(EN), Risø National Laboratory, Roskilde, Denmark.

35. Helmersson, A., (1995). *Methods for Robust Gain-Scheduling.* Ph.D. thesis, Linkoping University, Sweden.

36. Hespanha, J., and Morse, A. (1999). Stability of switched systems with average dwelltime. In: *Proceedings of the 46th IEEE Conference on Decision and Control*, Vol. 3, pp. 2655–2660.

37. Hespanha, J., and Morse, S., (2002). Switching between stabilizing controllers. *Automatica*, 38, 1905–1917.

38. Hinrichsen, E.N., and Nolen, P.J., (1984). Dynamics and stability of wind turbine generators. *IEEE Transactions on Power Apparatus and Systems*, 101, pp. 2640-2648.

39. Hui, J., and Bakhshai, A., (2008). A new adaptive control algorithm for maximum power point tracking for wind energy conversion systems. *IEEE Power Electronics Specialists Conference*, Kingston, Ontorio, pp. 4003-4007.

40. IEC 61400-3, (2006). Wind turbines-Part 3: Design requirements for offshore wind turbines. *International Electrotechnical Commission*, Draft 1st edition, Geneva, Switzerland.

41. Jafarnejadsani, H., and Pieper, J., (2013). L_1-optimal control of a linear parameter-varying model of a wind turbine in the transition region, *Proceedings of the 24th Canadian Congress of Applied Mechanics*, Saskatoon, Saskatchewan, Canada.

42. Jafarnejadsani, H., Pieper, J., and Ehlers, J. (2013). Adaptive control of a variable-speed variable-pitch wind turbine using RBF neural network. *IEEE Transactions on Control Systems Technology*, Vol. pp.

43. Jonkman B. J., and Buhl, M.L., (2006) *TurbSim User's Guide.* Technical Report NREL/EL-500-38230, National Wind Energy Technology Center, National Renewable Energy Laboratory, Golden, Colorado.

44. Jonkman B. J., and Buhl, M.L., (2006). *TurbSim User's Guide*. National Wind Energy Technology Center, National Renewable Energy Laboratory, Golden, Colorado.

45. Jonkman, J., Butterfield, S., Musial, W., and Scott, G., (2009). *Definition of a 5-MW Reference Wind Turbine for Offshore System Development*, Technical Report NREL/TP-500-38060, National Renewable Energy Laboratory, Golden, Colorado.

46. Khammash, M., (2000). A new approach to the solution of the ℓ_1 control problem: the scaled-Q method. *IEEE Transactions on Automatic Control* 45(2), 180-187.

47. Khammash, M., and Pearson, J.B., (1991). Performance robustness of discrete-time systems with structured uncertainty. *IEEE Transactions on Automatic Control,* 36(4), 398-412.

48. Khosravi, A., Jalali, A., (2008). A new LMI solution in the ℓ_1 optimal problem for wind turbine-induction generator unit. *Applied Mathematics and Computation* 206 pp.643–650.

49. Kos, J.M., (1978). Online control of a large horizontal axis energy conversion system and its performance in a turbulent wind environment. *Proceedings of the 13th Intersociety Energy Conversion Engineering Conference*. U.S.A., pp. 2064-2073.

50. Kraan, I., (1992). *Control Design for a Flexible Wind Turbine* (in Dutch). Deflt University of Technology, TUD-WBMRA- 613, 1992.

51. Laino, D., and Hansen, A., (2003) *YawDyn User's Guide-Version 12.14*. Prepared for the National Renewable Energy laboratory under subcontract No. TCX-9-29209-01.

52. Laino, D., and Hansen, A., (2003). Continued validation of the AeroDyn subroutines using NREL unsteady aerodynamics experiment data. *Proceedings of the 2003 ASME Wind Energy Symposium,* Reno, Nevada, pp. 84-93.

53. Lalor, G., Mullane, A., and O'Malley, M. (2005). Frequency control and wind turbine technologies. *IEEE Transactions on Power Systems* 20(4), 1905–1913.

54. Larsson, A. (2000). *The power quality of wind turbines*. Ph.D. thesis, Chalmers University of Technology, G¨oteborg, Sweden.

55. Leithead, W. and Connor, B. (2000). Control of variable speed wind turbines: design task. *International Journal of Control* 73(13), 1189–1212.

56. Leithead, W. and Connor, B. (2000). Control of variable speed wind turbines: dynamic models. *International Journal of Control* 73(13), 1173–1189.

57. Liebst, B.S., (1985). A pitch control system for the KaMeWa wind turbine. *Journal of Dynamic Systems and Control,* 107, 47.

58. Malaterro, P.O., and Khammash, M., (2000). ℓ_1 controller design for a high-order 5-Pool irrigation canal system. In: *Proceedings of 39th Conference of Decision and Control*, 38(5), 753-756.

59. Mattson, S.E., (1984). *Modeling and Control of Large Horizontal Axis Wind Power Plants*. Ph.D. Thesis, Department of Automatic Control, Lund Institute of Technology, Lund, Sweden.

60. Mayosky, M. A., and G. I. E. Cancelo, (1999). Direct adaptive control of wind energy conversion systems using Gaussian networks. *IEEE Transactions On Neural Networks*, Vol. 10, No. 4.

61. Molenaar, D.P., (2003). *Cost-effective Design and Operation of Variable Speed Wind Turbines*. Ph.D. Thesis, Mechanical Engineering and Systems and Controls Group, Delft University of Technology, Delft, The Netherlands.

62. Muljadi, E., and Butterfield, C., (2001). Pitch-controlled variable-speed wind turbine generation. *IEEE Transactions on Industry Applications* 37(1), 240–246.

63. Østergaard, K. Z., Brath, P., and Stoustrup, J., (2007). Estimation of effective wind speed, *Journal of Physics*, Conference Series 75.

64. Packard, A., and Doyle, J., (1993). The complex structured singular value. *Automatica* 29(1), 71-109.

65. Rieber, J. M., and Allgower, F., (2003). An approach to gain-scheduled L_1-optimal control of linear parameter-varying systems. *Proceedings of the 42nd IEEE Conference on Decision and Control*, Maui, Hawaii, USA.

66. Rieber, J. M., Fritsch, A., and Allgower, F., (2005). State-space formulas for gain-scheduled ℓ_1-optimal controllers. *American Control Conference*, Portland, OR, USA.

67. Rieber, J.M., (2007). *Control of Uncertain Systems with ℓ_1 and Quadratic Performance Objectives.* Ph.D. Thesis, Von der Fakultat Maschinenbau der Universitat Stuttgart, Germany.

68. Rieber, J.M., Scherer C.W., and Allgower, F., (2006b). Robust ℓ_1 performance analysis in face of parametric uncertainties. In: *Proceedings of 5th IFAC Symposium of Robust Control Design*, Toulouse, France. On CD-ROM, paper no. 248.

69. Rieber, J.M., Scherer C.W., and Allgower, F., (2008). Robust ℓ_1 performance for linear systems with parametric uncertainties. *International Journal of Control*, Vol. 81, pp. 851.

70. Rieber, J.M., Stemmer, A., and Allgower, F., (2005b). Experimental application of ℓ_1-optimal control in atomic force microscopy. In: *Proceedings of 16th IFAC World Congress, Prague, Czech Republic.* On DVD-ROM, paper no. 4660.

71. Rothman, E.A., (1978). The effects of control modes on rotor loads, *2nd International Symposium of Wind Energy Systems*. Amsterdam, The Netherlands, pp. 107- 117.

72. Rugh, W., and Shamma, J. (2000). Research on gain scheduling. *Automatica* 36(10), 1401–1425.

73. Sakar. D., and Modak, J.M., (2004). Genetic algorithms with filters for optimal control problems in fed-batch bioreactors. *Bioprocess and Biosystems Engineering*, 26, 295–306.

74. Sanchez-Pena, R.S., and Sznair, M., (1998). *Robust Systems-Theory and Applications.* John Wiley & Sons, New York, NY.

75. Scherer, C., Weiland, S., (2004). *Linear Matrix Inequality in Control*. Delft University of Technology, the Netherlands.

76. Scherer, C.W., (2000b). Robust mixed control and linear parameter-varying control with full block multipliers. In: *Recent Advances on LMI Methods in Control* (L. EL Ghaouri and Niculescu, Eds.), pp. 187-207. SIAM.

77. Schuler, S., Schlipf, D., Kühn, M., and Allgöwer, F., (2010). ℓ_1-optimal multivariable pitch control for load reduction on large wind turbines, *European Wind Energy Conference*, Scientific track, Warsaw, Poland.

78. Shamma, J.S., (1994). Robust stability with time-varying structured uncertainty. *IEEE Transactions on Automatic Control,* 39(4), 714-724.

79. Sim YC, Leng SB, Subramaniam V. A combined genetic algorithms-shooting method approach to solving optimal control problems. International Journal of Systems Science 2000; 31(1):83–89.

80. Skogestad, S., and Postlethwaite, I., (2005). *Multivariable Feedback Control*, second edition, John Wiley & Sons, Cheichester.

81. Sørensen, P., Hansen, A., Iov, F., Blaabjerg, F., and Donovan, M. (2005). *Wind farm models and control strategies*. Technical Report RISO-R-1464(EN), Risø National Laboratory, Roskilde, Denmark.

82. Spillman, M., and Ridgely, D.B., (1997). Flight control applications of ℓ_1 optimization. *Journal of Guidance, Control, and Dynamics, 20(1), 49-56.*

83. Stilwell, D., & Rugh, W. (2000). Stability preserving interpolation methods for the synthesis of gain scheduled controllers. Automatica, 36, 665–671.

84. Svensson, J.E. and Ulen, E., (1982). The control of the WTS-3, instrumentation and testing. *4th International Symposium on Wind Energy Systems*. Stockholm, Sweden, pp. 195-215.

85. Turner, M.C., Herrmann, G., and Postlethwaite, I., (Editors), (2007). *Mathematical Methods for Robust and Nonlinear Control*. LNCIS 367, pp. 123-142, Springer-Verlag Berlin Heidelberg.

86. Vidyasagar, M., (1986). Optimal rejection of persistent bounded disturbances. *IEEE Transactions on Automatic Control,* 31(6), 527-534.

87. Wasynczuk, O., Man, D.T. and Sullivan, J.P., (1981). Dynamic behavior of a class of wind turbine generators during random wind fluctuations. *IEEE Transactions on Power Apparatus and Systems*, 100, pp. 2837-2845.

88. Wilson, R.E., Walker, S.N. and Heh, P., (1999) *Technical and User's Manual for the FAST_AD Advanced Dynamics Code*, OSU/NREL Report 99-01, Corvallis, Oregon: Oregon State University.

89. Wright, A. D., (2004). *Modern Control Design for Flexible Wind Turbines.* Technical Report NREL-TP-500-35816, National Renewable Energy Laboratory, Golden, Colorado.

90. Xie W., and Eisaka, T., (2004). Design of LPV control systems based on Youla parameterization. *IEEE Proceedings of Control Theory Applications* Vol. 151, No. 4.

91. Youla, D.C, Jabr, H.A., and Bongiorno, J.J. (1976). Modern wiener-hopf design of optimal controllers Part2: the multivariable case. *IEEE Transactions on Automatic Control,* 21(3), 319-338.

Appendixes: Q-Parameterization

This section describes Q-Parameterization (or Youla Parameterization) which is a fundamental result of linear control theory. This theory has been developed by Kucera (1972) and Youla *et al.* (1976). The theory provides an affine parameterization of the set of all closed – loop transfer matrices which can be obtained by using a stabilizing finite order LTI controller in a standard finite order LTI feedback optimization setup. Here, we give a discrete-time description, but the same formulas hold in continuous time as well.

Lemma A.1: *Let a system G with state-space realization*

$$\begin{bmatrix} x(k+1) \\ z_1(k) \\ y(k) \end{bmatrix} = \begin{bmatrix} A & B_1 & B_2 \\ C_1 & D_{11} & D_{12} \\ C_2 & D_{21} & D_{22} \end{bmatrix} \begin{bmatrix} x(k) \\ w_1(k) \\ u(k) \end{bmatrix} \tag{A.1}$$

be given, and let F and L be such that $A + B_2F$ and $A + LC_2$ are asymptotically stable. Then all internally stabilizing finite-dimensional LTI output-feedback controllers $u = Ky$ are given by a *linear fractional transformation (LFT)*

$$\widehat{K}(z) = \mathcal{F}_\ell\big(J_i(z), Q_i(z)\big) \tag{A.2}$$

with $\hat{Q} \in \mathcal{RH}_\infty$, $\det\left(I + D_{22}\hat{Q}(\infty)\right) \neq 0$, and

$$\hat{J}(z) = \left[\begin{array}{cc|cc} A + B_2F + LC_2 + LD_{22}F & \vdots & -L & B_2 + LD_{22} \\ \cdots\cdots\cdots\cdots\cdots\cdots & \cdots & \cdots\cdots\cdots & \cdots\cdots \\ F & \vdots & 0 & I \\ -(C_2 + D_{22}F) & \vdots & I & -D_{22} \end{array}\right] \tag{A.3}$$

Furthermore, all internally stable closed-loop maps $z_1 = Gw_1$ are given by

$$\hat{G}(z) = \hat{H}(z) - \hat{U}(z)\hat{Q}(z)\hat{V}(z), \tag{A.4}$$

where

$$\widehat{H}(z) = \begin{bmatrix} A + B_2F & -B_2F & \vdots & B_1 \\ 0 & A + LC_2 & \vdots & B_1 + LD_{21} \\ \cdots\cdots\cdots\cdots & \cdots\cdots\cdots\cdots & \cdots\cdots & \cdots\cdots \\ C_1 + D_{12}F & -D_{12}F & \vdots & D_{11} \end{bmatrix},$$

$$\widehat{U}(z) = \begin{bmatrix} A + B_2F & \vdots & -B_2 \\ \cdots\cdots\cdots\cdots & \cdots & \cdots\cdots \\ C_1 + D_{12}F & \vdots & -D_{12} \end{bmatrix}, \quad \widehat{V}(z) = \begin{bmatrix} A + LC_2 & \vdots & B_1 + LD_{21} \\ \cdots\cdots\cdots\cdots & \cdots & \cdots\cdots\cdots\cdots \\ C_2 & \vdots & D_{21} \end{bmatrix} \qquad \text{(A.5)}$$

Appendixes: Proof of Theorem (4.1)

In this section, the proof for the Theorem (4.1) is presented. The continuous-time description of the theorem and its proof can be found in Binanchi and Sunchez-pena (2011).

Lemma A.2*: Given a set of matrices A_i associated to each vertex of the convex hull $\Theta = co\{\rho_1, \dots, \rho_{n_p}\}$, the following statements are equivalent.*

(i) *A_i has its eigenvalues in the open unit disk for all $i \in I_{n_p}$*

(ii) *There exists n_p matrix transformations T_i such that the LPV matrix*

$$\tilde{A}(\rho) = \sum_{i=1}^{n_p} \alpha_i(\rho)\tilde{A}_i = \sum_{i=1}^{n_p} \alpha_i(\rho) T_i A_i T_i^{-1} \tag{A.6}$$

has its eigenvalues in the open unit disk for all $\rho \in \Theta$, with $\alpha_i(\rho) = \alpha_i$ in $\rho = \sum_{i=1}^{n_p} \alpha_i \rho_i$ such that $\sum_{i=1}^{n_p} \alpha_i = 1$.

We use Lemma A.2 to prove Theorem 4.1. According to Youla parameterization, assuming$(D_{22} = 0)$, any stabilizing controller $\widetilde{K}_i$ for the plant $G_i(s)$ can be expressed as a linear fractional transformation (LFT):

$$\widetilde{K}_i(z) = \mathcal{F}_\ell\big(J_i(z), Q_i(z)\big) = \begin{bmatrix} \tilde{A}_{k,i} & \vdots & \tilde{B}_{k,i} \\ \dots\dots & \vdots & \dots\dots \\ \tilde{C}_{k,i} & \vdots & \widetilde{D}_{k,i} \end{bmatrix} \tag{A.7}$$

$$J_i(z) = \begin{bmatrix} A + B_2F_i + H_iC_2 & \vdots & -H_i & B_2 \\ \dots\dots\dots\dots\dots\dots & \dots\dots & \dots\dots\dots & \dots\dots \\ F_i & \vdots & 0 & I \\ -C_2 & \vdots & I & 0 \end{bmatrix}, \tag{A.8}$$

$$Q_i(z) = \begin{bmatrix} A_{q,i} & \vdots & B_{q,i} \\ \dots\dots & \vdots & \dots\dots \\ C_{q,i} & \vdots & D_{q,i} \end{bmatrix}, \tag{A.9}$$

with $A_{q,i}$ has its eigenvalues in the open unit disk. After some algebraic manipulations, it can be proved that, if

$$Q_i(z) = \left[\begin{array}{ccc} A + B_2 D_{k,i} C_2 & B_2 C_{k,i} & \vdots \quad B_2 D_{k,i} - H_i \\ B_{k,i} C_2 & A_{k,i} & \vdots \quad B_{k,i} \\ \cdots\cdots\cdots\cdots & \cdots\cdots\cdots\cdots & \cdots\cdots\cdots \quad \cdots\cdots\cdots \\ D_{k,i} C_2 - F_i & C_{k,i} & \vdots \quad D_{k,i} \end{array}\right], \tag{A.10}$$

the controllers $\widetilde{K}_i(z)$ are input to output equivalent to the original local controllers $K_i(z)$. Note that $A_{q,i}$ corresponds to the A matrix of closed-loop system $\mathcal{F}_\ell\big(G_i(z), K_i(z)\big)$, Hence $Q_i(z)$ is stable if the controller $K_i(z)$ stabilize $G_i(z)$. Then, replacing the controller matrices (LFT interconnection between (A.8) and (A.10)) in the closed-loop matrix

$$A_{cl,i} = \begin{bmatrix} A_i + B_2 \widetilde{D}_{k,i} C_2 & B_2 \tilde{C}_{k,i} \\ \tilde{B}_{k,i} C_2 & \tilde{A}_{k,i} \end{bmatrix}, \tag{A.11}$$

And applying a similarity transformation, the following result is obtained

$$A_{cl} = \sum_{i=1}^{n_p} \alpha_i(\rho) \begin{bmatrix} A_{H,i} & 0 & 0 \\ B_{q,i} C_2 & A_{q,i} & 0 \\ B_{H,i} C_2 & B_2 C_{q,i} & A_{F,i} \end{bmatrix} \tag{A.12}$$

with $A_{H,i} = A_i + H_i C_2,\ A_{F,i} = A_i + B_2 F_i$ and $B_{H,i} = B_2 D_{q,i} - H_i$.

Next, to ensure stability at any point in $\mathcal{P}$, a matrix $X_{cl} > 0$ must be computed such that $A_{cl}(\rho) X_{cl} A_{cl}(\rho) - X_{cl} < 0$. Due to the block triangle structure of $A_{cl}(\rho)$, the previous inequality is satisfied if the following three inequalities hold

$$\sum_{i=1}^{n_p} \alpha_i(\rho) \big(A_{H,i}(\rho) X_1 A_{H,i}(\rho) - X_1 \big) < 0, \tag{A.13}$$

$$\sum_{i=1}^{n_p} \alpha_i(\rho) \big(A_{q,i}(\rho) Y_2 A_{q,i}(\rho) - Y_2 \big) < 0, \tag{A.14}$$

$$\sum_{i=1}^{n_p} \alpha_i(\rho) \big(A_{F,i}(\rho) Y_3 A_{F,i}(\rho) - Y_3 \big) < 0, \tag{A.15}$$

with $X_{cl} = diag(X_1, Y_2, Y_3) \in \mathbb{R}^{(2n+n_q)\times(2n+n_p)}$.

Taking into account that $A_{q,i}$ are stable matrices by construction and the result in lemma A.2, if $X_{2,i} = T_i^T Y_2 T_i$, inequality (A.14) is equivalent to (4.23). On the other hand, using the vertex property (Apkarian *et al.*,1995), (A.13) and (A.15) can be reduced to prove the existence of positive definite matrices X_1 and $X_3 = Y_3^{-1}$ which satisfy (4.22) and (4.24) at each $i \in I_{n_p}$, with $W_i = X_1 H_i$ and $V_i = F_i X_3$. Note that we also used Schur complement lemma to obtain the equivalent LMIs for inequalities (A.13)-(A.15).